

Turkish Journal of

# Analytical Chemistry

Volume 6

Issue 1

June 2024

<https://dergipark.org.tr/tr/pub/turkjac>

Turkish Journal of  
**Analytical  
Chemistry**  
TurkJAC

**Volume 6  
Issue 1  
June 2024**

**Publication Type:** Peer-reviewed scientific journal

**Publication Date:** June 30, 2024

**Publication Language:** English

Published two times in a year (June, December)

## **Owner**

Prof. Miraç Ocak

Karadeniz Technical University, Faculty of Sciences, Department of Chemistry

## **Executive Editor**

Prof. Ümmühan Ocak

Karadeniz Technical University, Faculty of Sciences, Department of Chemistry

## **Co-Editor**

Ender Çekirge

Karadeniz Technical University, Institute of Forensic Sciences

## **Layout Editor**

Ender Çekirge

Karadeniz Technical University, Institute of Forensic Sciences

## **Editorial Secretary**

Ender Çekirge

Karadeniz Technical University, Institute of Forensic Sciences

## **Language Editors**

Nurhayat Özbek

Karadeniz Technical University, Faculty of Sciences, Department of Chemistry

Prof. Miraç Ocak

Karadeniz Technical University, Faculty of Sciences, Department of Chemistry

## **Copyeditor**

Nurhayat Özbek

Karadeniz Technical University, Faculty of Sciences, Department of Chemistry

Aslıhan Yılmaz Çamoğlu

Karadeniz Technical University, Faculty of Sciences, Department of Chemistry

Prof. Miraç Ocak

Karadeniz Technical University, Faculty of Sciences, Department of Chemistry

## **Proofreader**

Nurhayat Özbek

Karadeniz Technical University, Faculty of Sciences, Department of Chemistry

## **Editors**

Prof. Ümmühan Ocak

Karadeniz Technical University, Faculty of Sciences, Department of Chemistry

Prof. Miraç Ocak

Karadeniz Technical University, Faculty of Sciences, Department of Chemistry

Prof. Selehattin Yılmaz

Çanakale Onsekiz Mart University, Faculty of Science and Literature,  
Department of Chemistry

Prof. Ali Gündoğdu Karadeniz Technical University, Maçka Vocational School, Department of Pharmacy Services

## **Editor Board**

Prof. Selehattin Yılmaz Çanakkale Onsekiz Mart University, Faculty of Science and Literature, Department of Chemistry

Prof. Ali Gündoğdu Karadeniz Technical University, Maçka Vocational School, Department of Pharmacy Services

Prof. Hakan Alp Karadeniz Technical University, Faculty of Sciences, Department of Chemistry

Prof. Volkan Numan Bulut Karadeniz Technical University, Maçka Vocational School, Department of Chemistry and Chemical Processing Technologies

Prof. Celal Duran Karadeniz Technical University, Faculty of Sciences, Department of Chemistry

Asst. Prof. Aysel Başoğlu Gümüşhane University, Faculty of Health Sciences, Department of Occupational Health and Safety

Prof. Ayşegül İyidoğan Gaziantep University, Faculty of Science and Literature, Department of Chemistry

Prof. Sevgi Kolaylı Karadeniz Technical University, Faculty of Sciences, Department of Chemistry

Prof. Hüseyin Serencam Trabzon University, College of Applied Sciences, Department of Gastronomy and culinary arts

Assoc. Prof. Fatma Ağın Karadeniz Technical University, Faculty of Pharmacy, Department of Basic Pharmaceutical Sciences

Prof. Duygu Özdeş Gümüşhane University, Gümüşhane Vocational School, Department of Chemistry and Chemical Processing Technologies

Dr. Mustafa Z. Özel University of York, Department of Chemistry

Prof. Małgorzata Wiśniewska University of Maria Curie- Sklodowska, Faculty of Chemistry, Institute of Chemical Sciences, Department of Radiochemistry and Environmental Chemistry

Prof. Dilek Kul Karadeniz Technical University, Faculty of Pharmacy, Department of Basic Pharmaceutical Sciences

Prof. Sławomira Skrzypek University of Lodz, Faculty of Chemistry, Department of Inorganic and Analytical Chemistry

Prof. Fatih İslamoğlu Recep Tayyip Erdoğan University, Faculty of Science and Literature, Department of Chemistry

Asst. Prof. Zekeriyya Bahadır Giresun University, Faculty of Science and Literature, Department of Chemistry

Asst. Prof. Yasemin Çağlar Giresun University, Faculty of Engineering, Department of Genetic and Bioengineering

Prof. Agnieszka Nosal-Wiercińska	University of Maria Curie- Sklodowska, Faculty of Chemistry, Institute of Chemical Sciences, Department of Analytical Chemistry
Assoc. Prof. Dr. Halit Arslan	Gazi University, Faculty of Science, Department of Chemistry
Assoc. Prof. Cemalettin Baltacı	Gümüşhane University, Faculty of Engineering and Natural Sciences, Department of Food Engineering
Asst. Prof. Zafer Ocak	Kafkas University, Education Faculty, Mathematics and Science Education
Prof. Mustafa İmamoğlu	Sakarya University, Faculty of Science and Literature, Department of Chemistry
Assoc. Prof. Esra Bağda	Sivas Cumhuriyet University, Faculty of Pharmacy, Department of Basic Pharmaceutical Sciences, Analytical Chemistry Division
Assoc. Prof. Hüseyin Altundağ	Sakarya University, Faculty of Science and Literature, Department of Chemistry
Asst. Prof. Mehmet Başoğlu	Gümüşhane University, Faculty of Engineering and Natural Sciences, Department of Energy Systems Engineering

### **Publishing Board**

Prof. Latif Elçi	Pamukkale University, Faculty of Science and Literature, Department of Chemistry
Prof. Münevver Sökmen	Konya Food and Agriculture University, Faculty of Engineering and Architecture, Department of Bioengineering
Prof. Atalay Sökmen	Konya Food and Agriculture University, Faculty of Engineering and Architecture, Department of Bioengineering
Prof. Kamil Kaygusuz	Karadeniz Technical University, Faculty of Sciences, Department of Chemistry
Prof. Yaşar Gök	Pamukkale University, Faculty of Science and Literature, Department of Chemistry
Prof. Ayşegül Gölcü	İstanbul Technical University, Faculty of Science and Literature, Department of Chemistry
Prof. Mustafa Tüzen	Gaziosmanpaşa University, Faculty of Science and Literature, Department of Chemistry
Prof. Mustafa Soylak	Erciyes University, Faculty of Sciences, Department of Chemistry
Prof. Fikret Karadeniz	Kafkas University, Faculty of Science and Literature, Department of Chemistry
Prof. Mehmet Yaman	Fırat University, Faculty of Sciences, Department of Chemistry
Prof. Halit Kantekin	Karadeniz Technical University, Faculty of Sciences, Department of Chemistry
Prof. Esin Canel	Ankara University, Faculty of Sciences, Department of Chemistry
Prof. Dilek Ak	Anadolu University, Faculty of Pharmacy, Department of Basic Pharmaceutical Sciences

Prof. Mustafa K�uc�ukislamođlu	Sakarya University, Faculty of Science and Literature, Department of Chemistry
Prof. Salih Zeki Yildiz	Sakarya University, Faculty of Science and Literature, Department of Chemistry
Prof. Recai İnam	Gazi University, Faculty of Sciences, Department of Chemistry
Prof. Dr. Durıřehvar �nal	İstanbul University, Faculty of Pharmacy, Department of Basic Pharmaceutical Sciences
Prof. Mehmet T�ufek�i	Avrasya University, Faculty of Science and Literature, Department of Biochemistry
Prof. H�seyin Kara	Sel�uk University, Faculty of Sciences, Department of Chemistry
Prof. Sezgin Bakirdere	Yıldız Technical University, Faculty of Science and Literature, Department of Chemistry
Prof. Hasan Basri Őent�rk	Karadeniz Technical University, Faculty of Sciences, Department of Chemistry
Prof. Yusuf Atalay	Sakarya University, Faculty of Science and Literature, Department of Physics
Prof. Salih Zeki Yildiz	Sakarya University, Faculty of Science and Literature, Department of Chemistry

**Authorship, Originality, and Plagiarism:** The authors accept that the work is completely original and that the works of others have been appropriately cited or quoted in the text with the necessary permissions. The authors should avoid plagiarism. It is recommended that they check the article using appropriate software such as Ithenticate and CrossCheck. The responsibility for this matter rests entirely with the authors. All authors will be notified when the manuscript is submitted. If a change of author is needed, the reason for the change should be indicated. Once the manuscript is accepted, no author changes can be made.

### **Aims and Scope**

“Turkish Journal of Analytical Chemistry” publishes original full-text research articles and reviews covering a variety of topics in analytical chemistry. Original research articles may be improved versions of known analytical methods. However, studies involving new and innovative methods are preferred. Topics covered include:

- Analytical materials
- Atomic methods
- Biochemical methods
- Chromatographic methods
- Electrochemical methods
- Environmental analysis
- Food analysis
- Forensic analysis
- Optical methods
- Pharmaceutical analysis
- Plant analysis
- Theoretical calculations
- Nanostructures for analytical purposes
- Chemometric methods
- Energy

### **ETHICAL GUIDELINES**

TurkJAC follows ethical tasks and responsibilities are defined by the Committee on Publication Ethics (COPE) in publication procedure. Based on this guide, the rules regarding publication ethics are presented in the following sections.

#### **Ethical Approval**

Ethics committee approval must be obtained for studies on clinical and experimental regarding human and animals that require an ethical committee decision, this approval must be stated in the article and documented in the submission. In such articles, the statement that research and publication ethics are complied with should include. Information about the approval such as committee name, date, and number should be included in the method section and also on the first/last page of the article.

#### **Editors**

1. In the preliminary evaluation of a submission, the editor of the journal evaluates the article's suitability for the purpose and scope of the journal, whether it is similar to other articles in the literature, and whether it meets the expectations regarding the language of writing. When it meets the mentioned criteria, the scientific evaluation process is started by assigning a section editor if necessary.
2. A peer-reviewed publication policy is employed in all original studies, taking into full account of possible problems due to related or conflicting interests.

3. Section editors work on the articles with a specific subject and their suggestion is effective in the journal editor's decision about acceptance or rejection of the article.
4. No section editor contacts anyone except the authors, reviewers, and the journal editor about articles in the continued evaluation process.
5. In the journal editor's decision to accept or reject an article, in the addition of section editor's suggestion in consequence of scientific reviewing, the importance of the article, clarity and originality are decisive. The final decision, in this case, belongs to the journal editor.

### **Authors**

1. The authors should actively contribute to the design and execution of the work. Authorship should not be given to a person who does not have at least one specific task in the study.
2. Normally all authors are responsible for the content of the article. However, in interdisciplinary studies with many authors, the part that each author is responsible for should be explained in the cover letter.
3. Before the start of the study, it would be better to determine the authors, contributors, and who will be acknowledged in order to avoid conflict in academic credits.
4. The corresponding author is one of the authors of the article submitted to the journal for publication. All communications will be conducted with this person until the publication of the article. The copyright form will be signed by the corresponding author on all the authors' behalf.
5. It is unacceptable to submit an article that has already been published entirely or partly in other publication media. In such situation, the responsibility lies with all authors. It is also unacceptable that the same article has been sent to TurkJAC and another journal simultaneously for publication. Authors should pay attention to this situation in terms of publication ethics.
6. Plagiarism from others' publications or their own publications and slicing of the same study is not acceptable.
7. All authors agree that the data presented in the article are real and original. In case of an error in the data presented, the authors have to be involved in the withdraw and correction process.
8. All authors must contribute to the peer-reviewed procedure.

### **Reviewers**

1. Peer reviewers worked voluntarily are external experts assigned by editors to improve the submitted article.
2. It is extremely important that the referee performs the review on time so that the process does not prolong. Therefore, when the invitation is agreed upon, the reviewer is expected to do this on time. Also, the reviewer agrees that there are no conflicts of interest regarding the research, the authors, and/or the research funders.
3. Reviewers are expected not to share the articles reviewed with other people. The review process should be done securely.
4. Reviewers are scored according to criteria such as responding to the invitations, whether their evaluations are comprehensive and acting in accordance with deadlines, and the article submissions that they can make to TurkJAC are handled with priority.



# Contents

## Research Articles

- Validation of high-performance liquid chromatography method for the determination of doxorubicin in proliposomal drug delivery system formulation **1–10**  
*Mine Diril\*, Mehmet Ali Ege, H. Yeşim Karasulu*
- A comparative study of solvent effect on propolis extraction by ultrasound-assisted extraction **11–17**  
*Sevgi Kolaylı, Ceren Birinci\**
- Usability of calcite mineral, which develops in the crack fillings of carbonate rocks, as ornamental stone **18–24**  
*Murat Camuzcuoğlu*
- Investigation of antibiofilm and biological activities of *Vaccinium arctostaphylos* L. **25–31**  
*Uğur Kardil\*, Zeynep Akar, Azer Özad Düzgün*
- Validation study on spectrophotometric measurement of ethanol from beer and non-alcoholic beer samples distilled by micro steam distillation method **32–39**  
*Arda Akdoğan, Cemalettin Baltacı\**

## Reviews

- Voltammetric methods for determination of Allura Red AC in foods and beverages **40–49**  
*Elif Şişman, Fatma Ağım\**
- A comprehensive review on carbon quantum dots **50–60**  
*Mussarat JABEEN\*, Iqra Mutaza*



# Validation of high-performance liquid chromatography method for the determination of doxorubicin in proliposomal drug delivery system formulation

Mine Diril\* , Mehmet Ali Ege , H. Yeşim Karasulu 

Ege University, Faculty of Pharmacy, Department of Pharmaceutical Technology, 35100, İzmir, Türkiye

## Abstract

The objective of this study to develop a novel proliposome formulation containing Doxorubicin (Dox) and was to validate a sensitive and selective reversed-phase high-performance liquid chromatographic (HPLC) method for the evaluation of Dox concentrations of proliposome formulation. The samples were chromatographed on C18 column (Zorbax Eclipse Plus 5 $\mu$ m 4.6 x 250 mm) using a mobile phase with Sodium Lauryl Sulphate solution:Acetonitrile (50%:50%) at 254 nm. Linearity was confirmed in the concentration range of 10.0–75.0  $\mu$ g/mL. Specificity, linearity, working range, LOD, LOQ, accuracy, precision, robustness, and system suitability studies were done from HPLC validation parameters. Liposome formulation containing Dox was developed by pH gradient method then proliposome formulation was developed with lyophilisation technique. In the developed HPLC method, the encapsulation capacity (EE%) was found to be 90%  $\pm$  0.5 and the drug loading capacity (DL%) was found to be 100.0%  $\pm$  0.3. In vitro release studies and stability study results were evaluated with, validated HPLC method. It was observed that developed Dox-proliposome formulation increased Dox release at pH 5.5, pH 6.5, and pH 7.5 by 23.9%, 30.2%, and 14.8%, respectively, compared to commercial products. The result of F2 test performed in pH 7.5 media was 51.4%. According to the results of the physicochemical tests performed within the stability studies, it was observed that there was no significant change at the end of 12 months. These results show that the HPLC method developed, and validation study performed are important and applicable in the development, characterization, in vitro release, and stability studies of the novel proliposome formulation.

**Keywords:** Doxorubicin; proliposomal drug delivery systems; high-performance liquid chromatography; validation; in vitro release tests

## 1. Introduction

Doxorubicin (Dox) ([Fig. 1](#)) is a chemotherapeutic agent belonging to the anthracycline group [1,2]. Its primary mechanism of action is that Dox intervenes in DNA base pairs, causing DNA breakage, inhibiting both DNA and RNA synthesis. Dox inhibits topoisomerase II enzyme, causing DNA damage and induction of apoptosis and it is usually administered intravenously at 21-day intervals [3]. Side effects such as fatigue, hair loss, nausea and vomiting, and mouth sores are common after Dox administration, also associated with noteworthy cardiac toxicity so this limiting the long-term use of the drug [4,5]. Therefore, it is very important to develop formulations that will reduce the toxicity of Dox.

Lipids and fatty acids considered as the primary component of liposomes; They are structures that are considered biocompatible and biodegradable because they are found in the natural structure of cell membranes. Liposomes have become very interesting in recent years as they are versatile drug delivery systems

suitable for the encapsulation of both hydrophilic and hydrophobic substances. Moreover, these vesicular structures allow the encapsulation of both small ion-sized molecules and large molecules of several hundred thousand Daltons [6]. Liposomal encapsulation of drug molecules; it reduces systemic toxicity and improves tolerable dosing regimens for anticancer drugs. However, liposomes exhibit poor chemical and physical stability due to oxidation and hydrolysis of the lipids in their structure, which limits their shelf life.

Physical instability of the aqueous dispersion occurs due to vesicle aggregation and fusion of liposomes, leading to a change in vesicle size and leakage of the active substance. Chemical instability is associated with the tendency for hydrolysis and oxidation of phospholipids in liposomal drug delivery systems. Oxidation and hydrolysis of lipids can lead to the formation of short-chain lipids and subsequently less hydrophobic derivatives in the bilayers, resulting in the formation of liposomes with altered physicochemical

**Citation:** M. Diril, M.A. Ege, H.Y. Karasulu, Validation of high-performance liquid chromatography method for the determination of doxorubicin in proliposomal drug delivery system formulation, Turk J Anal Chem, 6(1), 2024, 1–10.

 <https://doi.org/10.51435/turkjac.1433347>

**Author of correspondence:** [mine.diril@gmail.com](mailto:mine.diril@gmail.com)

**Received:** February 7, 2024

**Tel:** +90 (232) 311 39 81

**Accepted:** April 5, 2024

**Fax:** +90 (232) 388 52 58

properties or disruption of the liposome structure and alteration of the drug release profile [7–9]. Therefore, removal of water in their structure can reduce or completely eliminate both hydrolysis and oxidation reactions [7]. Proliposome drug delivery system formulations have been developed to overcome the stability problems associated with the liposome [8]. Proliposomes are dry, free-flowing granular products that form liposomal dispersion on hydration or contact with biological fluids in the body and were discovered in 1986. They consist of water-soluble porous powder and phospholipids [9–11]. Proliposomes can be obtained by various methods such as fluidized bed method, supercritical anti-solvent method, lyophilization method [12].

The development and validation of analytical methods play important roles in the discovery, development, production, and stability monitoring of pharmaceuticals. The main purpose of the analytical method development and validation is to prove that proposed analytical method is accurate, specific, precise, and robust in the pharmaceutical industry for drugs. Therefore, analytical methodology development and validation has become essential activity for the development of new drug delivery systems [13,14]. Studies involving methods developed in recent years for the determination of Dox from drug delivery systems are listed in Table 1.

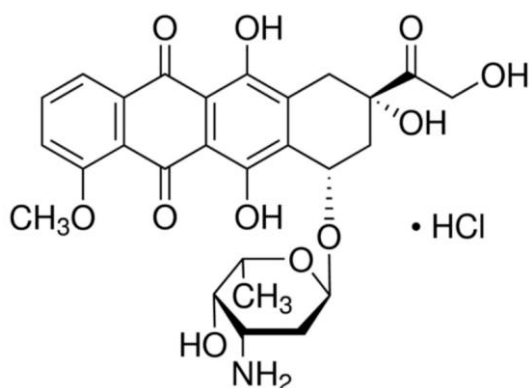


Figure 1. Doxorubicin-HCl chemical structure [15]

In this study, HPLC method was developed and validated to determine drug loading capacity, encapsulation capacity, evaluated *in vitro* release studies for different pH (pH 5.5, pH 6.5, and pH 7.5) and determined stability studies of Dox in the developed novel proliposome formulation. While HPLC methods were recommended for the determination of Doxorubicin in the developed liposome formulation containing Dox, no study was found in which Dox validation parameters were applied to the proliposome formulation and the results were shared in detail. Our study will contribute to the literature in this respect.

Table 1. List of quantification methods for Dox in pharmaceutical drug delivery systems last years

	Method	Purpose	Year Ref.
Rus et al.	UV-Vis	Dox Evaluation From Drug Delivery Systems	2021 [16]
Laxmi et al.	HPLC	Dox Determination Co-crystal	2019 [17]
Scheeren et al.	HPLC	Determine Dox in pH-sensitive chitosan nanoparticles	2018 [18]
Du et al.	HPLC	Dox Evaluation From Gold Nanoparticles	2018 [19]
Gowda et al.	RP-HPLC	Determination of Dox in Pure and Pharmaceutical Dosage Forms	2017 [20]

## 2. Experimental

### 2.1. Chemical and reagents

Doxorubicin hydrochloride (Dox) (99.8% purity) was selected as the active pharmaceutical ingredient donated from by DEVA Holding (Istanbul, Türkiye). Hydrogenated Soy L- $\alpha$ -phosphatidylcholine (HSPC), 1,2-distearoyl-sn-glycero-3-phosphocholine (DSPG), Cholesterol and 1,2-distearoyl-sn-glycero-3-phosphoethanolamine-N-[carboxy(polyethylene glycol) (DSPE-PEG(2000) Carboxylic Acid) were obtained from Avanti Polar Lipids (Birmingham, United States). Mannitol was obtained from Roquette (Lestrem, France). Sodium Lauryl Sulphate and ortho-phosphoric acid were purchased from Sigma (Burlington, United States). HPLC-grade acetonitrile was obtained from Carlo Erba (Val-de-Reuil, France). All chemicals used throughout the study were pharmaceutical grade or special analytical grade. Ultrapure water for all analyses was purified using the Millipore Direct-Q® 3 Water Purification System.

### 2.2. Instrumentation and analytical conditions

The HPLC-PDA system consisted of Shimadzu model of LC-20AT and PDA detector in series connected to a computer loaded with, LC Solution post-run programme (Duisburg, F.R. Germany). The chromatographic separation was performed on an Agilent Zorbax Eclipse Plus -C18 analytical column (150 mm  $\times$  4.6 mm, 5  $\mu$ m particle size, and 100 Å pore size). In addition, PDA detector was set at 254 nm. For the mobile phase, 2.88 grams of Sodium Lauryl Sulphate was weighed accurately and dissolved by adding approximately 990 mL of ultrapure water. The pH was adjusted to 2.5 by adding ortho-phosphoric acid and completed with water to a volume of 1000 mL. Acetonitrile was mixed with 50%-50% (v/v) of this solution and degassed in an ultrasonic bath for 10 minutes. The solution was filtered through a 0.2  $\mu$ m membrane filter. For the analysis, isocratic solvent elution was performed at a flow-rate of 1 mL/min. The column temperature was maintained at 25 °C and the injection volume was 5  $\mu$ L. On each day of

analysis, mobile phase flow was allowed from the column to equilibrate for 30 minutes.

### 2.3. Preparation and characterization of proliposome formulation

Liposome formulation was developed by a lipid hydration method and proliposome formulation was developed by lyophilisation technique. Because of Dox showed weak basic properties, pH gradient method was used to highly encapsulate the Dox in the liposome formulation [21,22]. Citric acid-sodium citrate buffer and 4-(2-hydroxyethyl)-1-piperazineethanesulfonic acid buffer systems (HEPES) were used to create the pH gradient method. Details of the liposome formulation developed by the lipid hydration method by creating a pH gradient are stated in the publication of the study by Mine et al [23]. Mannitol as lyoprotectant was added to the liposome dispersion and dissolved. Proliposome formulation was obtained by applying the lyophilisation. The liposome formulation samples were frozen at -65 °C. They were then subjected to gradual heating to 20 °C at 0.01 mbar pressure for 18 hours for primary drying in a lyophilization device. Secondary drying was carried out for 3 hours at 25 degrees Celsius under 0.01 mbar pressure. Characterization studies such as pH, viscosity, particle size (PS), polydispersity index (PDI), zeta potential (ZP), water content % and reconstitution time of proliposome formulation were performed. All analyses were carried out by dispersing, except water content, developed proliposome formulation in 5% dextrose solution ( $C_{\text{Dox}}=2$  mg/mL). The pH of Dox-proliposome formulation was measured using pH meter (Mettler Toledo, Switzerland) and viscosity was measured at  $37 \pm 1$  °C by using Ula spindle in a viscometer (Brookfield DVII + Pro, USA). The PS, PDI, and ZP values of the Dox-proliposome formulation were determined by using zetasizer (Malvern Nano ZS, England) device at room temperature ( $25 \pm 2$  °C). The water content of formulation was evaluated by Karl Fischer titration instrument (SI Analytics 7500, Germany). For reconstitution time analysis, the time taken for the developed Dox-proliposome formulation to be dispersed in 5% dextrose solution was observed with a stopwatch.

### 2.4. Preparation of Standard solutions and samples

#### 2.4.1. Stock standard solution

20 mg of Dox working standard was weighed accurately and transferred to a 100 mL flask, made up to volume with mobile phase, and mixed by shaking (main stock solution). 2.5 mL of this solution was taken and transferred to a 10.0 mL flask. For encapsulation efficiency and drug loading capacity, it was made up to volume with the same solvent and mixed by shaking. To

evaluate in vitro release studies, it was made up to volume with pH 5.5, pH 6.5, and pH 7.5 phosphate buffer, separately. They were filtered through a 0.20  $\mu\text{m}$  PTFE membrane filter (Sartorius Minisart SRD, Germany) then injected into the HPLC ( $C_{\text{Dox standard}} = 50$   $\mu\text{g/mL}$ ).

#### 2.4.2. Sample Proliposome solution preparation

To extract the drug from the proliposomal matrix, formulations were first mixed with 5 mL mobile phase then sonicated for 10 min. Then the solution was made up to 10 mL with mobile phase to a concentration of 50  $\mu\text{g/mL}$ . The sample was filtered through a 0.20  $\mu\text{m}$  PTFE membrane filter and injected HPLC. For the specificity parameter, placebo samples were prepared. Dox-free proliposome formulations were transferred to a 10 mL flask. Dox-free proliposome formulations were first mixed with 5 mL mobile phase and then sonicated for 10 min. The final solution was made up to volume with the mobile phase to a concentration of 50  $\mu\text{g/mL}$ . They were filtered through a 0.20  $\mu\text{m}$  PTFE filter and injected into the HPLC.

### 2.5. Validation of the HPLC method

The method has validated the requirements of the International Council for Harmonisation Q2(R2) guidelines. For this purpose, specificity, linearity, working range, accuracy, precision, robustness, and system suitability parameters were studied [24]. For the specificity parameter; Dox standard solution, unloaded proliposome formulation (placebo) solution, and doxorubicin-loaded proliposome (Dox-proliposome) formulation solution were injected. All peaks purity was analysed by PDA detector.

The linearity analysis was established through preparation of six concentration levels of standard linearity curve in the concentration range of 10.0–75.0  $\mu\text{g/mL}$  ( $n=3$ ). The calibration curve was plotted using the average of area versus known concentration. In order to evaluate in vitro release studies and to observe the effect of buffer solutions (pH 5.5, pH 6.5, and pH 7.5) to be used in the release medium, these buffer solutions were used as dilution solutions, and linearity, LOD, LOQ, and working range parameters were validated. Linearity assessment was done by the analysis of relative standard deviation of the slope ( $S_b\%$ ), y-residuals and correlation coefficient ( $r^2$ ) at a confidence level of 95%.

The LOD and LOQ were evaluated from the signal-to-noise ratio of chromatograms for blank samples ( $S/N=3$  for LOD and  $S/N=10$  for LOQ). Then it was expressed in concentration of via the relation with the signal-to-noise ratio of a 10.0  $\mu\text{g/mL}$  spiked blank [25]. For the working range analysis, six injections were studied with lowest concentration 10.0  $\mu\text{g/mL}$  and as highest concentration

of 75.0 µg/mL (for mobile phase, pH 5.5, pH 6.5, pH 7.5, separately). In addition, RSD% was evaluated for solvents.

Accuracy is the nearness of a measured value to the true or accepted value. Accuracy was evaluated by the standard addition method with placebo solutions. For the accuracy analysis; Dox-proliposome formulation solution samples were prepared at 80%, 100%, and 120% levels of assay test concentration and calculated recovery. A total of 9 samples were prepared, 3 for each level. The recovery% calculation is given in Equation 1.

$$\text{Recovery, \%} = \frac{\text{Concentration of analysis results}}{\text{Theoretical concentration}} \times 100 \quad (1)$$

The precision of the method was determined by intraday and interday studies. After the system suitability check with six standard solution injections, repeatability was performed by analyzing six samples of Dox-proliposomal formulation at the same concentration (50 µg/mL). The intermediate precision was evaluated by performing the analysis on two different days (interday) and also by different operators performing the analysis (interanalyst). For precision analysis, the standard deviation must be less than 2.0%.

The robustness of an analytical method indicates its ability to remain unaffected by small changes made in the parameters of the analytical method. For robustness study, one standard and two sample solutions were prepared. For each changed condition, six injections of the standard solution and two injections of the sample solutions were analyzed. These minor changes for method were mobile phase buffer pH ( $\pm 0.2$ ), flow rate ( $\pm 0.1$  mL/min), and column temperature ( $\pm 5$  °C). Theoretical plate number, retention time, and tailing factor were observed for each condition. RSD% of Dox assay between normal and modified working conditions were evaluated.

System suitability was determined from six replicate injections of standard solution containing 50 µg/mL of Dox. For the acceptance criteria; relative standard deviation (RSD%) was found less than 2% for peak area and retention time, greater than 2000 theoretical plates number, and tailing factor of less than 2.0 [26].

## 2.6. Studies with validated analytical method

### 2.6.1. Drug loading capacity.

Extraction of Dox encapsulated in proliposomal vesicles is important for the determination of drug loading capacity. For this purpose, an aliquot of the Dox-proliposome formulation was diluted in 5 mL mobile

phase and sonicated for 10 min to extract the drug. The final solution was made up to 10 mL with the mobile phase at a concentration of 50 µg/mL. It was calculated relative to a reference solution of the same concentration and represents the total drug content in the formulations.

### 2.6.2. Encapsulation efficiency

Encapsulation efficiency (EE%) of proliposome formulations was found by ultracentrifugation technique with Amicon Ultra 100 kDa EMD-Millipore (Billerica, MA). The unencapsulated drug was separated by ultrafiltration technique (Sigma 2-16P Centrifuge, Sigma, Germany) at 5000 rpm for 40 min. EE% was evaluated as the ratio of the analyzed drug amount to the initial drug amount using the HPLC method [27].

### 2.6.3. In vitro release study

The release conditions recommended by FDA in liposomal formulations containing Dox are pH 5.5 as endosomes and lysosomes of cancer cells, pH 6.5 as cancer tissues and pH 7.5 as normal tissues [28]. In vitro release studies were performed at different pH phosphate buffers (pH 5.5, pH 6.5, and pH 7.5) conditions using the dialysis membrane method. Proliposomal formulation was dispersed 5% dextrose solution ( $C_{\text{Dox}} = 2$  mg/mL) put in dialysis bag (Sigma-Aldrich, 14,000 Da molecular weight cut-off) and the dialysis bags were put into 100 mL of pH 5.5, pH 6.5 and pH 7.5 phosphate buffer solution, respectively. The systems were maintained at 47 °C in a stirred water bath at 100 rpm. 2 mL of samples were taken at predetermined time intervals (0, 0.5, 1, 2, 3, 6, 8, 12, 20, and 24 h) and then added with 2 mL of fresh buffer to maintain constant volume and sink conditions. Studies were also performed for commercial products. Calculation of the cumulative quantification of Dox was performed by HPLC method. To evaluate the effect and release results of the different release media used, the method was co-validated for linearity and working range using release media (PBS pH 5.5, 6.5, and 7.5) as diluent [18,29]. In addition, F2 similarity analysis was performed between the commercial product and the Dox-proliposome formulation.

### 2.6.4. Stability study

The stability of Dox-proliposomal formulation was investigated at  $5 \pm 3$  °C,  $25 \pm 2$  °C,  $60\% \pm 5$  relative humidity,  $30 \pm 2$  °C,  $65\% \pm 5$  relative humidity, and  $40 \pm 2$  °C,  $75\% \pm 5$  °C relative humidity. The sample was evaluated for physicochemical properties (pH, viscosity, PS, PDI, ZP, EE%, DL%, water content % and reconstitution time) under these stability conditions.

## 2.7. Statistical analysis

Student-t test or ANOVA variance analysis for parametric tests and Krusger Wallis analysis for nonparametric tests were preferred. \* $p < 0.05$  and \*\*\* $p < 0.001$  were considered significant and highly significant, respectively.

## 3. Results and Discussion

### 3.1. Preparation and characterization of proliposome formulation

The ratios of lipids, cholesterol, and pegylating agent were determined according to the pegylated liposomal commercial formulation containing of the active ingredient Dox (mol ratios phospholipid%:cholesterol%:pegylating agent%; 56:38:5) [30]. The physicochemical properties of Dox-proliposome formulation were done dispersed 5% dextrose solution, except the water content, and the results of physicochemical properties are shown Table 2. PDI is a measure of the heterogeneity of a sample based on size and distribution [31]. In addition, less than 0.5 PDI value indicates homogenous and stable particles [32]. The freeze thaw cycle enables the conversion of liposomal vesicles from MLVs to SUVs (Small unilamellar Vesicles) and Large Unilamellar Vesicles (LUVs), thus affecting PS and PDI results, while the extrusion process affects PS results [33]. As seen from the physicochemical results, low PS and acceptable PDI results were obtained, indicating that the extrusion and freeze thaw cycle processes applied to the Dox-proliposome formulation were successful. By lyophilizing liposomal formulations; hydrolysis, oxidation, drug leakage, and aggregation can be

prevented by removing aqueous structures from formulations [34].

In lyophilization, substances that protect formulations from stress conditions during freezing and drying are known as lyoprotectants. During the lyophilization phase of liposomal drug delivery systems, lyoprotectants maintain the stability of liposomes by protecting the lateral spaces of the head groups of phospholipids [35]. Mannitol, a lyoprotectant, is one of the excipients frequently used in liposomal drug carrier systems, which reduces redistribution time by providing cake formation after drying [36]. For this purpose, effective drying studies were carried out using Mannitol as a lyoprotectant in the study.

Effective drying accelerates the dispersion of particles and reduces the reconstitution time. Also, since the water contained in liposomes causes hydrolysis and oxidation, effective drying is very important to ensure stability [37]. In addition, water content analysis is very important to predict whether efficient drying is achieved by lyophilisation. The results of low water content and fast reconstitution time indicate that efficient drying was achieved by lyophilization in Dox-proliposome formulation.

**Table 2.** Physicochemical properties of Dox-proliposome formulation

Physicochemical properties	Results $\pm$ SD
pH	6.50 $\pm$ 0.95
Viscosity (cP)	12.63 $\pm$ 1.25
PS (nm)	120.6 $\pm$ 2.50
PDI	0.35 $\pm$ 0.21
ZP (mV)	-8.45 $\pm$ 1.25
Water Content (%)	0.053 $\pm$ 0.03
Reconstitution time (sec)	11.5 $\pm$ 1.1

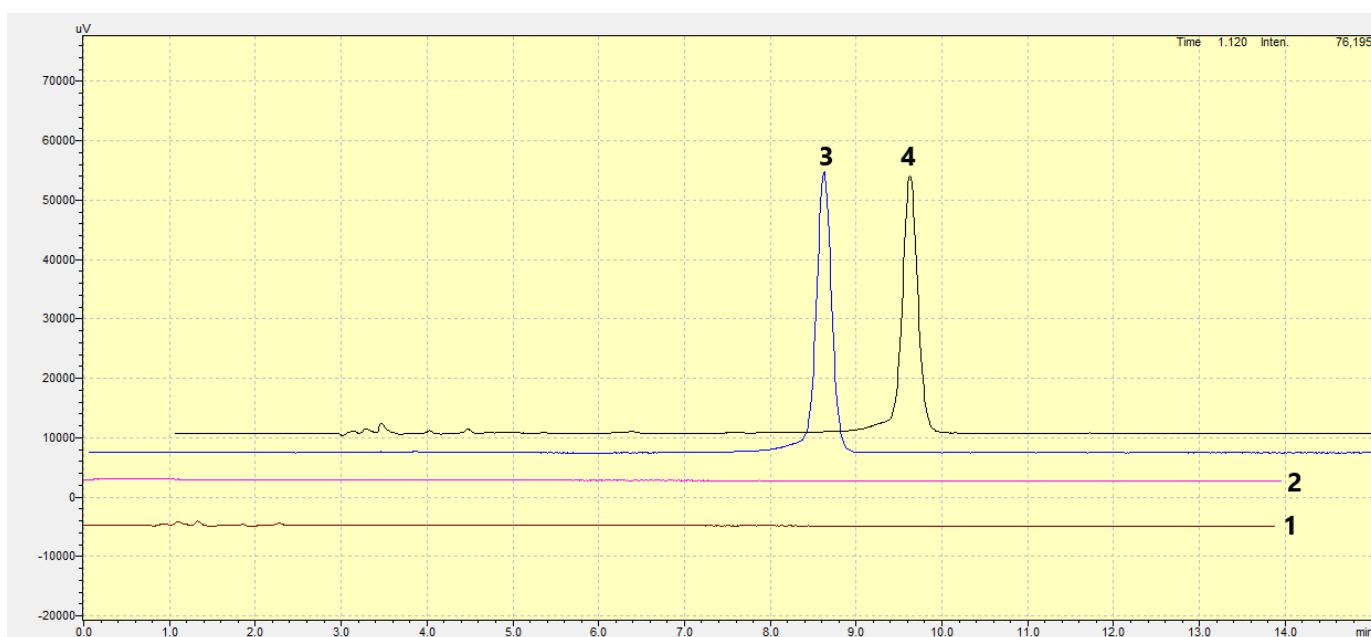


**Figure 2.** HPLC chromatograms from specificity parameter injection on HPLC where trace (1) represents unloaded proliposome formulation solution, (2) represents mobile phase, (3) represents Dox standard solution (10  $\mu\text{g}/\text{mL}$ ), (4) Dox-proliposome formulation solution

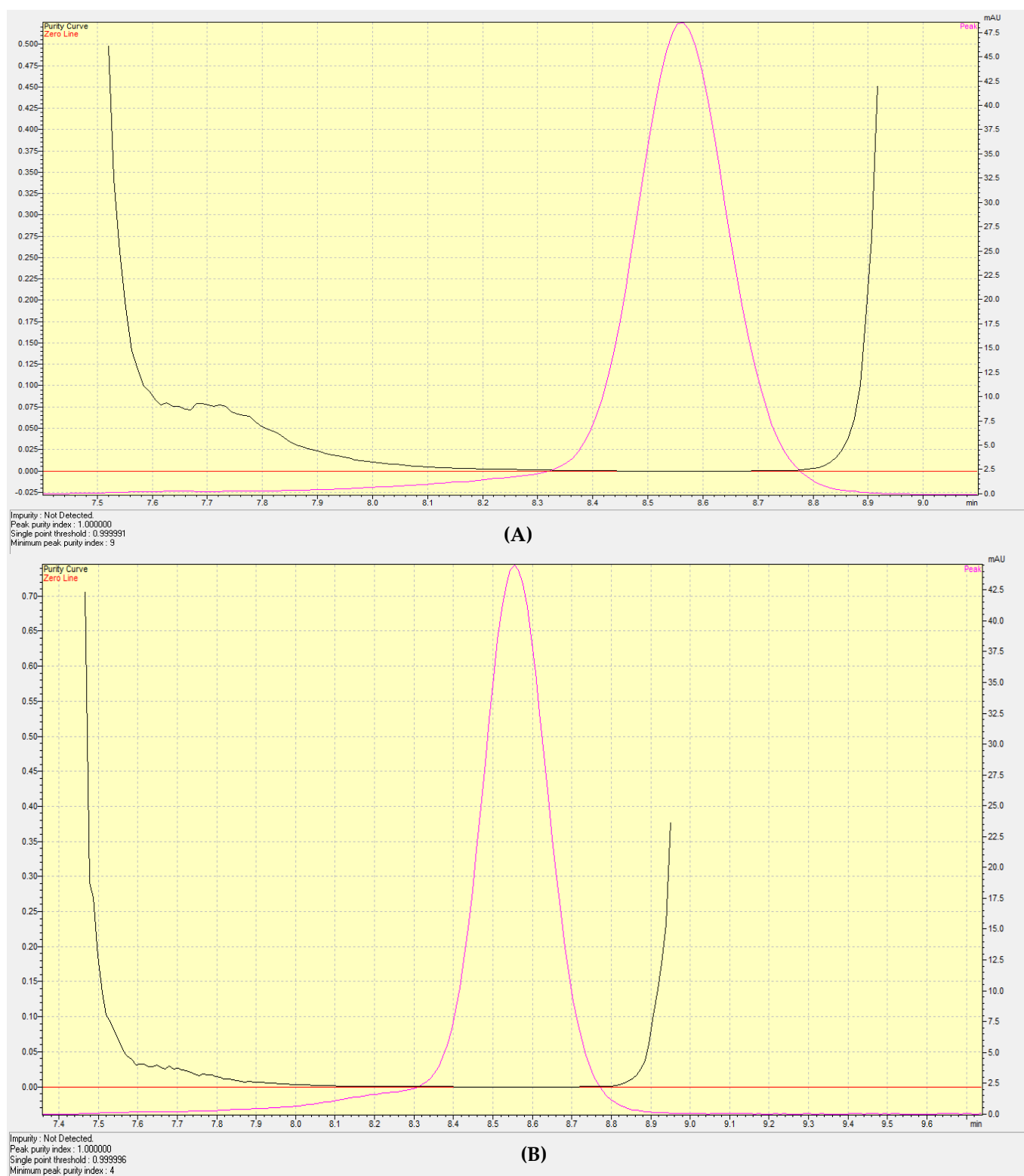


Figure 3. Peak purity of (A) Dox in standard solution, (B) Dox-proliposome formulation solution

### 3.2. Validation of the method

The specificity of the method for the quantitation of Dox was successfully achieved by demonstrating that there was no interference from the matrix components. The chromatograms (Fig. 2) showed that no signal was detected for the mobile phase and unloaded proliposome formulation solution. In order to show no interference in the HPLC method, peak purity testing was performed using PDA detector.

The peak purity index of chromatograms was evaluated for Dox standard and Dox-proliposome solutions and was higher than 0.9999. This indicates that there is no interference to the Dox peak from excipients or impurities. All these findings indicate that the method is specific (Fig. 3).

The data for the analytical curves constructed ( $n=3$ ) suggest acceptable linearity parameter of concentration range of 10 – 75  $\mu\text{g/mL}$  for mobile phase, pH 5.5, pH 6.5,

and pH 7.5, respectively. The linear regression equation was determined by the least squares method and thus the correlation coefficients were calculated, these results are shown in Table 3. LOD and LOQ were calculated using mobile phase, pH 5.5, pH 6.5 and pH 7.5 as solvent and the results are given in Table 3.

For the operating range analysis, the RSD% results of six injections at 10 µg/mL and 75 µg/mL in each solvent medium were calculated and the results are given in Table 4. Acceptance criterion of RSD% <2% was achieved.

Values between 98% and 102% are acceptable for accuracy analysis [38]. The recovery results for the accuracy parameter were between 98% and 102% for each concentration, with an RSD% of <2%, achieving the acceptance criterion (80%, 100%, and 120%) (Table 5).

For the precision parameter six different Dox-proliposome formulations batches, containing 50 µg/mL Dox, were extracted as part of the repeatability study and analysed. In the intermediate precision study performed as part of the precision parameter, six separate proliposome formulation samples were studied on two separate days and by two separate analysts. The results are shown in Table 5 and the RSD values obtained are lower than the 2.0% acceptance criterion.

The robustness test demonstrates the reliability of the analytical method against certain changes in parameters [39]. The method was considered robust because RSD% values for Dox assay were below 2% as seen in Table 6. System suitability tests represent an integral part used to ensure adequate performance of the analytical procedure and the chromatographic system for resolution and reproducibility [40]. For system suitability analyses, RSD% values calculated for the peak area, retention time and tailing factor were found 1.28, 0.11, 0.43, and 0.02%, respectively. The number of theoretical plates was found 16601.68 and RSD% 0.43%.

The data of all parameters performed in method validation studies were found within the acceptance criteria. This shows that the method can be applied successfully and is suitable for the analyses to be carried out. The advantages of these developed methods compared to the method in this study are evaluated in Table 7.

### 3.3. Studies with validated analytical method

As with all drug delivery systems, it is very important to achieve high drug loading capacity and encapsulation capacity in liposomal drug delivery systems during formulation development. To achieve optimum efficacy in a drug delivery system, it is necessary to encapsulate the maximum possible amount of toxic active substances, especially as Dox.

**Table 3.** Linearity, LOD, and LOQ results (Concentration range: 10–75 µg/mL)

Solutions	Equations	R <sup>2</sup>	LOD (µg/mL)	LOQ (µg/mL)
Mobile phase	$y = 12180037.469x + 7767.114$	0.9996	1.5	4.6
pH 5.5	$y = 12240914.436x - 3262.502$	0.9999	0.7	2.2
pH 6.5	$y = 12016875.912x + 629.902$	0.9994	1.9	5.6
pH 7.5	$y = 9785246.7153x - 10345.3163$	0.9996	0.8	2.3

**Table 4.** Working range analysis RSD% results for solvents

Concentration (µg/mL)	RSD%			
	Mobile phase	pH 5.5	pH 6.5	pH 7.5
10	0.7	0.7	0.2	0.8
75	0.1	0.2	0.1	0.5

**Table 5.** Repeatability, accuracy, and intermediate precision data of Dox-proliposome formulation solution

Validation parameters		Recovery ± RSD (%)
<b>Accuracy (n=3)</b>		
40 µg/mL		100.33 ± 0.85
50 µg/mL		100.73 ± 0.76
60 µg/mL		99.57 ± 0.35
<b>Precision</b>		
Intraday (n=6)		101.00 ± 1.2
Interday		
Day 1 (n=6)		99.60 ± 0.56
Day 2 (n=6)		99.30 ± 1.21
Mean (n=12)		99.45 ± 0.21
Between-analysts		
Analyst 1 (n=6)		100.23 ± 0.74
Analyst 2 (n=6)		99.56 ± 0.96
Mean (n=12)		99.90 ± 0.47

**Table 6.** Results of robustness parameter for Dox-proliposome formulation solution

Chromatographic parameter	Theoretical plates	Retention time (min)	Tailing Factor	Dox Assay (%)
Normal working condition	16459	8.2	0.94	99.7
pH 2.3	14599	7.9	0.96	98.3
pH 2.7	15340	8.2	0.93	99.4
Flow rate 0.9 mL/min	16229	8.4	0.94	99.1
Flow rate 1.1 mL/min	15322	8.1	0.96	99.2
Column temperature 20° C	16521	8.3	0.95	98.8
Column temperature 30° C	16673	8.1	0.96	98.6
Mean				99.0
RSD(%)				0.49

**Table 7.** Advantages of the method developed in this study compared to the literature

Advantages	
Scheeren et al. [18]	They showed similar retention times and peak shapes, but were studied with a higher injection volume (20 µl) than our method. Long use may cause peak shape distortion and low theoretical plate count.
Gowda et al. [20]	Retention time is 3 minutes. This is very close to the dead time and may increase the possibility of overlapping with possible peaks over time in stability studies.



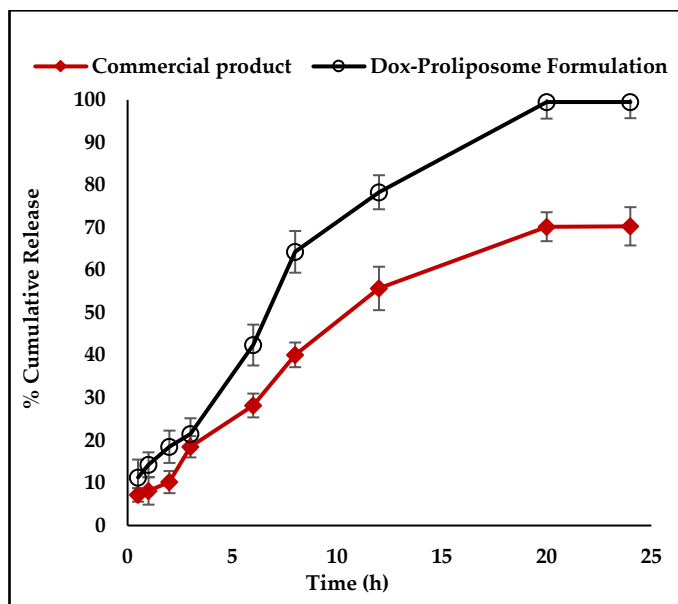


Figure 4. In vitro release of Dox from commercial product and Dox-proliposome formulation at pH:5.5

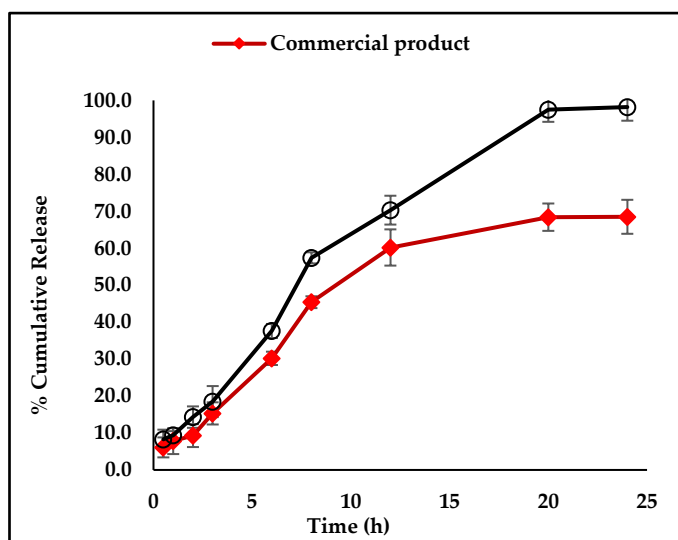


Figure 5. In vitro release of Dox from commercial product and Dox-proliposome formulation at pH:6.5

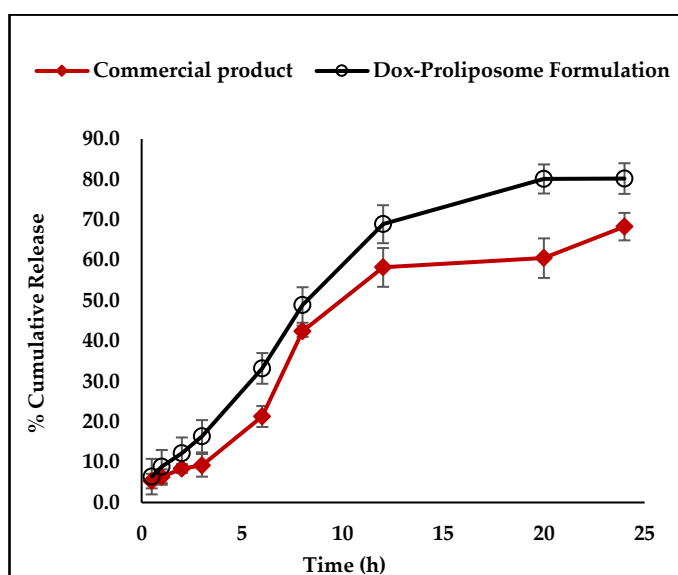


Figure 6. In vitro release of Dox from commercial product and Dox-proliposome formulation at pH:7.5

Dox encapsulated in liposome vesicles with high encapsulation efficiency provides high antitumor efficacy by altering tissue distribution and pharmacokinetics while reducing toxicity [41]. The drug loading capacity and encapsulation capacity of the proliposome formulation were determined during the development of the proliposome formulation with the validated HPLC method. The drug loading and encapsulation capacity of the developed optimal proliposome formulation were  $90\% \pm 0.5$  and  $100.0\% \pm 0.3$ , respectively ( $n=6$ ). RSD% were lower than 2.0% of each sample. In the study presented by Aghdam et al., which achieved high encapsulation into liposomal drug carrier systems with the pH gradient method, it was shown that clearance from the body could be reduced by 2.5 times with Dox [42]. This shows that liposomal Dox formulations, which can provide high encapsulation for in vitro studies, may be promising drug delivery systems in the in vivo environment. In addition, linearity and working range analyses were carried out to observe the effect of pH change in the in vitro release studies to be performed with the HPLC method developed. Dox assays of in vitro release studies performed in pH 5.5, pH 6.5 and pH 7.5 media were evaluated with linearity equations performed with these media for commercial product and Dox-proliposome formulation (Table 3). The release graphs of pH 5.5, pH 6.5, and pH 7.5 are given in Fig. 4, Fig. 5, and Fig. 6, respectively. It was observed that drug release increased because low pH values increase the hydrophilicity of Dox and its solubility in the liposome [43]. Similar to our study, in the study conducted by Mohammadi et al., higher release was observed at pH 5.5 compared to pH 7.4 for the developed liposomal formulations [44]. Therefore, Dox showed the highest release at pH 5.5 at the end of the 24th hour in the commercial product and the developed Dox-proliposome formulation. With the developed Dox-proliposome formulation, the release at the end of 24 hours was increased by 23.9%, 30.2%, and 14.8% at pH 5.5, pH 6.5, and pH 7.5, respectively, compared to the commercial product. The difference in vitro release values of the developed Dox-proliposome formulation compared to the commercial product may be due to the different lipids used in the developed proliposome formulation [45]. The lipid differentiation used can result in a change in the glass transition temperature, resulting in different release rates and kinetics [46]. In addition, due to the membrane-induced barrier effect of the vesicles in liposomal drug delivery systems, the release of the active substance occurs more slowly and in a controlled than the release of the active substance [47]. Obtained in vitro release results; the commercial product and the developed proliposomal drug delivery system formulation have shown that

controlled drug release is similar to the literature data [48,49].

In addition, according to the F2 similarity test between the commercial product and the developed Dox-proliposome formulation, the results in pH 5.5, pH 6.5, and pH 7.5 environments were found to be 37.5, 42.0, and 51.4, respectively. The fact that the F2 value between the two release profiles is between 50-100 indicates similarity by the FDA. [50]. F2 similarity ratio of Dox-proliposome formulation and commercial product in pH 7.5 medium was found to be 51.4% and it was found to comply with FDA similarity requirement. At 5.5 and 6.5, in vitro release profiles were not found to be similar to the commercial formulation, however, it was shown in Fig. 4 and Fig. 5 that the developed proliposome formulation was released more rapidly and in a controlled release than the commercial product in environments mimicking endosome and lysosomes of cancer cells (pH 5.5), cancer tissues (pH 6.5).

Moreover, there was no significant change in the results of the physicochemical analyses performed at all stability conditions to evaluate the stability for 12 months. This shows that the stability problem observed in liposomal drug delivery systems can be avoided with the developed proliposome formulations.

#### 4. Conclusion

The results of the study show that the proliposome formulation containing Dox was successfully developed and validation of Dox by HPLC was performed by the acceptance criteria. Altogether, the results showed that the validated HPLC method for the developed novel Dox-proliposome formulation is a suitable tool for the determination of drug loading capacity, determination of encapsulation capacity, measurement of release properties in different pH media, and evaluation of stability studies. In conclusion, the developed assay method and its validation have shown that promising results can be achieved at every stage of the development of the novel proliposome formulation and have greatly contributed to the study.

#### References

- [1] A.F. Yu, A.T. Chan, Steingart RM, Cardiac Magnetic Resonance and Cardio-Oncology: Does T 2 Signal the End of Anthracycline Cardiotoxicity, *J Am Coll Cardiol* 73(7), 2019, 792–4.
- [2] G. Marcq, E. Jarry, I. Ouzaid, J. Hermieu, F. Henon, J.C. Fantoni and E. Xylinas, Contemporary best practice in the use of neoadjuvant chemotherapy in muscle-invasive bladder cancer, *Therapeutic Advances in Urology*, 11, 2019, 1–8.
- [3] M. Kciuk, A. Gielecinska, S. Mujwar, D. Kołat, Z. Kałuzinska-Kołat, I. Celik, R. Kontek, Doxorubicin—An Agent with Multiple Mechanisms of Anticancer Activity, *Cells*, 659 (12), 2023, 1–30.
- [4] A.Z. Luu, B. Chowdhury, M. Al-Omran, H. Teoh, D.A. Hess, S. Verma, Role of Endothelium in Doxorubicin-Induced Cardiomyopathy, *JACC Basic to Transl Sci*, 3(6), 2018, 861–70.
- [5] M. Picpicz, V. Demján, M. Sárközy, T. Csont, Effects of cardiovascular risk factors on cardiac STAT3, *Int J Mol Sci*, 19(11), 2018, 1–29.
- [6] J. Shaji, V. Bhatia, Proliposomes: A brief overview of novel delivery system, *Int J Pharma Bio Sci*, 4(1), 2013, 150–60.
- [7] N.I. Payne, C.V. Ambrose, P. Timmins, M.D. Ward, F. Ridgway, Proliposomes: A novel solution to an old problem, *J Pharm Sci*, 75(4), 1986, 325–9.
- [8] D. Chordiya, S. Shilpi, D. Choudhary, Proliposomes: a potential colloidal carrier for drug delivery applications, *Advances in Pharmaceutical Product Development and Research*, 2020, 581–608.
- [9] K.Y. Janga, R. Jukanti, A. Velpula, S. Sunkavalli, S. Bandari, P. Kandadi, P.R. Veerareddy, Bioavailability enhancement of zaleplon via proliposomes: Role of surface charge. *Eur J Pharm Biopharm*, 80(2), 2012, 347–57.
- [10] C. Chu, S.S. Tong, Y. Xu, L. Wang, M. Fu, Y.R. Ge, J.N. Yu, X.M. Xu, Proliposomes for oral delivery of dehydrosilymarin: Preparation and evaluation in vitro and in vivo, *Acta Pharmacol Sin*, 32(7), 2011, 973–80.
- [11] N. Singh, P. Kushwaha, U. Ahmad, M. Abdullah, Proliposomes : An Approach for the Development of Stable Liposome Proliposomes: Una aproximación para el desarrollo de liposoma estables, *Ars Pharm*, 60(4), 2019, 231–40.
- [12] S. Muneer, Z. Masood, t S. But, S. Anjum, H. Zainab, N. Anwar, et al., Proliposomes as Pharmaceutical Drug Delivery System : A Brief Review Nanomedicine & Nanotechnology Proliposomes as Pharmaceutical Drug Delivery System : A Brief Review, 2017.
- [13] M. Doltade, R. Saudagar, Analytical Method Development and Validation: a Review, *Int J Pharm Biol Sci Arch*, 9(3), 2019, 563–70.
- [14] S. Sharma, S. Goyal, K. Chauhan, A review on analytical method development and validation, *Int J Appl Pharm*, 10(6), 2018, 8–15.
- [15] A. Rahdar, Hajinezhad, H. Hamishekar, A. Ghamkhari, G.Z. Kyzas, Copolymer/graphene oxide nanocomposites as potential anticancer agents, *Polym Bull*, 78(9), 2021, 4877–98.
- [16] I. Rus, M. Tertiş, V. Paşcalău, C. Pavel, B. Melean, M. Suci, C. Moldovan, T. Topală, C. Popa, R. Săndulescu, C. Cristea, Simple and fast analytical method for the evaluation of the encapsulation and release profile of doxorubicin from drug delivery systems, *Farmacia*, 69(4), 2021, 670–81.
- [17] P. Laxmi, A. Varma, A. Pai, M.B. Sathyanarayana, Experimental data of fabricated co-crystals of doxorubicin HCl with flavonoids, *Indian J Pharm Educ Res*, 53(3), 2019, S225–30.
- [18] L.E. Scheeren, D.R. Nogueira-Librelotto, J.R. Fernandes, L.B. Macedo, A.I.P. Marcolino, M.P. Vinardell, C.M.B. Rolim, Comparative Study of Reversed-Phase High-Performance Liquid Chromatography and Ultraviolet-Visible Spectrophotometry to Determine Doxorubicin in pH-Sensitive Nanoparticles, *Anal Lett*, 51(10), 2018, 1445–63.
- [19] Y. Du, L. Xia, A. Jo, R.M. Davis, P. Bissel, M.F. Ehrlich, et al, Synthesis and Evaluation of Doxorubicin-Loaded Gold Nanoparticles for Tumor-Targeted Drug Delivery, *Bioconjug Chem*, 29(2), 2018, 420–30.
- [20] Gowda BG, Hanumanthanaik D. Development and Validation of RP-HPLC Method for the Determination of Doxorubicin Hydrochloride in Pure and Pharmaceutical Dosage Forms, *Int J Adv Technol Eng Sci*, 2017, 5(6), 323–9.
- [21] J. Lee, M.K. Choi, I.S. Song, Recent Advances in Doxorubicin Formulation to Enhance Pharmacokinetics and Tumor Targeting, *Pharmaceuticals*, 16(6), 2023, 802.
- [22] M. Alyane, G. Barratt, M. Lahouel, Remote loading of doxorubicin into liposomes by transmembrane pH gradient to reduce toxicity toward H9c2 cells, *Saudi Pharm J*, 24(2), 2016, 165–75.
- [23] M. Diril, K.V. Özdokur, Y. Yıldırım, H.Y. Karasulu, In vitro evaluation and in vivo efficacy studies of a liposomal

- doxorubicin-loaded glycyrrhetic acid formulation for the treatment of hepatocellular carcinoma, *Pharm Dev Technol*, 28(10), 2023, 915–27.
- [24] European Medicines Agency, ICH guideline Q2(R2) on validation of analytical procedures, Vol. 2, 2022.
- [25] R. Rodriguez, E. Castillo, D. Sinuco, Validation of an HPLC method for determination of bisphenol-A migration from baby feeding bottles, *J Anal Methods Chem*, 2019.
- [26] A.K. De, P.P. Chowdhury, S. Chattopadhyay, Simultaneous Quantification of Dexpanthenol and Resorcinol from Hair Care Formulation Using Liquid Chromatography: Method Development and Validation, *Scientifica (Cairo)*, 2016.
- [27] L. Zou, F. Chen, J. Bao, S. Wang, L. Wang, M. Chen, C. He, Y. Wang, Preparation, characterization, and anticancer efficacy of evodiamine-loaded PLGA nanoparticles, *Drug Deliv*, 23(3), 2016, 908–16.
- [28] FDA, Draft Guidance on Doxorubicin Hydrochloride, Vol. 1, Draft Guidance on Doxorubicin Hydrochloride, 2018.
- [29] D.R. Nogueira, L.B. Macedo, L.E. Scheeren, M. Mitjans, Infante MR, Rolim CMB, et al., Determination of Methotrexate in pH-Sensitive Chitosan Nanoparticles by Validated RP-LC and UV Spectrophotometric Methods, *J Appl Biopharm Pharmacokinet*, 2, 2014,59–67.
- [30] L.E. Scheeren, D.R. Nogueira-Librelotto, J.R. Fernandes, L.B. Macedo, A.I.P. Marcolino, M.P. Vinardell, et al., Comparative Study of Reversed-Phase High-Performance Liquid Chromatography and Ultraviolet-Visible Spectrophotometry to Determine Doxorubicin in pH-Sensitive Nanoparticles, *Anal Lett*, 51(10), 2018, 1445–63.
- [31] S. Rao, Y. Song, F. Peddie, A.M. Evans, Particle size reduction to the nanometer range: a promising approach to improve buccal absorption of poorly water-soluble drugs, *Int J Nanomedicine*, 6, 2011,1245–51.
- [32] R.C. Lino, S.M. de Carvalho, C.M. Noronha, W.G. Sganzerla, M.R. Nunes, C.G. da Rosa, et al., Development and Characterization of Poly- $\epsilon$ - caprolactone Nanocapsules Containing carotene Using the Nanoprecipitation Method and Optimized by Response Surface Methodology, *Brazilian Arch Biol Technol*, 2020, 63.
- [33] J.D. Castile, K.M.G. Taylor, Factors affecting the size distribution of liposomes produced by freeze-thaw extrusion, *Int J Pharm*, 188(1), 1999, 87–95.
- [34] I. Sopyan, I. Sunan, D. Gozali, A Review: A Novel of Efforts to Enhance Liposome Stability as Drug Delivery Approach, *Sys Rev Pharm*, 2020, 11(6), 555 562.
- [35] Y. Wang, D.W., Grainger, Lyophilized liposome-based parenteral drug development: Reviewing complex product design strategies and current regulatory environments, *Adv Drug Deliv Rev*, 2019,151–152.
- [36] S.S. Kulkarni, R. Suryanarayanan, J.V. Rinella, Bogner RH, Mechanisms by which crystalline mannitol improves the reconstitution time of high concentration lyophilized protein formulations, *Eur J Pharm Biopharm*, 131, 2018, 70–81.
- [37] M.R. Toh, G.N.C. Chiu, Liposomes as sterile preparations and limitations of sterilisation techniques in liposomal manufacturing, *Asian J Pharm Sci*, 8(2), 2013, 88–95.
- [38] J. Ermer, Validation in pharmaceutical analysis, Part I: An integrated approach, *J Pharm Biomed Anal*, 24, 2001, 755–67.
- [39] N.N. Ferreira, F.I. Boni, F. Baltazar, M.P.D. Gremião, Validation of an innovative analytical method for simultaneous quantification of alpha-cyano-4-hydroxycinnamic acid and the monoclonal antibody cetuximab using HPLC from PLGA-based nanoparticles, *J Pharm Biomed Anal*, 2020, 190.
- [40] U.S. Department of Health and Human Services Food and Drug Administration, Guidance for Industry, 2015, 1-18.
- [41] S.M. Rafiyath, M. Rasul, B. Lee, G. Wei, G. Lamba, D. Liu, Comparison of safety and toxicity of liposomal doxorubicin vs. conventional anthracyclines: a meta-analysis, *Exp Hematol Oncol*, 1(1), 2012,1–9.
- [42] M.A. Abri, R. Bagheri, J. Mosafer, B. Baradaran, M. Hashemzaei, A. Baghbanzadeh, M. Guardia, A. Mokhtarzadeh, Recent advances on thermosensitive and pH-sensitive liposomes employed in controlled release, *J Control Release*, 315, 2019, 1–22.
- [43] F. Haghirsadat, G. Amoabediny, M.N. Helder, M.H. Sheikha, T. Forouzanfar, B. Zandieh-doulabi, A comprehensive mathematical model of drug release kinetics from nano-liposomes, derived from optimization studies of cationic PEGylated liposomal doxorubicin formulations for drug-gene delivery, *Artif Cells, Nanomedicine, Biotechnol*, 2017.
- [44] Z.A. Mohammadi, S.F. Aghamiri, A. Zarrabi, M. Reza Talaie, Liposomal Doxorubicin Delivery Systems: Effects of Formulation and Processing Parameters on Drug Loading and Release Behavior, *Curr Drug Deliv*, 13(7), 2016, 1065–70.
- [45] M. Anderson, A. Omri, The Effect of Different Lipid Components on the In Vitro Stability and Release Kinetics of Liposome Formulations, *Drug Delivery*, 11, 2004, 33–9.
- [46] G. Liu, K. McEnnis, Glass Transition Temperature of PLGA Particles and the Influence on Drug Delivery Applications, *Polymers (Basel)*, 14(5), 2022.
- [47] L. Peng, C. Guiliang, Jingchen Z., A Review of Liposomes as a Drug Delivery System: Current, *Molecules*, 27(1372), 2022, 1–23.
- [48] M. Fazel, M. Daeihamed, M. Osouli, A. Almasi, A. Haeri, S. Dadashzadeh, Preparation, in-vitro characterization and pharmacokinetic evaluation of brij decorated doxorubicin liposomes as a potential nanocarrier for cancer therapy, *Iran J Pharm Res*, 17, 2018, 33–43.
- [49] E. Cshuai, S. Kangarlou, T.X. Xiang, A. Ponta, P. Bummer, D. Choi, et al., Determination of key parameters for a mechanism-based model to predict doxorubicin release from actively loaded liposomes, *J Pharm Sci*, 104(3), 2015, 1087–98.
- [50] U.S. Food and Drug Administration (FDA), FDA guidance for industry dissolution testing of immediate release solid oral dosage forms, In: *Dissolution Testing of Immediate Release Solid Oral Dosage Forms US*, 1997.



# A comparative study of solvent effect on propolis extraction by ultrasound-assisted extraction

Sevgi Kolaylı , Ceren Birinci\* 

Karadeniz Technical University, Faculty of Sciences, Department of Chemistry, 61080, Trabzon, Türkiye

## Abstract

Propolis is a natural bee product obtained from beehives as raw propolis. Propolis extracts obtained from raw propolis with different polarities solvents are used as food supplement agent. The composition of propolis extracts depends on the raw propolis species, extraction methods and extraction solvent. In this study, it is expressed how the phenolic composition of propolis extracts varies depending on the solvent polarity used. The ultrasonic-assisted maceration technique was used to extract an Anatolian raw propolis sample with five different polarity solvents, namely water, methanol, ethanol, isopropanol, and n-butanol using sequential and gradual extractions. The extraction capacity was evaluated by total phenolic substance content (TPC), total flavonoid substance content (TFC), individual phenolic compounds, and antioxidant capacity. The phenolic compositions were analyzed by High Performance Liquid Chromatography (HPLC-PDA) according to the twenty-five phenolic standards. As a result, propolis directly extracted with water, methanol (98%), ethanol (98%), isopropanol (98%), n-butanol (98%) and 70% ethanol, TPC value of 147.98 mg GAE/g, TFC value of 47.18 mg QUE/g, FRAP value of 1144.33  $\mu\text{M FeSO}_4 \cdot 7\text{H}_2\text{O/g}$  and DPPH analysis results of 0.03 SC50 (mg/mL). It was determined that 70% ethanolic extract contained the highest phenolic compounds and had the highest antioxidant capacity compared to propolis extracted with solvents gradually.

**Keywords:** Propolis, extraction, solvent, polyphenols, antioxidant

## 1. Introduction

Propolis is a natural substance produced by honeybees (*Apis mellifera*) from resin-like materials from plant sources collected in the hive or in special propolis traps. Honeybees use propolis as an isolation, antifungal and antimicrobial agent [1,2]. After being removed from the hives, raw propolis is extracted in different solvents and using various extraction techniques. It is consumed in liquid or capsule form in complementary medicine. Raw propolis is a mixture of wax (5-30%), balsam (20-50%), and volatile compounds (1%), the majority of its bioactive components being in the balsamic portion [3,4]. The balsamic fraction obtained by extraction with ethanol is rich in polyphenols. The types and amounts of polyphenols in propolis samples vary according to the flora of the region where it is produced and the needs of the bee population. However, caffeic acid and its esters and flavonoids such as chrysin and pinocembrin are abundant in all propolis specimens [4-6]. Propolis extracts exhibit a wide range of antioxidant, [5-8] antimicrobial, [6-8], antiviral, [9-11] antidiabetic [12] and

antitumoral [13] activities and is used in traditional and complementary medicine as supplementary food [6,14].

One crucial factor in preparing propolis extracts from raw propolis involves the selection of the extraction technique, solvent type, and raw propolis ratio. These elements significantly affect the resulting extract's composition and properties. Various extraction techniques, such as maceration, ultrasonic extraction, Soxhlet extraction, and microwave and supercritical extraction, are used for the preparation of commercial propolis extracts [6,14-16]. Different polarity solvents such as water, ethanol, polypropylene glycol (PPG), and green solvents are used in the extraction [3,17]. However, ethanol is regarded as the optimal solvent for extraction [18,19]. Most propolis extracts consumed as a food supplement are produced using dietary ethanol, such as alcohols made from wheat, sugar beet, or sugar cane [6,15,19]. A number of studies have shown that ultrasound-assisted maceration is the most practical and economical technique in the extraction of raw propolis [14,18-20].

**Citation:** S. Kolaylı, C. Birinci, A comparative study of solvent effect on propolis extraction by ultrasound-assisted extraction, Turk J Anal Chem, 6(1), 2024 11-17.

**Author of correspondence:** [cerendidar.birinci@gmail.com](mailto:cerendidar.birinci@gmail.com)

**Received:** March 1, 2024

**Tel:** +90 (462) 377 25 25

**Accepted:** May 14, 2024

**Fax:** +90 (462) 325 31 96

 <https://doi.org/10.51435/turkjac.1445121>

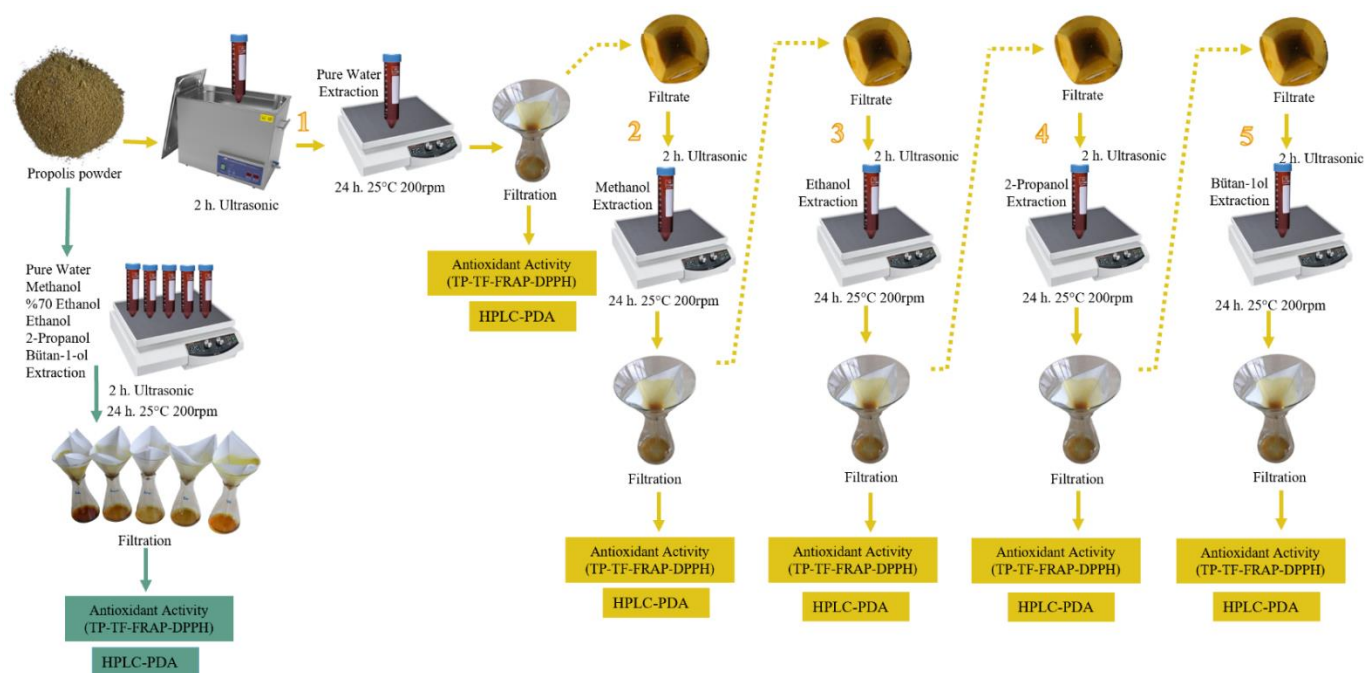


**Figure 1.** Schematic of the extraction procedure of propolis sample

However, due to the known disadvantages of ethanol, the search for ecological and green solvents for propolis continues. In addition to organic solvents, a variety of deep eutectic solvents, green solvents and alkaline or acidic extractions are also available [21–24].

In addition, which solvent would be more appropriate for the polyphenols found in raw propolis is still a matter of debate. The aim of this study is to investigate which solvent or solvents would be more useful for elucidating the composition of propolis. This research therefore evaluated the effects of solvent polarities on the ultrasonically-assisted propolis extractions.

## 2. Materials and methods

### 2.1. Chemicals

Methanol (Merck, 106009), ethanol (Symras, 3050500), isopropanol (Merck, 1.00272), and n-butanol (Sigma Aldrich, 34867), diethyl ether (Sigma Aldrich, 24004), ethyl acetate (Sigma Aldrich, 27227), acetic acid (Sigma Aldrich, 27225), acetic acid (Sigma Aldrich, 27225), acetonitrile (Sigma Aldrich, 34851) were used as analytical purity. The phenolic standards of quercetin (Sigma Aldrich, Q4951), gallic acid (Sigma Aldrich, G7384), caffeic acid (Sigma Aldrich, C0625), protocatechuic acid (Sigma Aldrich, 03930590), p-OH benzoic acid (Sigma Aldrich, 240141), syringic acid (Sigma Aldrich, S6881), epicatechin (Sigma Aldrich, E1753), p-coumaric acid (Sigma Aldrich, C9008), ferulic acid (Sigma Aldrich, 128708), rutin (Sigma Aldrich, R5143), myricetin (Sigma Aldrich, M6760), resveratrol

(Sigma Aldrich, R5010), daidzein (Sigma Aldrich, D7802), luteolin (Sigma Aldrich, L9283), trans-cinnamic acid (Sigma Aldrich, C80857), hesperetin (Sigma Aldrich, W431300), chrysin (Sigma Aldrich, C80105), pinocembrin (Sigma Aldrich, P5239), caffeic acid phenethyl ester (CAPE) (Sigma Aldrich, C8221), chlorogenic acid (Sigma Aldrich, C3878), m-OH-benzoic acid (Sigma Aldrich, 36333), ellagic acid (Sigma Aldrich, E2250), apigenin (Sigma Aldrich, 10798), rhamnetin (Sigma Aldrich, 17799), and curcumin (Alfa Aesar, B21573) were used.

### 2.2. Extraction procedure

Raw propolis samples obtained from 10 different regions of Anatolia of Türkiye, were mixed and turned into a single propolis sample. The raw propolis mixture was frozen in a deep freeze, pulverized with the help of an electric grinder, and returned to the deep freeze. The extraction process was carried out in two parts. In the first part, propolis was extracted separately in different solvents (pure water, methanol ethanol, isopropanol, and n-butanol), while in the second part, the sample was extracted gradually with these solvents. For each extraction, 30 mL of solvent was added to 3 g of powdered propolis. The mixture was placed in a falcon tube and then extracted in an ultrasonic bath (Everest Ultrasonic CleanEX N-1011, Türkiye) for 2 hours with 99 amplitudes. The mixture was next extracted by maceration in a shaker (Heidolph MR 3001, Germany) for 24 hours at room temperature. Following the extraction, the mixtures were filtered through filter paper (Sartorius Stedim Grade 391) and used for analysis (Fig. 1).

### 2.3. Total phenolic content (TPC)

The TPC of propolis extract was measured for each solvent using the classic Folin-Ciocalteu's method [25]. For this purpose, 20  $\mu\text{L}$  of extract and 400  $\mu\text{L}$  of 0.2 N Folin-Ciocalteu's reagent were mixed in a test tube, to which was added 680  $\mu\text{L}$  of distilled water. After 3 min of incubation, 400  $\mu\text{L}$  of 10% sodium carbonate was added, and the mixture was incubated for 2 h at room temperature. Following incubation, the absorbance was read on a spectrophotometer (Thermo Scientific Evolution TM 201, UV-VIS Spectrophotometer, USA) at 760 nm. Different concentrations of gallic acid (0.5, 0.25, 0.125, 0.0625, 0.03125, and 0.015625 mg/mL) were used in the preparation of the standard graph. This was produced with the absorbance values corresponding to the concentration, and the amount of phenolic substance as gallic acid equivalent was determined using the drawn graph.

### 2.4. Total flavonoid content (TFC)

The TFC of each propolis extract was measured following spectrophotometric assay [26]. Briefly, to 250  $\mu\text{L}$  of each extract were added 2.15 mL absolute methanol (Merck, 106009), 50  $\mu\text{L}$  10% aluminum nitrate (Sigma Aldrich, 237973), and 50  $\mu\text{L}$  1 M ammonium acetate. The mixture was then incubated for 40 min at room temperature. After incubation, absorbance was measured at 415 nm. Different concentrations of quercetin (0.5; 0.25; 0.125; 0.125; 0.0625; 0.03125, and 0.015625 mg/mL) were used to prepare the standard graph. This was drawn with the absorbance values at 415 nm against the concentration, and the amount of quercetin equivalent flavonoid substance was determined according to the graph.

### 2.5. Determination of Iron (III) reducing antioxidant power-(FRAP)

The ferric reducing antioxidant power assay (FRAP) was used to measure total antioxidant capacity [27]. Freshly prepared FRAP reagent was prepared by mixing 300 mM pH 3.6 sodium acetate buffer, 10 mM TPTZ, and 20 mM  $\text{FeCl}_3$  (Carlo Erba, 451695) solutions (10:1:1). Briefly, 1.5 mL of FRAP reagent and 0.05 mL of sample were placed in a test tube. After incubation at 37 $^\circ\text{C}$  for 4 min, the absorbance was read at 595 nm. Different concentrations (31.25, 62.5, 125, 125, 250, 500, and 1000  $\mu\text{M}$ ) of  $\text{FeSO}_4 \cdot 7\text{H}_2\text{O}$  (Merck, 103965) were used to prepare the standard graph. The results were expressed as  $\text{FeSO}_4 \cdot 7\text{H}_2\text{O}$  equivalent antioxidant power.

### 2.6. DPPH $\cdot$ Radical scavenging activity

It was detected by the decrease in the maximum absorbance of the purple-violet colored commercial DPPH $\cdot$  (2,2-diphenyl-1-picrylhydrazyl) radical at 517

nm in the presence of antioxidant substance. Equal amounts of DPPH solution and sample solutions were mixed and left at room temperature for 50 minutes and absorbances were measured. SC50 values were calculated by plotting the concentrations corresponding to the absorbances found[28]

### 2.7. Phenolic component analysis by HPLC-PDA

Before measuring the phenolic component in the propolis extracts in different solvents using HPLC-PDA analysis, phenolic component enrichment was performed by liquid-liquid extraction. The solvents of propolis extracts in different solvents were removed in a rotary evaporator (IKA $^\circ$ -Werke RV 05 Basic) at 40 $^\circ\text{C}$ . Then, 10 ml of pH:2 distilled water was added and extracted, first with diethyl ether and then with ethyl acetate and combined. After all the solvents had been removed, the residue remaining in the flasks was dissolved with 2 ml of absolute methanol, passed through a 0.45  $\mu\text{m}$  filter (Isolab 094.01.003), and then transferred to an instrument for phenolic analysis.

In the phenolic composition analysis method, all validations were completed against 25 phenolic standards using an RP-HPLC system (Shimadzu Corporation LC 20AT, Japan) coupled with a photodiode-array (PDA) detector. The sample was injected into the HPLC system with a reverse phase C18 column (250 mm  $\times$  4.6 mm, 5 mm; Fortis). Acetonitrile, water, and acetic acid were used for the mobile phase by applying a programmed gradient. The mobile phase consisted of (A) 2% acetic acid in water and (B) acetonitrile: water (70:30). Samples and standard injection volume was set to 20  $\mu\text{L}$ , column temperature to 30  $^\circ\text{C}$  and flow rate to 1.0 mL/min[19]. Standard calibration curves of phenolic compounds were constructed with chromatograms recorded at 250, 280, 320, or 360 nm as their maximum absorbance, and the results were expressed in  $\mu\text{g/g}$ .

### 2.8. Statistics

The Kruskal Wallis non-parametric test was applied to investigate the solvent differences in propolis samples. Since a non-parametric test was used, the results are expressed as mean  $\pm$  standard deviation, mean rank, and median values. The Kruskal-Wallis test comparing these groups revealed a statistically significant difference between the median values ( $p < 0.05$ ). Dunn's post-hoc test was applied to determine which group or groups caused the difference between the solvent groups. IBM SPSS version 25 software was used for all statistical analyses.

**Table 1.** Total phenolics and antioxidant capacities of direct propolis extractions

	TPC mg GAE/g			TFC mg QUE/g			FRAP $\mu\text{M FeSO}_4 \cdot 7\text{H}_2\text{O/g}$			DPPH SC <sub>50</sub> (mg/mL)		
	Mean $\pm$ Std. Dev.	Mean Rank	Median	Mean $\pm$ Std. Dev.	Mean Rank	Median	Mean $\pm$ Std. Dev.	Mean Rank	Median	Mean $\pm$ Std. Dev.	Mean Rank	Median
	<b>Water</b>	3.43 $\pm$ 0.24	2.00	3.20 <sup>a</sup>	0.18 $\pm$ 0.02	2.00	0.18 <sup>a</sup>	35.58 $\pm$ 0.10	2.00	35.55 <sup>a</sup>	1.03 $\pm$ 0.02	17.00
<b>Methanol (98%)</b>	147.50 $\pm$ 5.07	14.33	148.50 <sup>bd</sup>	33.07 $\pm$ 0.90	14.00	33 <sup>bcd</sup>	801.53 $\pm$ 8.67	8.00	799.58 <sup>ac</sup>	0.04 $\pm$ 0.01	5.83	0.04 <sup>ac</sup>
<b>Ethanol (98%)</b>	146.33 $\pm$ 1.53	12.67	146 <sup>bc</sup>	30.14 $\pm$ 1.49	11.00	30.68 <sup>bcd</sup>	1020.67 $\pm$ 3.06	14.00	1020 <sup>bc</sup>	0.04 $\pm$ 0.01	5.83	0.04 <sup>ac</sup>
<b>Isopropanol (98%)</b>	130.69 $\pm$ 3.05	8.00	130.08 <sup>acd</sup>	25.21 $\pm$ 1.60	7.17	24.60 <sup>ad</sup>	981.67 $\pm$ 5.51	11.00	982 <sup>bc</sup>	0.08 $\pm$ 0.01	13.83	0.08 <sup>bc</sup>
<b>n-Butanol (98%)</b>	96.33 $\pm$ 2.00	5.00	97.80 <sup>ac</sup>	24.01 $\pm$ 0.98	5.83	24 <sup>ac</sup>	465.67 $\pm$ 6.03	5.00	465 <sup>ac</sup>	0.06 $\pm$ 0.01	10.83	0.06 <sup>ab</sup>
<b>Ethanol (70%)</b>	147.98 $\pm$ 2.42	15.00	148.60 <sup>bd</sup>	47.18 $\pm$ 1.48	17.00	47.43 <sup>b</sup>	1144.33 $\pm$ 7.09	17.00	1143 <sup>b</sup>	0.03 $\pm$ 0.01	3.67	0.03 <sup>a</sup>
<b>p-value</b>		<.01			<.01			<.01			<.01	

The different letters of a, b, c and d indicated a significant difference between the solvent groups ( $p < 0.05$ )

### 3. Result and discussion

Ultrasonic extraction of the raw propolis sample was carried out using five species' polarity solvents. The same extraction method was applied in two different ways, as direct and consecutive extractions. The extraction efficiency or capacity was evaluated according to the total phenolic contents and antioxidant capacities. The results of the first extraction values are shown in Table 1. Comparison of the total phenolic contents (TPC) of the five different solvents from polar to apolar solvent, revealed that ethanol and methanol were the phenolic substances with the highest contents, followed by isopropanol, n-butanol, and water. Among the five solvents, water is the most polar solvent, followed by methanol, ethanol, isopropanol, and n-butanol. The results showed that ethanol and methanol exhibited similar extraction capacities to the sample. Although propolis is an overly complex natural product, polyphenols represent the majority of biomolecules that can be extracted with different solvents [3,24]. Although the polyphenols in propolis have different polarities, water is not a good solvent for propolis in general, as confirmed by the results of the present study. While the amount of TPC in water was 3.43 mg GAE/g, the equivalent value in ethanol (70%) was 147.98 mg GAE/g. The TPC values of the methanolic and ethanolic solvents were remarkably close to one another. Methanol exhibits

higher polarity than ethanol and was identified as a good solvent for raw propolis as ethanol. However, since methanol is a toxic solvent, it is not used for supplemental propolis extraction. A comparison of the TPC values of the two solvents with lower polarity, isopropanol and n-butanol, revealed that isopropanol had a higher TPC. However, both solvents contained smaller amounts of TPC than ethanol and methanol [29]. No significant difference was observed between the two ethanolic solvents' TPC values (Table 1). Indeed, in a previous propolis extraction study using varying percentages (from 10% to 90%) of ethanolic solutions, ethanolic solvent between 65% and 70% was identified as most effective [18].

Total flavonoid contents (TFC) were also measured in addition to TPC in this study. The amounts of TFC in the five different solvents ranged from 0.18 to 47.18 mg QUE/g. The lowest amount was found in water, and the highest in the ethanolic (70%) extract. No significant difference was determined between the 98% methanolic and ethanolic extracts. Although there were no significant differences in TPC values between these ethanolic solvents, significant differences were observed in TFC values. Analysis revealed that 70% ethanolic solvent was more successful in the extraction of flavonoids. In this study, the antioxidant capacity of the propolis extracts was determined by means of two different tests, FRAP and DPPH radical scavenging

**Table 2.** Total phenolics and antioxidant capacities of consecutive propolis extractions

		TPC mg GAE/g			TFC mg QUE/g			FRAP $\mu\text{M FeSO}_4 \cdot 7\text{H}_2\text{O/g}$			DPPH SC <sub>50</sub> (mg/mL)		
		Mean $\pm$ Std. Dev.	Mean Rank	Median	Mean $\pm$ Std. Dev.	Mean Rank	Median	Mean $\pm$ Std. Dev.	Mean Rank	Median	Mean $\pm$ Std. Dev.	Mean Rank	Median
		<b>Water</b>	<b>1.step</b>	3.38 $\pm$ 0.16	8.00	3.35 <sup>a</sup>	0.19 $\pm$ 0.02	2.00	0.18 <sup>ac</sup>	36.68 $\pm$ 0.22	8.00	36.50 <sup>a</sup>	1.10 $\pm$ 0.09
<b>Methanol (98%)</b>	<b>2.step</b>	130.30 $\pm$ 1.63	14.00	130 <sup>ad</sup>	41.30 $\pm$ 1.18	14.00	41.6 <sup>acd</sup>	1016.67 $\pm$ 5.74	1016	799.58 <sup>acd</sup>	0.04 $\pm$ 0.001	2.00	0.04 <sup>bc</sup>
<b>Ethanol (98%)</b>	<b>3.step</b>	15.00 $\pm$ 0.82	11.00	15 <sup>ade</sup>	3.40 $\pm$ 0.03	11.00	3.42 <sup>a</sup>	120.00 $\pm$ 1.63	11.00	120 <sup>ac</sup>	0.41 $\pm$ 0.02	5.00	0.42 <sup>ab</sup>
<b>Isopropanol (98%)</b>	<b>4.step</b>	2.00 $\pm$ 0.16	5.00	2 <sup>bd</sup>	1.63 $\pm$ 0.06	8.00	1.62 <sup>bc</sup>	19.77 $\pm$ 1.11	5.00	20 <sup>bc</sup>	5.20 $\pm$ 0.10	11.00	5.2 <sup>ac</sup>
<b>n-Butanol (98%)</b>	<b>5.step</b>	0.40 $\pm$ 0.02	2.00	0.4 <sup>bce</sup>	0.87 $\pm$ 0.06	5.00	0.84 <sup>bd</sup>	2.70 $\pm$ 0.22	2.00	2.6 <sup>bcd</sup>	51.23 $\pm$ 2.70	14.00	50.20 <sup>a</sup>
<b>p-value</b>			<.01			<.01			<.01			<.01	

The different letters of a.b.c and d are indicated a significant difference between the solvent groups ( $p < 0.05$ )

activity. The ferric reducing antioxidant power (FRAP) ranged from 35.58 to 1144.33  $\mu\text{M FeSO}_4 \cdot 7\text{H}_2\text{O/g}$ . The highest FRAP value was found in 70% ethanolic extracts and the lowest in water. When similar concentrations of methanol and ethanolic propolis extracts were compared, 98% ethanol exhibited a greater antioxidant capacity. The greater antioxidant capacity of the ethanolic extracts may be attributable to their higher flavonoid content. The lowest DPPH radical scavenging activity ( $\text{SC}_{50}$ ) value was in the ethanolic extracts, similarly to the FRAP values, and the highest was observed in water and isopropanol.

Since one of the aims of the study was to classify the polyphenols in propolis according to their polarity, propolis extraction was performed by gradual extraction. The data obtained by sequential extraction are given in Table 2. The powdered raw propolis sample was first extracted with distilled water, followed sequentially by methanol, ethanol, isopropanol, and butanol. This low TPC value indicates that a very small part of the total phenolic substance in the raw propolis

was dissolved in water. After aqueous extraction, the remaining propolis pulp was extracted with 98% methanol using a similar extraction technique. The TPC value obtained in the methanolic extract was 130.30 mg GAE/g, most of the phenolic substances being extracted from the raw propolis. The TPC values of the ethanolic extraction was found very lower (15 mg GAE/g) since the extraction was second, first methanolic extraction mostly phenolic were extracted. The TPC values in isopropanol and butanol were very low, since most of the phenolic components in propolis (approximately 95%) were extracted with methanol and ethanol. In the sequential extraction, the majority of flavonoid substances were obtained from metabolic extraction, although a small amount was extracted in ethanol. The highest antioxidant values were observed in methanolic extract, similarly to the TPC and TFC values in sequential extraction.

The phenolic components of the extracts obtained in both extractions were analyzed using HPLC-PDA. The measurement results based on twenty-five phenolic

**Table 3.** Phenolic composition of direct and sequential propolis extracts

Phenolic Standards ( $\mu\text{g/g}$ )	Water	98% Methanol	98% Ethanol	98% isopropanol	98% n-butanol	70% Ethanol	Water (1)	Methanol (2)	Ethanol (3)	2-Propanol (4)	Butan-1-ol (5)
<i>Hydroxybenzoic acids</i>											
<i>p</i> -OH Benzoic acid	47	48	—	36	—	74	45	46	6	2	1
<i>m</i> -OH Benzoic acid	—	—	—	—	—	—	—	—	—	—	—
Protocatechuic acid	63	—	—	—	—	—	48	—	—	—	—
Gallic acid	13	31	—	—	—	—	12	—	—	—	—
Chlorogenic acid	—	—	35	—	—	99	—	—	—	—	—
Syringic acid	—	—	—	—	—	27	—	—	—	—	—
Ellagic acid	153	—	—	—	—	—	230	—	—	36	—
<i>Hydroxycinnamic acids</i>											
<i>t</i> -cinnamic acid	7	373	289	205	195	331	40	384	47	7	2
Ferulic acid	251	1544	1344	1214	756	2121	344	1255	152	18	4
<i>p</i> -Coumaric acid	170	1192	1054	856	574	1561	335	893	114	13	3
Caffeic acid	753	1335	1121	1023	636	1719	912	1025	131	17	3
CAPE	—	2150	1785	1530	1112	2237	—	2207	255	—	—
<i>Flavonol</i>											
Rhamnetin	—	390	—	—	—	—	—	360	—	—	—
Quercetin	—	301	256	144	164	451	—	272	72	3	—
Rutin	—	—	—	—	—	—	—	—	—	—	—
Myricetin	—	—	—	—	—	—	—	—	—	—	—
<i>Flavan-3-ols</i>											
Epicatechin	—	—	—	—	—	—	—	—	—	—	—
<i>Flavones</i>											
Chrysin	15	5534	5046	4878	3106	7851	21	5928	744	74	16
Daidzein	—	—	—	—	—	—	—	—	—	—	—
Apigenin	—	609	509	555	298	741	—	443	59	7	2
Luteolin	—	—	—	—	—	19	—	—	—	—	—
<i>Flavanones</i>											
Pinocembrin	16	5466	5072	5162	3116	8013	25	5645	705	76	15
Hesperetin	87	2496	2240	2095	1318	441	101	2655	322	27	5
<i>Other polyphenols</i>											
Curcumin	—	—	—	—	—	—	—	—	—	—	—
Resveratrol	—	—	—	—	—	—	—	—	—	—	—

(—): not detected



compounds are given in Table 3. In the first extraction technique, the majority of the phenolic acids (hydroxybenzoic and hydroxycinnamic acids) were detected in water extract, although a small number of flavonoids were also detected. The most abundant phenolic acid in the aqueous extract was caffeic acid. A previous study using honey as a green solvent also reported that aqueous propolis extract is rich in caffeic acid [24]. This is one of the derivatives of hydroxycinnamic acids, and the hydroxyl groups it contains bestow a polar character on it. However, since this polarity is lower than in water, it is more prone to dissolve in ethanolic and methanolic solvents. Derivatives of hydroxycinnamic acids from polyphenol subclasses emerged as leachable with all the solvents used. In addition, the derivatives of hydroxycinnamic acids, one of the subclasses of polyphenols, emerged as the molecules with the highest extractable quality in the five solvents. Chrysin, one of the flavone derivatives, was soluble in all organic solvents except for water, but was extracted at the highest level with 70% ethanol. Chrysin, one of the major components of propolis, is an important component of complementary medicine due to its high biological activity [30].

The methanolic and ethanolic propolis extracts in this study exhibited similar phenolic compositions. However, ethanol should be used in consumable propolis extracts due to the toxic effect of methanol, although methanol can be used as a suitable solvent for analytical studies. In the present study, two different concentrations of ethanol were used, and it may be concluded that 70% ethanol is more suitable for propolis extraction. Phenolic compounds derived from hydroxybenzoic acids were detected at low levels in the propolis sample, while water and 70% ethanolic were the most suitable for these compounds. The isopropanol and n-butanolic extracts were found to be rich in flavonoids.

CAPE, the most important compound in propolis, was detected at the highest level in methanol and 70% ethanol. CAPE is a polyphenol compound that has attracted considerable attention in recent years due to its high antioxidant properties, as well as significant anti-inflammatory, neuroprotective, and antitumoral activities [30–33]. The first aqueous extraction was performed using the sequential extraction technique. The profiles of phenolic compounds obtained in both aqueous extractions were very similar, although there were small differences between the amounts of phenolic compounds. Similarly to the first extraction, the methanol and ethanolic extracts were found to be rich in both phenolic acid and flavonoids in the second extraction. A large amount of CAPE was extracted with methanol. The phenolic component profiles of isopropanol and butanolic extracts were similar to one

another but contained very small amounts of phenolic compounds.

## 4. Conclusion

Ethanolic propolis extracts exhibited high phenolic acid and flavonoid contents and were also the most antioxidant-rich extracts. Solvents with higher polarities also contained larger amounts of phenolic acids, while lower polarity solvents exhibited larger quantities of flavonoids. The solvent with the highest phenolic components and antioxidant capacity was 70% ethanol.

## Funding

None.

## Declaration of competing interest

The authors declare no competing interest.

## Author contributions

Sevgi Kolaylı: Designed the hypotheses, statistical analysis, evaluated the results, and drafted the manuscript. Ceren Birinci: Formol analyses and HPLC studies.


## References

- [1] Ç. Akçay, Ü. Ayata, E. Birinci, M. Yalçın, S. Kolaylı, Some Physical, Biological, Hardness, and Color Properties of Wood Impregnated with Propolis, *Forestist*, 2022, 72:283–93.
- [2] P.M. Cuce, S. Kolaylı, E. Cuce, Enhanced performance figures of solar cookers through latent heat storage and low-cost booster reflectors, *International Journal of Low-Carbon Technologies*, 2020, 15:427–33.
- [3] V. Bankova, B. Trusheva, M. Popova, Propolis extraction methods: a review, *Journal of Apicultural Research*, 2021, 60(5), 734743.
- [4] A. Kurek-Górecka, Ş. Keskin, O. Bobis, R. Felitti, M. Górecki, M. Otręba, et al, Comparison of the Antioxidant Activity of Propolis Samples from Different Geographical Regions, *Plants (Basel)*, 2022, 11.
- [5] S. Kolaylı, U.Z. Ureyen Esertas, Y. Kara, The Antimicrobial, Anti-Quorum Sensing, and Anti-Biofilm Activities of Ethanolic Propolis Extracts Used as Food Supplements, *Biology Bulletin*, 2022;49: S21–30.
- [6] M.F. Abo El-Maati, S.A. Mahgoub, S.M. Labib, A.M.A. Al-Gaby, M.F. Ramadan, Phenolic extracts of clove (*Syzygium aromaticum*) with novel antioxidant and antibacterial activities, *European Journal of Integrative Medicine*, 2016, 8:4, 494-504.
- [7] S. Kolaylı, C. BİRİNCİ, Y. Kara, A. Ozkok, A.E. Tanuğur Samancı, H. Sahin, et al, A melissopalynological and chemical characterization of Anatolian propolis and an assessment of its antioxidant potential, *European Food Research and Technology* 2023, 249:1213–33.

- [8] K. Pobiega, K. Kraśniewska, M. Gniewosz, Application of propolis in antimicrobial and antioxidative protection of food quality - A review, *Trends Food Sci Technol*, 2019,83:53–62.
- [9] M. Cora, C.K. Buruk, S. Ünsal, N. Kaklikkaya, S. Kolaylı, Chemical Analysis and in Vitro Antiviral Effects of Northeast Türkiye Propolis Samples against HSV-1, *Chem Biodivers*, 2023; 20.
- [10] H.I. Guler, G. Tatar, O. Yildiz, A.O. Belduz, S. Kolaylı, Investigation of potential inhibitor properties of ethanolic propolis extracts against ACE-II receptors for COVID-19 treatment by molecular docking study, *Arch Microbiol*, 2021,203:3557.
- [11] A. Odunkiran, M. Şengül, S. Ufuk, Some Characteristics of Honey and Propolis and Their Effects on Covid-19, *J. Apit.Nat.*,2021,4:2, 129-153.
- [12] R. El Adaouia Taleb, N. Djebli, H. Chenini, H. Sahin, S. Kolaylı, In vivo and in vitro anti-diabetic activity of ethanolic propolis extract, *J Food Biochem*, 2020;44.
- [13] R.D. Oliveira, S.P. Celeiro, C. Barbosa-Matos, A.S. Freitas, S.M. Cardoso, M. Viana-Pereira, Portuguese Propolis Antitumoral Activity in Melanoma Involves ROS Production and Induction of Apoptosis, *Molecules*, 2022, 27.
- [14] A. Braakhuis, Evidence on the Health Benefits of Supplemental Propolis, *Nutrients* 2019, 11.
- [15] H. Zaidi, S. Ouchemoukh, N. Amessis-Ouchemoukh, N. Debbache, R. Pacheco, M.L. Serralheiro, et al, Biological properties of phenolic compound extracts in selected Algerian honeys-The inhibition of acetylcholinesterase and  $\alpha$ -glucosidase activities, *European Journal of Integrative Medicine*, 2019,25:77–84.
- [16] A. Huseynova, A. Ali Alakbarlı, Spectrophotometric Analysis of Flavonoid Quantity in Pollen of *Amygdalus communis* L. and Determination of Biomarkers, *J.Apit.Nat.*, 2023, 6:1, 22–29.
- [17] V.A. Taddeo, F. Epifano, S. Fiorito, S. Genovese, Comparison of different extraction methods and HPLC quantification of prenylated and unprenylated phenylpropanoids in raw Italian propolis, *J Pharm Biomed Anal*, 2016, 129:219–23.
- [18] N. Pujirahayu, H. Ritonga, Z. Uslinawaty, Properties And Flavonoids Content In Propolis Of Some Extraction Method Of Raw Propolis, *International Journal of Pharmacy and Pharmaceutical Sciences*, 2014, 6:6, 338-340
- [19] Y. Kara, Z. Can, S. Kolaylı, Applicability of Phenolic Profile Analysis Method Developed with RP-HPLC-PDA to some Bee Product, *Brazilian Archives of Biology and Technology*, 2022, 65.
- [20] M. Oroian, F. Dranca, F. Ursachi, Comparative evaluation of maceration, microwave and ultrasonic-assisted extraction of phenolic compounds from propolis, *J Food Sci Technol* 2020, 57:70.
- [21] K.L. Yeo, C.P. Leo, D.J.C. Chan, Ultrasonic Enhancement on Propolis Extraction at Varied pH and Alcohol Content, *Journal of Food Process Engineering*, 2015, 38:562–70.
- [22] B. Yurt, Effect of Hydrogen-Enriched Solvents on the Extraction of Phytochemicals in Propolis, *ACS Omega*, 2023, 7:8(15):14264-14270.
- [23] Y.C. Kung, L.S. Chua, M.F. Yam, J. Soo, Alkaline hydrolysis and discrimination of propolis at different pH values using high throughput 2D IR spectroscopy and LC-MS/MS, *Bioresour Technol Rep*, 2022,18.
- [24] M. Kekeçoğlu, A. Sorucu, Determination of the effect of green extraction solvents on the phenolic acids and flavonoids of propolis, *Journal of Research in Veterinary Medicine*, 2022, 41:49–54.
- [25] V.L. Singleton, R. Orthofer, R.M. Lamuela-Raventós, Analysis of total phenols and other oxidation substrates and antioxidants by means of folin-ciocalteu reagent, *Methods Enzymol*, 1999, 299:152–78.
- [26] L.R. Fukumoto, G. Mazza, Assessing Antioxidant and Prooxidant Activities of Phenolic Compounds, *J Agric Food Chem*, 2000, 48:3597–604.
- [27] I.F. Benzie, J.J. Strain, The ferric reducing ability of plasma (FRAP) as a measure of "antioxidant power": the FRAP assay, *Anal Biochem*, 1996 ,15:239(1), 70-6.
- [28] M. Cuendet, K. Hostettmann, O. Potterat, W. Dyatmiko, Iridoid Glucosides with Free Radical Scavenging Properties from *Fagraea blumei*, *Helvetica Chimica Acta*, 1997, 80, 1144-1152.
- [29] M.G. Miguel, S. Nunes, S.A. Dandlen, A.M. Cavaco, M.D. Antunes, Phenols and antioxidant activity of hydro-alcoholic extracts of propolis from Algarve, South of Portugal, *Food and Chemical Toxicology*, 2010, 48:3418–23.
- [30] M. Stompor-gorący, A. Bajek-bil, M. Machaczka, Chrysin: Perspectives on Contemporary Status and Future Possibilities as Pro-Health Agent, *Nutrients*, 2021, 13, 2038.
- [31] M. Balaha, B. De Filippis, A. Cataldi, V. Di Giacomo, CAPE and Neuroprotection: A Review, *Biomolecules*, 2021,11:1–28.
- [32] C. Omene, M. Kalac, J. Wu, E. Marchi, K. Frenkel, O.A. O'Connor, Propolis and its active component, Caffeic acid phenethyl ester (CAPE), modulate breast cancer therapeutic targets via an epigenetically mediated mechanism of action, *J Cancer Sci Ther*, 2013, 5:334–42.
- [33] L. Saftić, Ž. Peršurić, E. Fornal, T. Pavlešić, S. Kraljević Pavelić, Targeted and untargeted LC-MS polyphenolic profiling and chemometric analysis of propolis from different regions of Croatia, *J Pharm Biomed Anal*, 2019, 165:162–72.



# Usability of calcite mineral, which develops in the crack fillings of carbonate rocks, as ornamental stone

Murat Camuzcuoğlu 

Bayburt University, Faculty of Applied Sciences, Department of Emergency Aid and Disaster Management, 69000, Bayburt, Türkiye

## Abstract

Türkiye has a geologically significant amount of mineral content and offers essential resources, especially in the mining field (ornamental stone production). This study develops methods for extracting, processing, and usability calcite minerals, which develop as vein-filling (secondary formations) among fragmented limestones along the Bayburt-Erzurum highway for ornamental stone purposes. The chemical and crystallographic properties of the mineral were determined by XRD and FT-IR analyses. In the XRD analysis performed on the powder sample obtained from the mineral, a value of 80000 (cps) corresponding to 30 theta was found, which was determined to be a pure calcite mineral. In the FT-IR analysis performed to support the XRD analysis, peak values of 2513-1795  $\text{cm}^{-1}$  and 1406-873-712  $\text{cm}^{-1}$  were detected, and the value was observed to belong to the pure calcite mineral. Calcite mineral was used in jewelry production and was evaluated in terms of durability, aesthetics, and rarity in producing ornamental stones. Epoxy (durable, clean, and transparent) was used as a binding material in ornamental stone production. In general, calcite minerals are widely used in various industrial areas, but their use as ornamental stones is limited due to their low hardness. This study offers a new perspective on evaluating calcite minerals as ornamental stones, revealing that it is possible to process a low-hardness mineral as an ornamental stone using a binding material.

**Keywords:** Geology, calcite, ornamental stone, XRD analysis, FTIR analysis

## 1. Introduction

Ornamental stone refers to various colored rocks, minerals, and organic materials processed after being extracted from the earth's crust and used as ornaments and jewelry [1,2]. Ornamental stones are generally formed by abundant elements, such as carbon, aluminum, oxygen, silicon, magnesium, and calcium [2].

Hardness is essential when considering using minerals or stones as ornamental stones [3]. This is due to the necessity of processing, polishing, and preserving the stone's structure. For a material to be suitable for this purpose, it must be of a similar hardness to that of quartz, which has a Mohs hardness scale value of 7.

In particular, ornamental stones have been cut into various shapes, processed, and polished using multiple techniques, enhancing their visual appeal and appealing to people. They have also been used as a status marker throughout human history [4].

The study area is at the exit of Kop Mountain on the Bayburt-Erzurum Road and generally consists of thin, medium-layered, beige, yellowish, and brown-colored sandy limestones, thin-layered sandstones in green tones and gray-colored marl alternating clastic

limestones. Limestones include the sandy levels in the north and south of the ultramafic massif and have a darker color than these units. Pure calcite mineral developed as veins in the crack fillings between clastic limestones.

The hardness of the calcite mineral is 3 according to the Mohs hardness scale, and its density is approximately 2.6 [5]. This mineral mainly forms the main mineral of carbonate rocks such as marble and limestone. Calcite mineral is mixed with different minerals (aragonite, etc.) with the same chemical content ( $\text{CaCO}_3$ ), and such minerals with similar chemical content can be distinguished from each other by determining their chemical and crystallographic contents through XRD and FT-IR analyses. Today, calcite mineral is used in many sectors, such as paper, paint, construction, ceramics, food, and feed [5]. In addition to its uses in such sectors, it uses an ornamental stone. Pure crystalline calcite mineral generally occurs in the crack fillings of rocks existing in limestone formations, but it has yet to be produced commercially due to its small amount.

**Citation:** M. Camuzcuoğlu, Usability of calcite mineral, which develops in the crack fillings of carbonate rocks, as ornamental stone, Turk J Anal Chem, 6(1), 2024, 18–24.

**Author of correspondence:** [muratacamuzcuoglu@bayburt.edu.tr](mailto:muratacamuzcuoglu@bayburt.edu.tr)

**Received:** May 24, 2024

**Tel:** +90 (458) 211 11 53

**Accepted:** June 11, 2024

**Fax:** +90 (458) 333 20 43

 <https://doi.org/10.51435/turkjac.1489684>

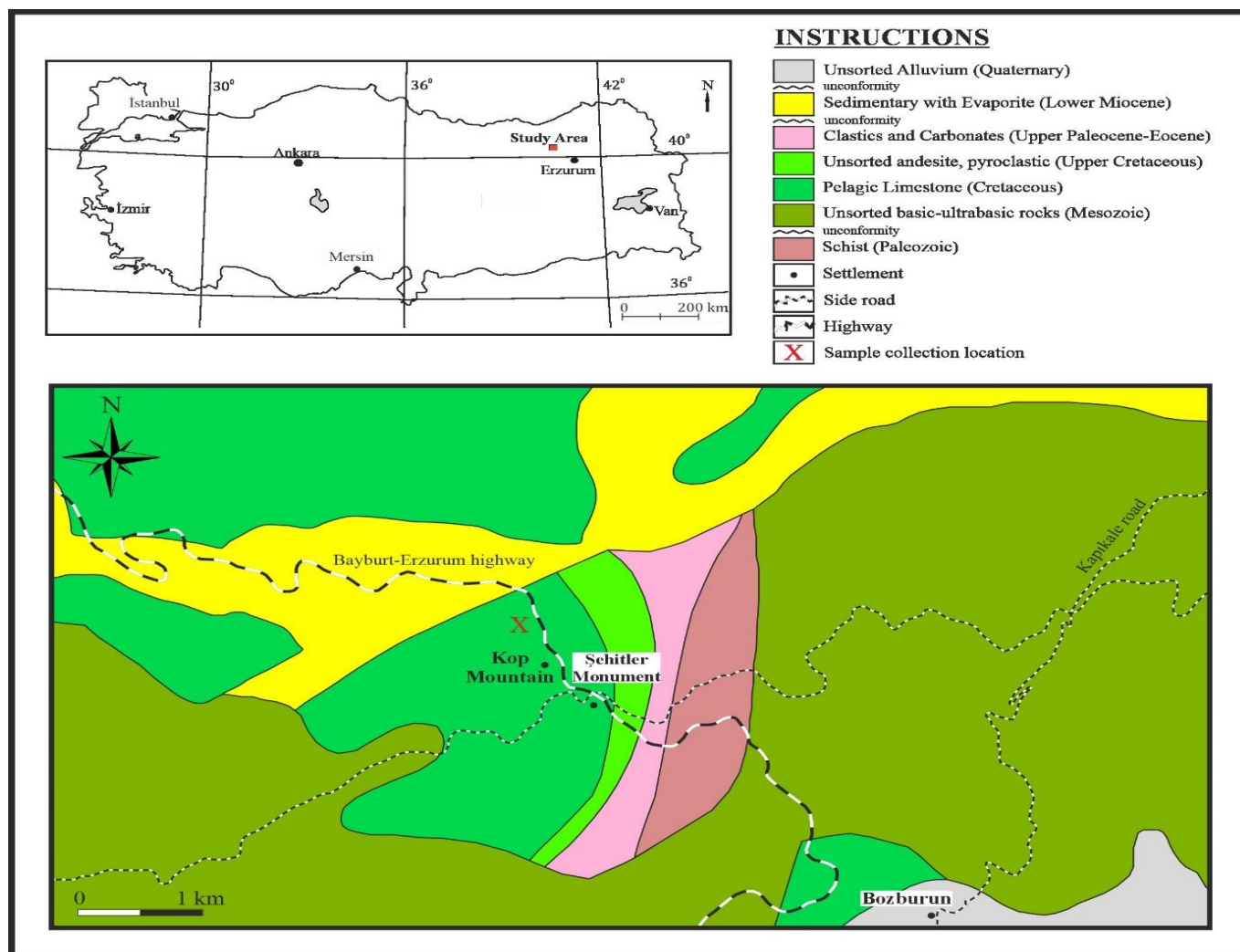


Figure 1. Modified study area location map

This study investigated the usability of pure crystalline calcite minerals occurring in crack fillings of limestone formation as ornamental stone (jewelry). The hardness of calcite is three, and the hardness of jewelry made by coating it with epoxy is determined to be 5.5-6. This hardness value is sufficient to harden the mineral that may be soft in jewelry production. Calcite minerals can be used as jewelry by being coated with epoxy when evaluated in terms of rarity and hardness. Studies in the literature generally examine composite materials, and in jewelry works, there are applications where powder paints are mixed with epoxy. This study has determined in the literature that new products can be obtained by bonding minerals with epoxy in jewelry making.

## 2. Material and methods

### 2.1. Material

It consists of pure crystalline calcite mineral, which develops as veins in the crack fillings between clastic limestones at the exit of Kop Mountain on the Bayburt-Erzurum Road and consists of  $\text{CaCO}_3$  as its main element. The sampling location of the calcite mineral

taken from the crack fillings of carbonate clastic rocks (Pelagic limestone) in the study area was recorded on the 1/25000 map taken from the Mineral Research and Exploration (MTA) earth sciences portal [6] (Fig. 1).

### 2.2. Preparation of calcite mineral for various applications

Since the pure calcite minerals taken in the study area developed in rock fillings, they were first removed (with the help of a hammer and tweezers) and made ready for analysis and gemstone applications. Since the calcite crystals will be used for ornamental stone application, they were carefully sorted to avoid damaging the crystal structure. During the sorting phase, the broken calcite crystals were pulverized in an agate mortar for XRD and FT-IR analyses, along with the ornamental stones produced from the powder sample.

### 2.3. Determination of XRD and FT-IR analyses

Calcite minerals from the field were ground in an agate mortar and turned into powder for XRD and FT-IR analyses. XRD and FT-IR analyses were conducted at Bayburt University Central Research Laboratory

Application and Research Center (BUMER). XRD Analysis was performed on a Bruker D8 Discover computer-controlled X-ray Diffractometer XRD to determine the mineralogical composition of the rock. For XRD analyses, diffraction Pattern Capture for Powder Samples took 1-30 minutes. The rock's chemical composition was determined using a PerkinElmer brand FT-IR spectrometer. In FT-IR analysis, vibrations occur between the bonds when infrared light interacts with matter. The energies from the vibrations are converted into spectra according to their wavelengths.

#### 2.4. Production of ornamental stone

Epoxy resin was applied to the jewelry tool and allowed to dry slightly to make it easier to work. The crystals of the calcite mineral were arranged and prepared on a jewelry apparatus with the help of tweezers. No epoxy was applied to the calcite crystals on the surface to prevent them from losing their shine and naturalness. On the other hand, the calcite powder samples, which had been crushed and sieved, were poured into the prepared molds and filled. On the other hand, the epoxy resin prepared in a 2:1 ratio (epoxy and hardener) was poured into these molds. The epoxy was waited at 24 °C (at room temperature) for 24 hours and was allowed to dry, and after this period, the ready-made final products were removed from the molds.

#### 2.5. Properties of the epoxy used

Epoxy resins are known for their high adhesion strength, chemicals, and water resistance. The epoxy used in the study is resistant to alkalis (concentrated and dilute), acids (dilute), solvent-containing substances (diesel, gasoline, alcohol, etc.), cleaning groups (disinfectant, detergent, etc.), oils (animal, vegetable, mineral) and seawater can show durability. For wet environments, epoxy can withstand temperatures up to 50 °C, while in dry environments, epoxy resin can withstand temperatures up to 130 °C. In the study, the application was made by mixing epoxy and hardener in a ratio of 2:1.

### 3. Geology

The study area covers Kop Mountain on the Bayburt-Erzurum highway. When the geology of the region is examined, there are unsorted basic-ultrabasic rock units belonging to the ophiolitic units represented by the Paleozoic-aged Schist rock unit at the base and the Mesozoic-aged units unconformably overlying it. These units are Cretaceous-aged Pelagic limestones overlie the sampling was done. The pelagic limestones from which the sampling was made were overlain by Upper Cretaceous-aged unsorted andesite and pyroclastic rock

units and by Upper Paleocene - Eocene-aged clastic and carbonate units. Upper Paleocene-Eocene aged units were unconformably overlain by Lower Miocene aged evaporite sedimentary units, and all these rock units were unconformably covered by Quaternary-aged alluvial material. Since there was no detailed geological map or study in the study area, the map of the region was modified and drawn from the Earth Sciences Portal of Mineral Research and Exploration (MTA) [6] (Fig. 1). Sample collection in the study was carried out at the exit of Kop Mountain on the Bayburt - Erzurum Road towards Erzurum.

## 4. Results and Discussion

#### 4.1. Ornamental stones

Ornamental stones (precious and semi-precious) have been popular for centuries due to their association with wealth and beauty. Some essential criteria are accepted worldwide for precious and semi-precious stones to be considered ornamental [7]. These criteria;

- The term 'durability' is defined as resistance to (external factors). This is represented by resistance to brittleness, impacts, and hardness.
- Beauty is inherently subjective, yet specific characteristics of the stone are universally regarded as aesthetically pleasing. These include its capacity for rapid processing, transparency, cleanliness, and a diverse array of attractive colors.
- Rarity is a critical factor in determining the value of a stone or an object.

In addition to the aforementioned essential criteria, several desired features are commonly sought in ornamental stones. These include the ability to reflect light (light refraction) and the ease with which they can be cut and polished. While no universally accepted definition differentiates precious stones from semi-precious stones, it is widely understood that stones such as sapphires, rubies, diamonds, and emeralds represent precious stones. Conversely, other stones are typically described as semiprecious stones. Sapphire, diamond, ruby, and emerald (precious stones) are considered noble when subjected to specific processes [8].

Ornamental stones result from various geological processes, including metamorphism, igneous activity, and hydrothermal activity. In magmatic and pegmatites, metamorphic rocks, and hydrothermal deposit areas, ornamental stones can be found on or near the surface [9]. Tectonic movements, such as faulting and volcanism, result in the stones being exposed at the Earth's surface.

While stones of natural origin are often the first thing that comes to mind when one thinks of ornamental stones, the term also encompasses materials of organic origin (pearl, amber, coral, etc.) and materials produced



Figure 2. Calcite minerals terrain view

synthetically (imitation) in a laboratory environment. Ornamental stones produced in laboratory environments have become a highly sought-after product worldwide in recent years. Natural stone is a material that is used extensively in the global market. It is frequently used to decorate interiors and exteriors, produce medical and dental products, and facade coatings. Moreover, natural stone's utilization in jewelry materials and ornaments is also rising. Consequently, further research is required to expand the use of natural (ornamental) stones, including semi-precious and precious stones.

Although a sub-discipline of mineralogy, Gemology is a branch of science that deals with ornamental stones and helps identify, examine, and classify materials. It is generally closely associated with stone cutting and jewelry making.

#### 4.2. Macroscopic examinations

Coarse crystalline calcite minerals, which develop as veins in the crack fillings between the clastic limestones cropping out on the Bayburt-Erzurum Road, are observed in transparent white tones in the study area (Fig. 2).

Calcite minerals used as ornamental stones were carefully removed from the vein part of the rock to prevent their crystals from breaking. To ensure the homogeneity of the calcite crystals, small pieces were separated to prevent the crystals from being crushed too much. At the same time, any unwanted parts that could cause color were removed with tweezers. Then, the

calcite minerals to be used as ornamental stones were set aside, and the remaining and very crushed calcite minerals were ground in an agate mortar for analysis and for producing ornamental stones from the powder sample (Fig. 3).

#### 4.3. XRD analyses

X-rays are sent to the sample, which must have a smooth surface so that the X-rays are refracted and scattered at the right angle. The X-ray hitting the sample is reflected at different angles ( $\alpha$ ,  $\beta$ ,  $\gamma$ ) and intensities [10]. Thus, X-rays detect the mineralogical and elemental composition of the analyzed substance. From the peak values from quantitative calculations of the correct selection of different mineral parameters and the intensity ratio



Figure 3. Preparing the calcite mineral for ornamental stone production and chemical analysis

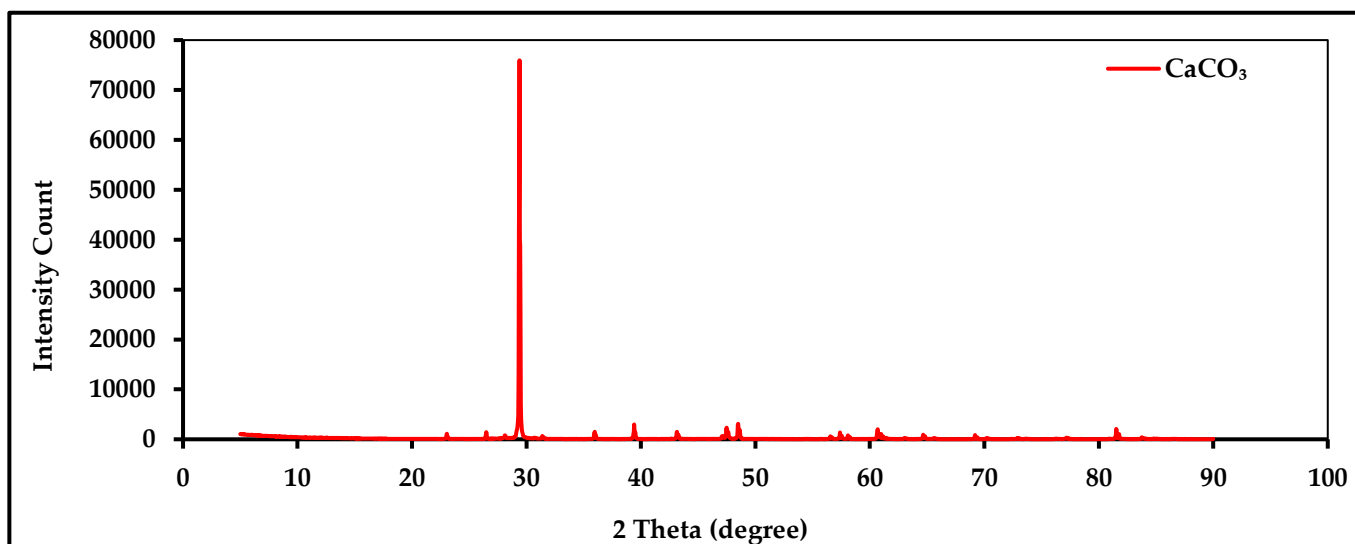


Figure 4. X-ray diffraction patterns of calcite

according to degree, the crystal system of the powder sample used and ground in the study was identified and determined to be a calcite mineral (Fig. 4).

Calcite and aragonite minerals are often confused due to their similar properties (structure and colors). Because these minerals are polymorphs of each other and have the same chemical composition ( $\text{CaCO}_3$ ). The only distinguishing method is their crystal systems: calcite mineral crystallizes in the trigonal system, and aragonite mineral crystallizes in the hexagonal system. XRD analyses generally determine the elements and minerals in building materials, ores, and manufactured goods. As a result of XRD analyses, mineral names are determined using different crystal systems of minerals with the same chemical structure. In XRD imaging, the density of the coarse crystalline calcite mineral reaches up to 80000 (cps). The 80000 (cps) value reached is used to determine the purity of the calcite mineral and the calcite mineral. In the XRD analysis, the 80000 (cps) peak corresponds to the pure calcite peak compared to the 30-theta peak [11]. This high-density value increases depending on the prepared powder sample's surface orientation and the mineral's degree of crystallization. Although the same minerals are captured in some XRD images, the intensity varies depending on the purity of the mineral. The calcite mineral used in the study offers a density value close to pure.

#### 4.4. FT-IR examinations

FT-IR spectroscopy allows for obtaining information about individual minerals and non-crystalline inclusions and detecting organic matter's presence. The absorption of IR by solids generally depends on the atom's strength, mass, and length of the interatomic bonds in the structure of the minerals. Additionally, it is subject to the constraints of the global symmetry of the local and the unit cell site symmetry (site symmetry) of each other

atom within the unit cell [12]. Furthermore, the absorption of IR is significantly influenced by the size and shape of the mineral particles [13] and, to a certain extent, by the crystalline arrangement [14]. In the FT-IR analysis, the sample examined was not a rock but a mineral, so no peak value of any foreign material was obtained. In FT-IR spectroscopy, which can provide some helpful information about the structure of the molecules, it appears to have absorption bands at  $2513\text{--}1795\text{ cm}^{-1}$ . Moreover, Asymmetric peak values of  $1406\text{--}873\text{--}712\text{ cm}^{-1}$  were reached. IR spectra are consistent with the characteristic vibrations of calcite [15,16]. The peak values by the FT-IR analysis showed that the examined sample had pure  $\text{CaCO}_3$  content and supported the XRD measurements (Fig. 5).

#### 4.5. Gemstone applications

The study proposed that by binding natural stones or minerals with different binding materials, their usability as ornamental stones would be enhanced in terms of visual appeal by imparting various properties such as shine and durability. For this purpose, epoxy has been selected due to its high resistance to multiple chemicals and temperatures and ease of workability and cleanability (transparency). In addition to its strength and durability, which have been widely utilized recently, epoxy exhibits these properties. Epoxy is employed in a multitude of applications, including exterior coatings, the production of adhesives for forest products (furniture, wood, etc.), high-performance floors (waterproof floors, mosaic floors, colored aggregate flooring, chip flooring etc.), the construction industry (paint, lining, coating, etc.), aviation, industry, and the space industry. Furthermore, epoxy is employed in numerous artistic and decorative areas. In the creative field, various products, including earrings, coasters, necklaces, and rings are produced by combining different colors into epoxy resins. Nevertheless, further

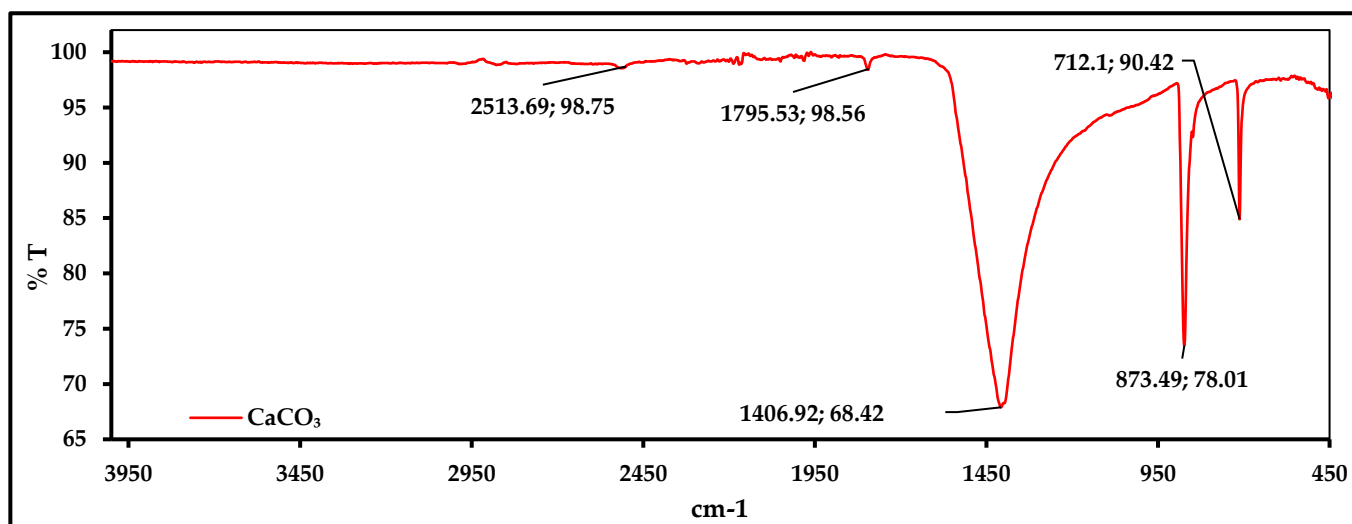


Figure 5. Fourier transform infrared spectroscopy (FT-IR) spectra:  $\text{CaCO}_3$  (Calcite)

studies are required to expand the knowledge base on jewelry products with epoxy binders made using natural minerals. In this study, the excellent adhesion properties and durability of the epoxy used as a binder were employed to enhance the durability of the low-strength calcite mineral. Furthermore, minerals with low hardness can be utilized as ornamental stones by imparting them with distinctive properties due to epoxy binder material.

The color content of the coarse crystalline calcite observed in the study area, its pure, clean, bright, and transparent appearance, its ability to be quickly processed, and its less (in secondary rock vein fillings) make it rare. These properties of the calcite mineral increase its usability as an ornamental and jewelry material and show that it has an economic value. Although there is a cost of using epoxy in jewelry production, the cost of epoxy can be neglected because the product obtained using calcite mineral is valuable.

The study obtained two products (calcite crystal and powder) using calcite as an ornamental stone (Fig. 6a). In accessory products made from calcite powder samples (ring stone, pendant, etc.), calcite powder reacted with epoxy and caused a color change (white-yellow) (Fig. 6b). No color change was observed in the accessory

product made of calcite crystals (Fig. 6c). Ornamental stone production involves combining natural minerals with various binding materials, and more research and development are needed for these processes.

## 5. Conclusions

A classification of the usability of the product obtained from the study as jewelry (bracelet, earring, and ring stone) according to the existing categories in the classification of ornamental stones is presented below.

- In terms of durability, the hardness of calcite is 3. Although it has low strength, it has been found that calcite is suitable for use in jewelry making as the epoxy used as a binding material has sufficient chemical and physical resistance.
- Although visibility is a relative concept, the calcite mineral's crystalline structure increases the product's visibility and potential as a gemstone.
- In terms of rarity, although calcite mineral is not rare compared to other precious and semi-precious minerals, it can be considered valuable due to its secondary formation and formation in crack fillings of detrital limestones (occurrence in small amounts).



Figure 6. a) Jewelry produced in calcite mineral, b and c) Close-up photographs of the jewelry made



As a result, this study shows that the low-hardness calcite mineral (coarse crystalline and developing secondary in rock crack fillings) with different usage areas can be used as a gemstone by bonding with a binding material (epoxy). Furthermore, it has been established that the epoxy employed as a binder can be utilized for diverse applications in the fabrication of ornamental stones, encompassing both cleanliness (transparency) and durability (chemical and physical resistance).

## References

- [1] Y. Eşme, Anadolu'da Bilinen Önemli Süstaşları Jeolojik ve Ekonomik Potansiyeli (Unpublished), Bornova, İzmir, 1994.
- [2] İ.K. Akbudak, Z. Başbüyük, M. Gürbüz, Yozgat "Aydıncık" kalsedon-ametist oluşumlarının mineralojisi-petrografisi ve ekonomikliğinin incelenmesi, DÜMF Mühendislik Dergisi 9(1), 2018, 313-324.
- [3] S. Ghorbani, S.H. Hoseinie, E. Ghasemi, T. Sherizadeh, A review on rock hardness testing methods and their applications in rock engineering, Arab J Geosci, 15 (11) (2022).
- [4] M. Camuzcuoğlu, Peridotitin Epoksi (Reçine) İçerisinde Renk Verici Pigment Olarak Kullanılabilirliği ve Süstaşı Yapımı, European Confereces 2nd International Conference on Health, Engineering and Applied Science, 4-6 August, Belgrade, 2023.
- [5] Mineral Research and Exploration (MTA), Türkiye, 2024, <https://www.mta.gov.tr/v3.0/bilgi-merkezi/kalsit> (Access; 18.05.2024)
- [6] Mineral Research and Exploration (MTA), Yerbilimleri, Türkiye, 2024 <http://yerbilimleri.mta.gov.tr/anasayfa.aspx> (Access; 27.04.2024)
- [7] T. Rızaoğlu, M. Camuzcuoğlu, Usability of Obsidian with Special Refraction as an Ornamental Stone by Bonding with Epoxy Resin, Systemy Wspomagania w Inżynierii Produkcyj, 11(2), 2022, 96-103.
- [8] <https://www.mta.gov.tr/v3.0/bilgi-merkezi/sustasi> (Access; 12.05.2024)
- [9] C. Simonet, E. Fritsch, B. Lasnier, 2008). A classification of gem corundum deposits aimed towards gem exploration, Ore Geol Rev, 34 (1-2), 2008, 127-133.
- [10] W. Harris, W.G. Norman, X-ray diffraction techniques for soil mineral identification. In Methods of Soil Analysis Part 5- Mineralogical Methods, American Society of Agronomy and Soil Science Society of America, 2015, 81-115.
- [11] MinDAT 2024 <https://www.mindat.org/min-859.html> (Access; 07.06.2024)
- [12] D.S. Volkov, O.B. Rogova, M.A. Proskurnin, Organic Matter and Mineral Composition of Silicate Soils: FTIR Comparison Study by Photoacoustic, Diffuse Reflectance, and Attenuated Total Reflection Modalities, Agronomy, 11(9), 2021,1-30.
- [13] M. Fan, D. Dai, B. Huang, Fourier transform infrared spectroscopy for natural fibres. Fourier transform-materials analysis, 3, 2012, 45-68.
- [14] R. Bardestani, G.S. Patience, S. Kaliaguine, Experimental methods in chemical engineering: specific surface area and pore size distribution measurements-BET, BJH, and DFT, Can J Chem Eng, 97(11), 2019, 2781-2791.
- [15] D. Shan, S. Wang, H. Xue, S. Cosnier, Direct electrochemistry and electrocatalysis of hemoglobin entrapped in composite matrix based on chitosan and CaCO<sub>3</sub> nanoparticles. Electrochem Commun, 9, (2007), 529-534.
- [16] S. Hajji, T. Turki, A. Boubakri, M. Ben Amor, N. Mzoughi, Study of cadmium adsorption onto calcite using full factorial experiment design, Desalin Water Treat, 83, (2017), 222-233.



## Investigation of antibiofilm and biological activities of *Vaccinium arctostaphylos* L.

Uğur Kardil<sup>1\*</sup> , Zeynep Akar<sup>2</sup> , Azer Özad Düzgün<sup>3</sup> 

<sup>1</sup> Gümüşhane University, Department of Medical Services and Techniques, Gümüşhane University Vocational School of Health Services, 29000, Gümüşhane, Türkiye

<sup>2</sup> Gümüşhane University, Department of Genetics and Bioengineering, Faculty of Engineering and Natural Sciences, 29000, Gümüşhane, Türkiye

<sup>3</sup> Gümüşhane University, Department of Occupational Health and Safety, Faculty of Health Sciences, 29000, Gümüşhane, Türkiye

### Abstract

This study investigated the total phenolic and flavonoid contents and the antioxidant, antimicrobial, antibiofilm and  $\alpha$ -glucosidase inhibitory activities of the methanol extract from *Vaccinium arctostaphylos* L. leaf and fruit parts. The highest antioxidant activity determined in leaf part with 53  $\mu$ M TEAC and 8.4  $\mu$ g/mL  $SC_{50}$  using the ferric reducing antioxidant power (FRAP) and 2,2-diphenyl-1-picrylhydrazyl (DPPH $\bullet$ ) radical scavenging assays, respectively. The data indicated that the leaf of the plant had the higher total phenolic content (49  $\mu$ g/mL GAE) and total flavonoid content (0.071  $\mu$ g/mL QAE) compared to fruit. The  $\alpha$ -glucosidase enzyme activity of the leaves ( $IC_{50}$ : 0.179 mg/mL) was observed to be higher than that of the fruits ( $IC_{50}$ : 0.386 mg/mL). The MIC values of the leaf and fruit parts of *V. arctostaphylos* were 6.25 mg/mL and 3.125 mg/mL, respectively. The results of this study indicate that the leaf extract was found to significantly reduce the biofilm-forming capacity of the *Acinetobacter baumannii* isolate by approximately 3-fold, whereas the fruit extract was observed to have only a marginal effect, reducing the biofilm-forming capacity by approximately 1.4-fold. The effects of plant extracts on microbial biofilms may be examined with a view to combating antibiotic resistance. Also, results suggesting that it might be an effective medical plant to prevent or treat diseases associated with oxidative damage and bacterial infections.

**Keywords:** Antibiofilm, antioxidant activity, *Vaccinium arctostaphylos* L.,  $\alpha$ -glucosidase

### 1. Introduction

Medicinal plants contain bioactive compounds that are used instead of drugs in traditional treatment methods. The use of plants containing secondary metabolites, including phenolics and flavonoids, in alternative therapies is a growing area of research. These metabolites have been shown to have therapeutic effects in the treatment or suppression of a number of diseases [1]. Secondary metabolites which have antioxidant activity considered able to scavenging and prevent free radicals that cause oxidative damage in biomolecules [2]. In addition, natural alternatives with much fewer side effects are preferred instead of synthetic antioxidants in the treatment of diseases [3]. Therefore, there is a growing interest in the identification of natural compounds that can prevent oxidative damage and the harmful effects of free radicals.

The genus *Vaccinium* L., which belongs to the family Ericaceae, includes nearly 450 species worldwide [4].

Türkiye, which has an important flora in terms of medicinal plants, is home to several of the *Vaccinium* species. The literature contains numerous reports of the biological activities of *Vaccinium* [5,6]. Previous studies have indicated that *Vaccinium* species exhibit bioactivity properties, including antioxidant, antimicrobial and antidiabetic effects [7–9].

*Vaccinium arctostaphylos* L. is a compact shrub with a height of approximately 1.5-2.5 m, found between 1600-1800 m above sea level. Fruits of the *V. arctostaphylos* contain approximately levels of 30% sugar, 15% protein, and 2% fat. Phenolics with antioxidant properties are the highly important metabolites in the leaves and fruits of *V. arctostaphylos* [10]. The plant is widely have been used as an antidiabetic agent for a long time in traditional medicine [11].

It has been reported that the fruit and leaves of this plant have serum glucose and lipid level lowering

**Citation:** U. Kardil, Z. Akar, A.Ö. Düzgün, Investigation of antibiofilm and biological activities of *Vaccinium arctostaphylos* L., Turk J Anal Chem, 6(1), 2024, 25–31.

**Author of correspondence:** [ugurkardil\\_61@hotmail.com](mailto:ugurkardil_61@hotmail.com)

**Received:** March 25, 2024

**Tel:** +90 (458) 211 11 53

**Accepted:** June 10, 2024

**Fax:** +90 (458) 333 20 43

 <https://doi.org/10.51435/turkjac.1489982>

activities and are also used in the treatment of hypertension [4]. Moreover, previous studies have reported that caffeic acid is the main phenolic compound of *V. arctostaphylos*, which contains various phenolic compounds [12].

One of the most important public health problems in the world is the high resistance of gram-negative bacteria to antibiotics. Infections caused by these bacteria are associated with high morbidity and mortality due to limited treatment options [13]. It is essential to research and develop more effective natural antibacterial agents to combat bacterial infections caused by pathogens.

To date, there have been few studies investigating the antimicrobial activity of *V. arctostaphylos* fruit and leaf extracts. Furthermore, to the best of our knowledge, no study has been conducted on the antibiofilm activity of these extracts. Thus, the present study aimed to evaluate the antioxidant, antidiabetic, antimicrobial and antibiofilm activities of the fruit and leaf methanolic extracts of *V. arctostaphylos*.

## 2. Materials and methods

### 2.1. Chemicals and reagents

Methanol, ethanol, NaOH, NaCl, HCl, Na<sub>2</sub>CO<sub>3</sub>, Trolox (6-hydroxy-2,5,7,8-tetramethylchroman-2-carboxylic acid), DPPH• (2,2-diphenyl-1-picrylhydrazyl), FeCl<sub>3</sub>.6H<sub>2</sub>O, acetic acid, gallic acid, quercetin, ammonium acetate, ammonium nitrate,  $\alpha$ -Glucosidase (*Saccharomyces cerevisiae*, lyophilized powder,  $\geq 10$  units/mg protein), 4-nitrophenyl- $\alpha$ -D-glucopyranoside, Folin-Ciocalteu's phenol reagent and yeast extract were purchased from Sigma Aldrich (St. Louis, MO, USA). TPTZ (2,4,6-tris(2-pyridyl)-s-triazine), tryptone and crystal violet were purchased from Merck (Darmstadt, Germany).

### 2.2. Plant material and sample preparation

*V. arctostaphylos* leaves and fruits were collected from Sürmene, Trabzon, Türkiye, in September 2023. The leaves and fruits were subjected to a drying process at room temperature over a period of four months. Subsequently, the dried samples were pulverized using a grinder, after which the pulverized samples were extracted with methanol solvent in a shaker for a period of two hours. Following the shaking process, the extracts were filtered through 0.45  $\mu$ m syringe filters (Whatman) to produce clear solutions. Methanol, used as solvent was evaporated with a rotary evaporator under low pressure. Both the fruit and leaf extracts were dissolved in methanol to the desired concentration. The extracts were stored at a temperature of 4 °C until further use in subsequent experiments.

### 2.3. Determination of antioxidant activities

#### 2.3.1. DPPH radical scavenging activity

The DPPH• radical scavenging activities of methanol extracts of the leaf and fruit parts were investigated using the method described by Brand-Williams et al. [14]. The method was applied by mixing the extracts with DPPH• solution and keeping them at ambient temperature and in the dark for 50 minutes. The changes in the absorbance of the DPPH• treated with extracts and standard antioxidant were measured at a wavelength of 517 nm. A graph was drawn according to the concentrations that corresponded to these absorbance values. In this graph, the amount of sample required to halve the concentration of DPPH• was determined in  $\mu$ g/mL and expressed as the SC<sub>50</sub> value. The SC<sub>50</sub> values were compared with the standard antioxidant Trolox.

#### 2.3.2. Ferric reducing antioxidant power (FRAP)

The FRAP values of extracts were evaluated using the method described by Benzie and Strain [15], whereby the total reduction capacity determined indirectly. Each extract and standard solution were mixed newly prepared FRAP reagent. Then solutions were vortexed and kept for 20 min incubation period at ambient temperature and the absorbance values were read at 595 nm. The FRAP activities of the extracts were expressed as  $\mu$ M TEAC (Trolox Equivalent Antioxidant Capacity), which was obtained by using the calibration graph of Trolox.

### 2.4. Determination of total phenolic and flavonoid contents

#### 2.4.1. Total phenolic content (TPC)

The total phenolic content of the extracts was evaluated *in vitro* using the Folin-Ciocalteu reagent method, as described by Slinkard and Singleton [16]. Each extract and standard solution were mixed Folin reagent. Then, the Na<sub>2</sub>CO<sub>3</sub> (7.5%) was added to the solution and it was vortexed. The reaction solutions were incubated for a period of two hours at a temperature of ambient. The total phenolic content was calculated based on absorbance measurement at 765 nm, with the values expressed as  $\mu$ g of gallic acid equivalent per mL of extract ( $\mu$ g/mL GAE) using calibration graph.

#### 2.4.2. Total flavonoid content (TFC)

The total flavonoid content of the extracts was determined in accordance with the method of Fukumoto and Mazza [17]. The calibration curve was obtained with quercetin (QAE) and the results expressed as quercetin equivalent ( $\mu$ g/mL QAE).

## 2.5. Determination of antimicrobial activity

### 2.5.1. Determination of minimum inhibitory concentrations of extracts

Both the leaf and fruit parts of the *V. arctostaphylos* were extracted. The final concentrations were determined as 50 mg/mL, and these concentrations were used as the starting concentration (50-0.097 mg/mL) in the liquid microdilution method to determine minimum inhibitory concentrations (MIC). MIC values of the extracts were investigated against the previously determined clinical antibiotic-resistant *Acinetobacter baumannii* isolate with biofilm-forming capacity. All experiments were performed in 96 well plates and in triplicate [18].

### 2.5.2. Investigation of antibiofilm properties of extracts

After determining the MIC values of *V. arctostaphylos* leaves and fruit parts against the antibiotic-resistant *A.baumannii* isolate, 1/2 MIC values were used as reference values for the antibiofilm experiment. The experiment was carried out in 96 well plates and in triplicate. *A. baumannii* was incubated in 3 mL of LB medium at 37 °C overnight. After incubation, 1/100 diluted *A. baumannii* isolate along with 1/2 MIC leaf and fruit extracts were added to 96 well plates and incubated again overnight. Then, the suspension in the plate was poured and the plate was washed three times with distilled water. 200 µL of 1% crystal violet dye was added to each well and left at room temperature for 20 minutes. Crystal violet was removed from the plate and the washing process was repeated with distilled water. After washing the plate, it was left to dry for 15 minutes at room temperature. Then, 200 µL of 95% ethanol was added to the wells. *Escherichia coli* Dh5@ was used as a negative control (Ac). Optical absorbance (A) value was measured at 620 nm in the spectrometer. The evaluation was made according to four different criteria: 1.  $A \leq A_c$  Negative, 2.  $A_c < A \leq 2A_c$  Weak positive, 3.  $2A_c < A \leq 4A_c$  Moderately positive, 4.  $A > 4A_c$  Strong positive [18].

## 2.6. Determination of enzyme inhibition

### 2.6.1. $\alpha$ -Glucosidase inhibition assay

The  $\alpha$ -glucosidase enzyme activity of fruit and leaf extracts of *V. arctostaphylos* was investigated in a modified method of Yu et al. [19]. Initially, 650 µL of buffer solution (pH 6.8, concentration 0.1 M), 20 µL sample and 30 µL enzyme (*Saccharomyces cerevisiae*, lyophilized powder,  $\geq 10$  units/mg protein) were mixed. The mixture was maintained at a temperature of 37 °C for a period of 10 minutes, after which 75 µL of the substrate (4-nitrophenyl- $\alpha$ -D-glucopyranoside) was added. Following a 20-minute incubation period at 37 °C, 650 µL of 1 M  $\text{Na}_2\text{CO}_3$  was added to halt the reaction. The absorbance values were determined by measuring them at a wavelength of 405 nm using a UV/VIS spectrophotometer.

Acarbose was employed as the positive control, with different concentrations employed as the standard inhibitor. The study was conducted in triplicate and in reagent-sample blinds.  $\text{IC}_{50}$  values (the concentration of the sample that halves the enzyme activity) were calculated for both acarbose and the samples.

## 3. Results and discussion

### 3.1. Evaluation of antioxidant activity

In this study, antioxidant activities of methanolic extracts of *V. arctostaphylos* leaf and fruit were determined using DPPH and FRAP methods (Table 1). DPPH•, a stable free radical, is a widely used method to evaluate the antioxidant activity of extracts. The FRAP test, which measures the reducing capacity of an extract, is an indirect method for determining its antioxidant activity.

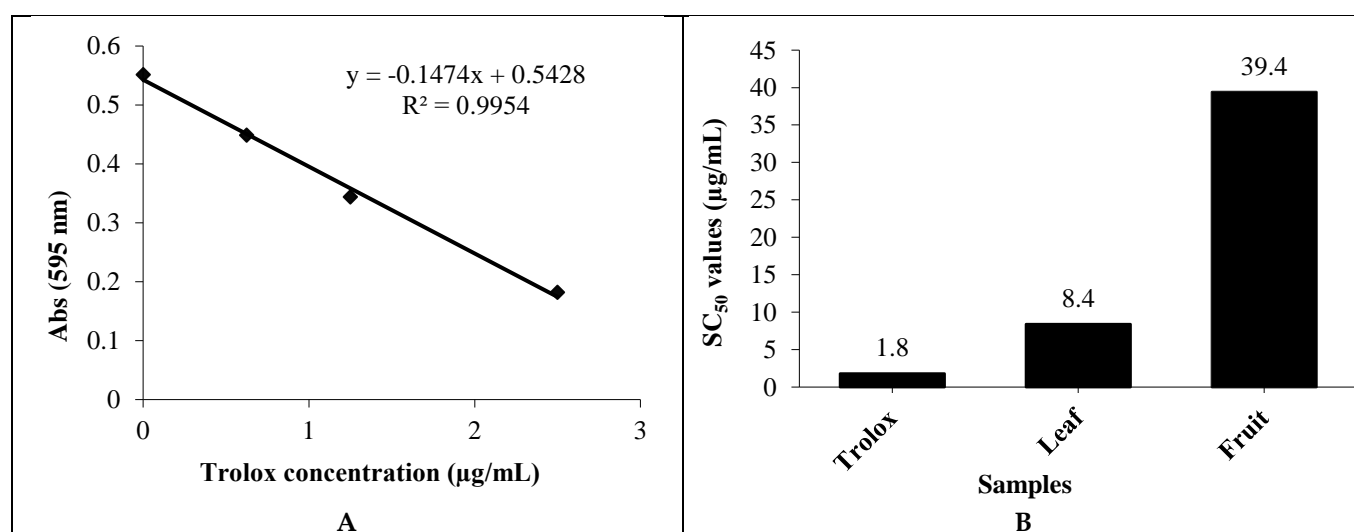


**Figure 1.** A: The graph depicts the changes in absorbance of the DPPH radical in the presence of varying concentrations of Trolox, B:  $\text{SC}_{50}$  values of *V. arctostaphylos* leaf and fruit extracts and Trolox

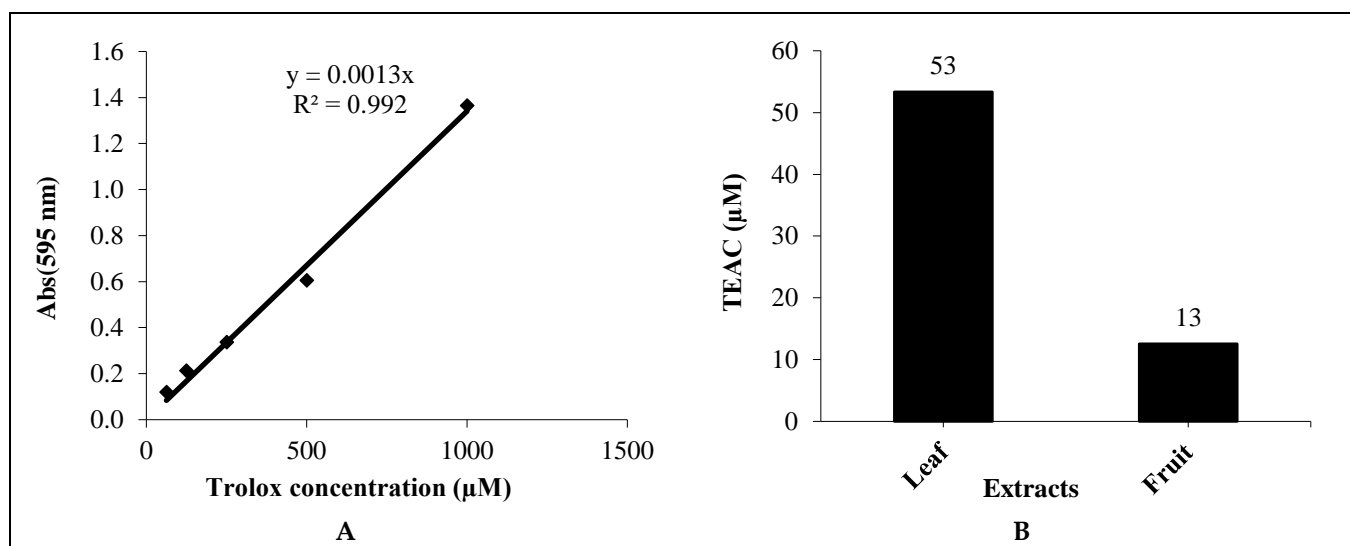


**Figure 2.** A: Graph of calibration corresponding to changes in absorbance of iron (III) reduction potential of the with different concentrations of Trolox, B: TEAC (μM) values of the leaf and fruit parts of the *V. arctostaphylos* extracts

In a previous study, Mahboubi et al. [20] reported that the  $SC_{50}$  values of DPPH radical scavenging in leaf and fruit samples were 60 and 35 μg/mL, respectively. In another study Musavi et al. [21] reported that the  $SC_{50}$  values of DPPH radical scavenging activity in the methanolic extract of the leaf and fruit parts of *V. arctostaphylos* were 3.20 and 2.98 μg/mL, respectively. In contrast to these studies, the  $SC_{50}$  values of the DPPH radical scavenging of the extracts were 8.4 and 39.4 μg/mL in leaf and fruit, respectively in our study (Fig. 1). Trolox, which was evaluated as standard, showed 4.5 times higher the radical scavenging activity from the leaf extract with an  $SC_{50}$  value of 1.8 μg/mL (Fig. 1). Leaf extracts of *V. arctostaphylos* L. showed higher than fruit extract DPPH• scavenging activity. Moreover, the *in vitro* outcomes exhibited a positive correlation of the total phenolic and flavonoid content of the extracts (Table 1).

In a study conducted by Hasanloo et al. [22] it was found that the leaf and fruit of *V. arctostaphylos* exhibited remarkable reducing activities across a range of

genotypes. In another study, Güder et al. [23] reported that ethanolic extract of *V. arctostaphylos* fruit exhibited notable FRAP activities at varying concentrations. In the present study, when the iron (III) reduction potential of the extracts was examined by the FRAP method, it was found that the antioxidant power of the leaf extract was 4 times higher than the fruit extract, with  $53 \pm 2.72$  μM TEAC (Fig. 2).

**Table 1.** Antioxidant activity, TPC, and TFC values of the leaf and fruit parts of the *V. arctostaphylos* extracts

	DPPH $SC_{50}$ (μg/mL)	FRAP TEAC (μM)	TPC GAE (μg/mL)	TFC QAE (μg/mL)
Leaf	$8.4 \pm 0.5$	$53 \pm 2.72$	$49 \pm 3.47$	$0.071 \pm 0.0030$
Fruit	$39.4 \pm 6.1$	$13 \pm 1.08$	$12 \pm 1.92$	$0.008 \pm 0.0006$

### 3.2. Evaluation of total phenolic and flavonoid contents

Phenolic and flavonoid compounds, which are secondary metabolites, are responsible for a multitude of biological activities, including antioxidant, antidiabetic, and antimicrobial effects. [22,24,25]. In this study, evaluation of total phenolic and flavonoid contents was

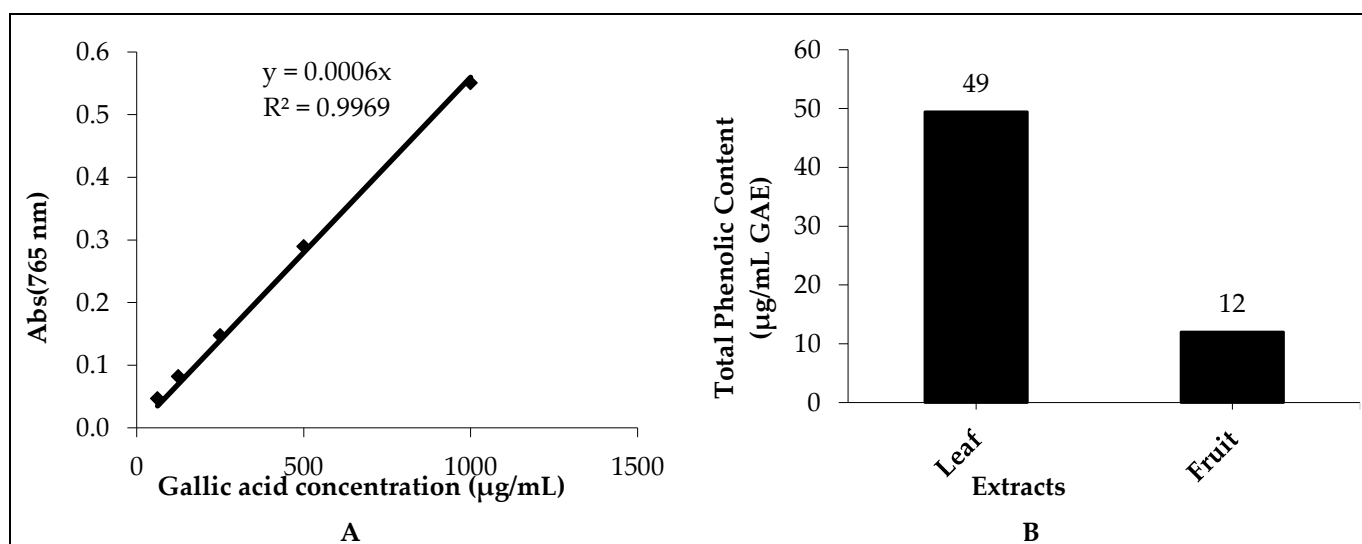


**Figure 3.** A: The standard curve of gallic acid, B: The TPC of leaf and fruit parts of the *V. arctostaphylos* expressed as μg/mL GAE

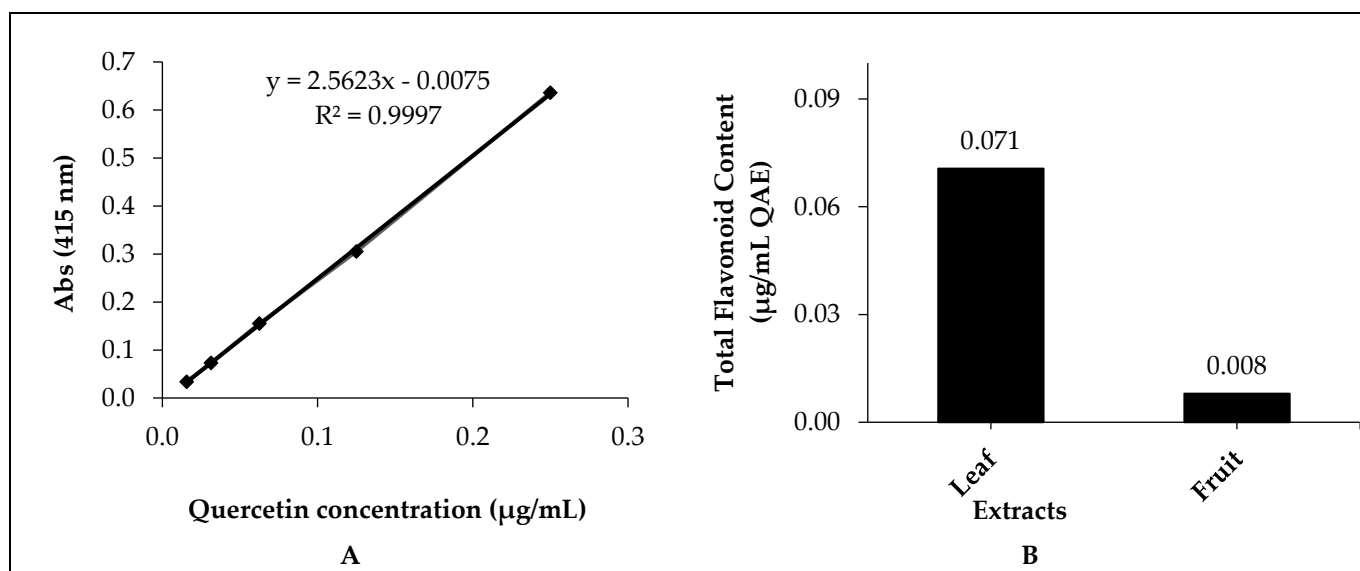


Figure 4. The standard curve of quercetin, B: The TFC of leaf and fruit parts of the *V. arctostaphylos* expressed as µg/mL QAE

determined of the both the leaf and fruit parts of the *V. arctostaphylos* (Table 1). A standard curve of gallic acid was used to determine total phenolic content (Fig. 3), with the results expressed in terms of µg/mL GAE. A standard curve of quercetin was used in order to determine the total flavonoid content (Fig. 4), and the results were expressed as µg/mL QAE. Leaf extract of *V. arctostaphylos* had the highest total phenolic and flavonoid content, with  $49 \pm 3.47$  µg/mL GAE and  $0.071 \pm 0.0030$  µg/mL QAE, respectively (Fig. 3 and Fig. 4). In the literature, Saral et al. [26] reported that the total phenolic and flavonoid contents of methanolic extracts of *V. arctostaphylos* fruits from different regions ranged from 20.74 to 11.54 mg GAE/g and 1.93 to 2.16 mg QAE/g dry weight of sample, respectively. Mahboubi et al. [20] found that the leaf parts of *V. arctostaphylos* methanolic extracts contained higher amounts of flavonoids compared to the fruit parts. In their study, Shamilov and colleagues identified 10 phenolic compounds in the leaves of *V. arctostaphylos* [6]. Also, the previous studies reported that caffeic acid is the major phenolic compound of *V. arctostaphylos* [12].

A scatter graph of the antioxidant activity, TPC and TFC values for the leaf and fruit extracts of *V. arctostaphylos* was created (Fig. 5). The results demonstrated that there was a positive correlation between DPPH, FRAP, TPC and TFC antioxidant activity results of the plant extracts leaf and fruit parts ( $R^2: 0.9999$ ).

### 3.3. Evaluation of antimicrobial activity

Antimicrobial and antibiofilm activities of methanol extracts of leaves and fruit parts of *V. arctostaphylos* were investigated against the antibiotic-resistant clinical isolate *A. baumannii*. The MIC value of the leaf part of *V. arctostaphylos* was determined as 6.25 mg/mL, and the

MIC value of the fruit part was determined as 3.125 mg/mL (Table 2).

After the MIC values were determined, the antibiofilm activities of the extracts were evaluated using 1/2 MIC values. *E. coli* Dh5@ isolate was used as a control. All evaluations were made based on the OD value (Ac: 0.1915) of the biofilm-forming capacity of the control isolate. The biofilm formation capacity of the control strain was taken as a reference point, and it was determined that the *A. baumannii* clinical isolate exhibited a moderate capacity for biofilm formation. In the experiment where the antibiofilm activity was investigated, it was determined that the biofilm-forming property of *A. baumannii* treated with the leaf extract decreased to negative, and in the experiments conducted with the fruit part, the biofilm-forming property of the isolate decreased from moderate to weak (Table 2). The findings demonstrate that the leaf part of *V. arctostaphylos* exhibits a higher antibiofilm activity than the fruit part.

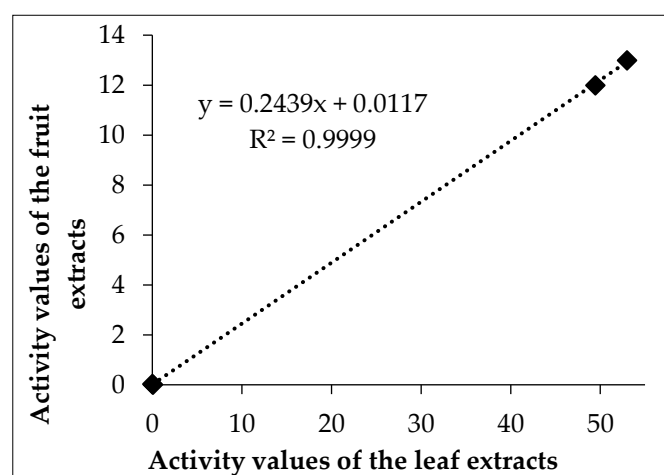


Figure 5. Correlations of total phenolics, FRAP, total flavonoids and DPPH antioxidant activity results of the leaf and fruit parts the *V. arctostaphylos* extracts

**Table 2.** MIC and antibiofilm results of the leaf and fruit parts of the *V. arctostaphylos* extracts

	MIC Value (mg/mL)	Biofilm Value / OD
Leaf	6.250	0.1372
Fruit	3.125	0.2930
A73 ( <i>A.baumannii</i> )	—	0.4132
<i>E.coli</i> Dh5@ (control)	—	0.1915

Despite the continuing global public health threat posed by antimicrobial resistance, there are also constraints on the discovery and development of new antimicrobial agents. Biofilm formation represents a significant mechanism of resistance employed by a multitude of pathogens, rendering them increasingly challenging to treat [27,28]. Microorganisms can form biofilms that protect them from the effects of natural host defenses and antimicrobial agents [27,29]. This is one of the mechanisms by which bacteria become resistant to antibiotics. Plants are a rich source of compounds with biological activity, making them an excellent resource for the discovery of useful and novel antimicrobial products [27,30,31]. Plant extracts may demonstrate antimicrobial activity when used in their own or may serve as a source of effective antimicrobial compounds that can act against biofilms of pathogens. Consequently, the investigation of the antibiofilm activities of plants against pathogenic bacteria may represent an important contribution towards the development of treatments for diseases [27]. Additionally, further research is needed to isolate compounds from plants with antibiofilm effects and determine the mechanism of activity.

#### 3.4. Evaluation of $\alpha$ -glucosidase inhibitory effects of extracts

The  $\alpha$ -glucosidase enzyme activity of fruit and leaf extracts of *V. arctostaphylos* was measured as IC<sub>50</sub>; 0.386 and 0.179 mg/mL, respectively (Table 3). The  $\alpha$ -glucosidase enzyme inhibition value of the leaf part of the plant is higher than that of the fruit part. The  $\alpha$ -glucosidase enzyme plays a pivotal role in non-insulin-based treatments for diabetes, as it catalyzes the final step in the digestion of carbohydrates, which is a crucial aspect of the metabolic process [32]. In the literature, there are few studies on the  $\alpha$ -glucosidase enzyme activity of the fruit parts of this plant. In a study, the fruit part of the plant was extracted with different solvents (Ethanol, Methanol and distilled water) and  $\alpha$ -glucosidase enzyme inhibition values were determined. Inhibition was observed in all three solvents in the results obtained. The IC<sub>50</sub> value of the methanol extract in this study was 0.477 mg/mL [33]. The results of this test demonstrated that the leaves of this plant, which are typically consumed as fruit, also possess significant enzyme activity.

**Table 3.**  $\alpha$ -Glucosidase enzyme inhibition activity of *V. arctostaphylos*

Sample	IC50 (mg/mL)	R2
Acarbose	0.029 ± 0.02	0.9971
Leaf	0.179 ± 0.03	0.9912
Fruit	0.386 ± 0.05	0.9957

## 4. Conclusions

This study presented the total phenolic and flavonoid contents and the antioxidant, antimicrobial, antibiofilm, and  $\alpha$ -glucosidase inhibitory activities of methanol extract from *V. arctostaphylos* leaf and fruit parts. The study data demonstrated that leaf extract of this plant had the higher biological activities compared to the fruit extracts. In addition, the similar results between antioxidant activity and total phenolic and flavonoid contents resulted in a very good correlation (R<sup>2</sup>: 0.9999). The findings show that *V. arctostaphylos* has antibiofilm activity, and the leaf part exhibits a higher antibiofilm activity than the fruit part. The results of our study indicate that *V. arctostaphylos* may be a promising candidate for the prevention and treatment of diseases associated with oxidative damage and bacterial infections. Consequently, further research on these biological activities *V. arctostaphylos* may lead to the development of treatment options. Also, to be suggest for the treatment of human diseases, it must undergo thorough evaluation in various clinical trials.

## Acknowledgments

—

## Funding

None.

## Conflicts of Interest

The authors declare no conflict of interest.

## Authors' contribution

UK: Conducted the extraction, antioxidant activity experiments and wrote the article. ZA: Conducted the extraction, enzyme activity and antioxidant activity experiments. AÖD: Performed the antibiofilm experiments and contributed to the article writing.

## References

- [1] R.C. Fierascu, I. Fierascu, A.M. Baroi, A. Ortan, Selected aspects related to medicinal and aromatic plants as alternative sources of bioactive compounds, *Int J Mol Sci*, 22(4), 2021, 1521.
- [2] L.A. Tziveleka, M.A. Tammam, O. Tzakou, V. Roussis, E. Ioannou, Metabolites with antioxidant activity from marine macroalgae, *Antioxidants*, 10(9), 2021, 1431.
- [3] C. Nirmala, M.S. Bisht, H.K. Bajwa, O. Santosh, Bamboo: A rich source of natural antioxidants and its applications in the food and pharmaceutical industry, *Trends Food Sci Tech*, 77, 2018, 91-99.
- [4] A. Ahmadi, M. Khalili F. Mashae B. Nahri-Niknafs, The effects of solvent polarity on hypoglycemic and hypolipidemic activities of *Vaccinium arctostaphylos* L. Unripe fruits, *Pharm Chem J*, 50, 2017, 746-752.
- [5] S.I. Papanov, E.G. Petkova, I.G. Ivanov, Polyphenols content and antioxidant activity of bilberry juice obtained from different altitude samples, *J Pharm Res Int*, 33, 2021, 218-223.
- [6] A.A. Shamilov, D.N. Olennikov, D.I. Pozdnyakov, V.N. Bubenchikova, E.R. Garsiya, M.V. Larskii, Caucasian blueberry: Comparative study of phenolic compounds and neuroprotective and antioxidant potential of *Vaccinium myrtillus* and *Vaccinium arctostaphylos* leaves, *Life*, 12(12), 2022, 2079.
- [7] M. Abidov, A. Ramazanov, M. Jimenez Del Rio, I. Chkhikvishvili, Effect of Blueberin on fasting glucose, C-reactive protein and plasma aminotransferases, in female volunteers with diabetes type 2: double-blind, placebo controlled clinical study, *Georgian Med News*, 141, 2006, 66–72.
- [8] S. Silva, E.M. Costa, M.F. Pereira, M.R. Costa, M.E. Pintado, Evaluation of the antimicrobial activity of aqueous extracts from dry *Vaccinium corymbosum* extracts upon food microorganism, *Food Control*, 34(2), 2013, 645-650.
- [9] T. Jurikova, S. Skrovankova, J. Mlcek, S. Balla, L. Snopek, Bioactive compounds, antioxidant activity, and biological effects of European cranberry (*Vaccinium oxycoccos*), *Molecules*, 24(1), 2018, 24.
- [10] M. Gharbavi, M. Mousavi, M. Pour-Karim, M. Tavakolizadeh, A. Sharafi, Biogenic and facile synthesis of selenium nanoparticles using *Vaccinium arctostaphylos* L. fruit extract and anticancer activity against *in vitro* model of breast cancer, *Cell Biol Int*, 46(10), 2022, 1612-1624.
- [11] B. Nickavar, G. Amin, Anthocyanins from *Vaccinium arctostaphylos* berries, *Pharm Biol*, 42(4-5), 2004, 289-291.
- [12] F.A. Ayaz, S. Hayirlioglu-Ayaz, J. Gruz, O. Novak, M. Strnad, Separation, characterization, and quantitation of phenolic acids in a little-known blueberry (*Vaccinium arctostaphylos* L.) fruit by HPLC-MS, *J Agr Food Chem*, 53, 2005, 8116–8122.
- [13] R. Rangarajan, R. Venkataraman, Antibiotics targeting Gram-negative bacteria, In *Drug Discovery Targeting Drug-Resistant Bacteria*, Editors: P. Kesharwani, S. Chopra, A. Dasgupta, 2020, United Kingd, Andre Gerhard Wolff.
- [14] W. Brand-Williams, M.E. Cuvelier, C. Berset, Use of a free radical method to evaluate antioxidant activity, *Lwt-Food Sci Technol*, 28 (1), 1995, 25–30.
- [15] I.F.F. Benzie, J.J. Strain, The ferric reducing ability of plasma (FRAP) as a measure of “antioxidant power”: the FRAP assay, *Anal Biochem*, 239 (1), 1996, 70–76.
- [16] K. Slinkard, V.L. Singleton, Total phenol analysis: Automation and comparison with manual methods, *Am J Enol Viticult*, 28, 1977, 49–55.
- [17] L.R. Fukumoto, G. Mazza, Assessing antioxidant and prooxidant activities of phenolic compounds, *J. Agric. Food Chem*, 48 (8), 2000, 3597–3604.
- [18] M. Çimen, A.Ö. Düzgün, Antibiotic induced biofilm formation of novel multidrug resistant *Acinetobacter baumannii* ST2121 clone, *Acta Microbiol Imm H*, 68, 2020, 80–86.
- [19] Z. Yu, Y. Yin, W. Zhao, J. Liu, F. Chen, Anti-diabetic activity peptides from albumin against  $\alpha$ -glucosidase and  $\alpha$ -amylase, *Food Chem*, 135, 2012, 2078–2085.
- [20] M. Mahboubi, N. Kazempour, M. Taghizadeh, *In vitro* antimicrobial and antioxidant activity of *Vaccinium arctostaphylos* L. extracts, *J Biol Active Prod Nature*, 3(4), 2013, 241-247.
- [21] A.K. Musavi, M. Mazandarani, S. Rahimian, M. Ghafourian, Ecological Requirement, Ethnopharmacology, Phytochemical and Antioxidant Capacity of *Vaccinium arctostaphylos* L. in Gilan Province (North of Iran), *J Med Plants By-Prod*, 5(1), 2016, 89-95.
- [22] T. Hasanloo, R. Sepehrifar, H. Hajimehdipoor, Levels of phenolic compounds and their effects on antioxidant capacity of wild *Vaccinium arctostaphylos* L.(Qare-Qat) collected from different regions of Iran, *Turk J Biol*, 35(3), 2011, 371-377.
- [23] A. Güder, M.S. Engin, M. Yolcu, M. Gür, Effect of Processing Temperature on the Chemical Composition and Antioxidant Activity of *Vaccinium Arctostaphylos* Fruit and Their Jam, *J Food Process Pres*, 38(4), 2014, 1696-1704.
- [24] A.M. Feshani, S.M. Kouhsari, S. Mohammadi, *Vaccinium arctostaphylos*, a common herbal medicine in Iran: molecular and biochemical study of its antidiabetic effects on alloxan-diabetic Wistar rats, *J Ethnopharmacol*, 133(1), 2011, 67-74.
- [25] B. Ozturk, O. Karakaya, S.M. Celik, M. Karakaya, S.K. Guler, T. Yartilgac, H. Aydın, A. Ozturk, The effect of cold storage on the bioactive components and physical properties of caucasian whortleberry (*Vaccinium arctostaphylos* L.) a preliminary study, *Acta Sci Pol-Hortoru*, 15(2), 2016, 77-93.
- [26] Ö. Saral, Z. Ölmez, Comparison of antioxidant properties of wild blueberries (*Vaccinium arctostaphylos* L. and *Vaccinium myrtillus* L.) with cultivated blueberry varieties (*Vaccinium corymbosum* L.) in Artvin region of Turkey, *Turk J Agric-Food Sci Tech*, 3(1), 2015, 40-44.
- [27] I.M. Famuyide, A.O. Aro, F.O. Fasina, J.N. Eloff, L.J. McGaw, Antibacterial and antibiofilm activity of acetone leaf extracts of nine under-investigated south African *Eugenia* and *Syzygium* (Myrtaceae) species and their selectivity indices, *Bmc Complem Altern M*, 19, 2019, 1-13.
- [28] C. De La Fuente-Núñez, V. Korolik, M. Bains, U. Nguyen, E.B.M Breidenstein, S. Horsman, S. Lewenza, L. Burrows, R.E.W. Hancock, Inhibition Of Bacterial Biofilm Formation And Swarming Motility By A Small Synthetic Cationic Peptide, *Antimicrob Agents Ch*, 56(5), 2012, 2696.
- [29] M. Jamal, W. Ahmad, S. Andleeb, F. Jalil, M. Imran, M.A. Nawaz, T. Hussain, M. Ali, M. Rafiq, M.A. Kamil, Bacterial biofilm and associated infections, *J Chin Med Assoc*, 81(1), 2018, 7–11.
- [30] A. Romulo, Z. Ea, J. Rondevaldova, L. Kokoska, Screening of *in vitro* antimicrobial activity of plants used in traditional Indonesian medicine, *Pharm Biol*, 56(1), 2018, 287–93.
- [31] I.C. de O. Ribeiro, E.G.A. Mariano, R.T. Careli, F. Morais-Costa, F.M. de Sant’Anna, M.S. Pinto, M.R. de Souza, E.R. Duarte, Plants Of The Cerrado With Antimicrobial Effects Against *Staphylococcus* Spp. And *Escherichia coli* from Cattle, *Bmc Vet Res*, 14(1), 2018, 32.
- [32] S. Kumar, S. Narwal, V. Kumar, O. Prakash,  $\alpha$ -glucosidase inhibitors from plants: A natural approach to treat diabetes, *Pharmacogn Rev*, 5(9), 2011, 19.
- [33] B. Barut, E.N. Barut, S. Engin, A. Özel, F.S. Sezen, Investigation of the Antioxidant,  $\alpha$ -Glucosidase Inhibitory, Anti-inflammatory, and DNA Protective Properties of *Vaccinium arctostaphylos* L., *Turk J Pharm Sci*, 16(2), 2019, 175–183.





# Validation study on spectrophotometric measurement of ethanol from beer and non-alcoholic beer samples distilled by micro steam distillation method

Arda Akdoğan , Cemalettin Baltacı\* 

Gümüşhane University, Faculty of Engineering and Natural Sciences, Department of Food Engineering, 29100, Gümüşhane, Türkiye

## Abstract

In this study, a new spectrophotometric method based on the oxidation of sodium dichromate was proposed for the determination of ethanol percentage (v/v) in beer and non-alcoholic beer after distillation with the micro water vapor method, and the method was validated with various parameters. The Harmonized Guidelines for Single-Laboratory Validation of Methods of Analysis were used to validate the analytical method we provided. The following aspects of the method were assessed: precision, recovery, linearity, measuring range, limit of detection (LOD), limit of quantification (LOQ), method detection limit (MDL), and measurement uncertainty. The LOD, LOQ, and MDL values obtained for ethanol were 0.04%, 0.05%, and 0.15%, respectively. The relative standard deviation (RSD) values were less than 2.36% and 4.12% for both repeatability and within-laboratory reproducibility, respectively. Recovery percentages of analytes added to the sample at certain levels were determined to be quantitative between 97% and 102%. These findings fulfill the minimal performance standards outlined in AOAC Official Methods of Analysis Appendix F: Guidelines for Standard Method Performance Requirements. In conclusion, the method validated with various parameters in this study has proven to be effectively usable for the routine analysis of ethanol in beer and non-alcoholic beer. This developed analysis method stands out as an innovative approach in terms of collecting ethanol from beers with the help of micro-distillation water vapor and measuring the color resulting from oxidation.

**Keywords:** Beer, ethanol, method validation, micro water vapor distillation, non-alcoholic beer

## 1. Introduction


One of the first known alcoholic beverages, beer, is made from cereals fermented by yeast [1]. Low- or non-alcoholic beer is produced by reducing the alcohol content or eliminating the ethanol in alcoholic beer using a variety of techniques involving physical and biological procedures. Thermal and membrane techniques are examples of physical procedures. The varying volatilities of ethanol and water serve as the basis for the thermal processes of distillation, falling film evaporator, and spinning cone columns. The four types of membrane-based processes include pervaporation, osmotic distillation, dialysis, and reverse osmosis. The idea behind the biological method is to use particular yeasts or limit the amount of ethanol produced by partial fermentation [2].

Due to regulatory restrictions on drivers' alcohol consumption, sports, diet (calorie intake), and health concerns, there has been a surge in interest in non-alcoholic and low-alcoholic beer in recent years [3]. As a

result, the brewing industry's market for producing non-alcoholic beer is growing [4]. Beer is a widely consumed alcoholic beverage that has different legal definitions in different nations. The legal restrictions on the alcohol by volume (ABV) of non-alcoholic and low-alcoholic beer vary across nations. Beers with low alcohol content are divided into two categories in the majority of EU countries: non-alcoholic beer with an ABV of less than or equal to 0.5% and low-alcoholic beer with an ABV of no more than 1.2% [5]. According to Turkish law, the ABV of low-alcoholic beer and non-alcoholic beer is less than 0.5%, and 0.5–3.0%, respectively.

Numerous beers with varying alcohol percentages are available on the market. In the brewing sector, it's critical to precisely and properly determine the alcohol concentration for several reasons, including compliance with laws, label verification, quality control, and production consistency [6]. Various techniques, including physical and biological procedures, have been

**Citation:** A. Akdoğan, C. Baltacı, Validation study on spectrophotometric measurement of ethanol from beer and non-alcoholic beer samples distilled by micro steam distillation method, Turk J Anal Chem, 6(1), 2024, 32–39.

 <https://doi.org/10.51435/turkjac.1498318>

**Author of correspondence:** [cbaltaci11@gmail.com](mailto:cbaltaci11@gmail.com)

**Received:** June 9, 2024

**Tel:** +90 (456) 233 17 93

**Accepted:** June 21, 2024

**Fax:** N/A

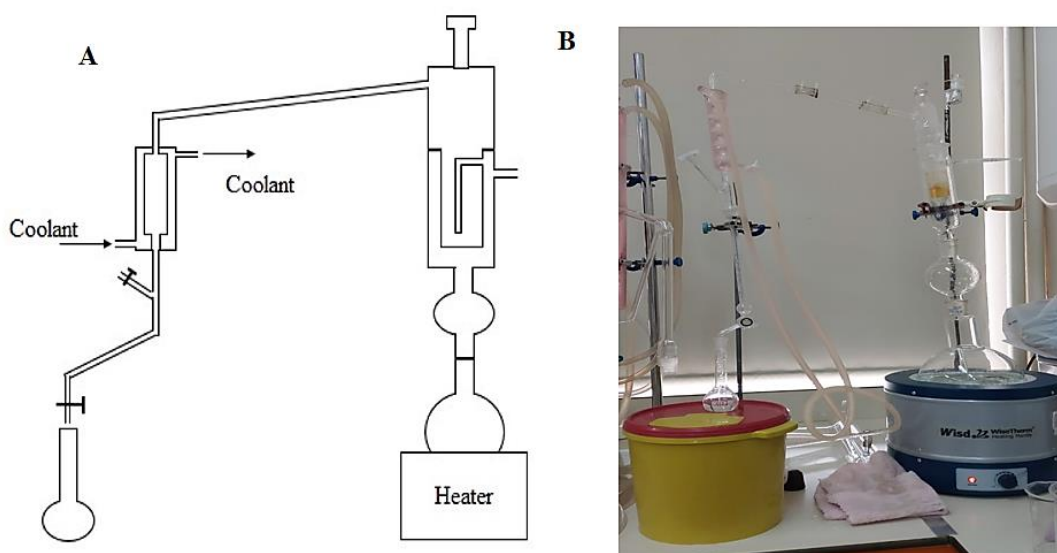


**Figure 1.** Micro water vapor distillation apparatus (A) diagram and (B) picture

proposed in the literature to reduce or eliminate the alcohol content in alcoholic beer to produce low-alcohol or non-alcoholic beer. [7–10].

There are different methods for determining the alcohol content of beer. Beer's ethanol concentration can be found by enzymatic analysis [11], distillation, refractometry [12], gas chromatography [13], catalytic combustion and near-infrared spectroscopy [14]. Volumetric and gravimetric measurements of the distillate's specific gravity serve as the foundation for the distillation process. The distillate is measured both gravimetrically and volumetrically using the labor-intensive conventional distillation method. The spectrophotometric approach uses color to quantify absorbance in the materials. Measuring mistakes can therefore be decreased, in contrast to volumetric and gravimetric approaches.

As a result, the innovative approach of the research is that it can determine the ethanol concentration in a very small sample fraction with an effective model design. Therefore, the study aims to determine the ethanol content in traditional fermented alcoholic beverages spectrophotometrically based on sodium dichromate oxidation after extraction from beer by micro water vapor distillation and to validate the method.

## 2. Materials and methods

The alcohol in beer was rapidly distilled with the micro water vapor distillation method in this study. Instead of volumetric and gravimetric measurements of distillate, it aimed to determine the alcohol content of beer samples with the standard curve by measuring absorbance with a spectrophotometer. The method was based on a reaction between ethanol and sodium dichromate

forming green-colored chromate ions in the presence of sulfuric acid and acetate buffer.

### 2.1. Sample

Yeast (*Saccharomyces cerevisiae*) and malt extract (Pilsner, Muntions Plc, Cedar Maltings Stowmarket, Suffolk, UK) were used in this study. After adjusting the malt extract/water ratio recommended by the manufacturer, the yeast was fermented at 20 °C. A custom-made, airtight fermentation tank (SAIER Verpackungstechnik GmbH & Co. KG, Alpirsbach, Germany) equipped with temperature monitoring capabilities was used for this purpose. Once fermentation was complete, the samples were bottled and kept at +4 °C until needed. Beer and non-alcoholic beer samples were collected from markets in Trabzon and Gümüşhane. All samples were stored at +4 °C until analysis.

### 2.2. Chemicals and devices

HPLC-grade solvents and analytical chemicals were supplied by Merck company (Darmstadt, Germany). The standard ethanol (99.99%) was provided by Sigma-Aldrich (St. Louis, Missouri, United States). A UV-Vis 1800 spectrophotometer device was used (Shimadzu, Kyoto, Japan) for the quantitative analysis.

### 2.3. Determination of ethanol

A spectrophotometric approach based on the oxidation of sodium dichromate was used to analyze ethanol. After adding a 5 mL aliquot of beer to the sample cell, micro water vapor distillation was carried out until 25 mL of distillate was collected (Fig. 1).

Following a 2-hour incubation period at room temperature, 500 µL of sodium dichromate (40 mg/L), 500 µL of sodium acetate buffer (pH 4.60) solution, and 2.5 mL of 1 N H<sub>2</sub>SO<sub>4</sub> were added to 500 µL of the distillate sample. The samples' absorbance was then

measured in the UV-Vis spectrophotometer at 578 nm. The standard curve was created using ethyl alcohol standards at various concentrations (0.10, 0.25, 0.50, 1.00, and 2.00% (v/v)) [15].

#### 2.4. Method validation

Validating methods for ethanol detection in beer samples is crucial for accurate and reliable results.

A method's selectivity defines its capacity for detection. Sensitivity means the smallest analyte concentration that the method could reliably measure and also indicates the method's ability to detect low levels of ethanol in the samples. Linearity evaluates the relationship between the concentration of ethanol in the sample and the response of the detection method. It confirms that the method produces results directly proportional to the current ethanol concentration. Linearity evaluates the relationship between the concentration of ethanol in the sample and the response of the detection method. It confirms that the method produces results that are directly proportional to the current ethanol concentration. Ethanol was used in the study at concentrations of 0.10%, 0.25%, 0.50%, 1.00%, and 2.00%.

The limit of detection, or LOD for short, is the lowest analyte concentration that any technique can detect, and also LOD aids in figuring out the method's realistic detection limit. LOD can be calculated by taking 3 times the standard deviation (SD) [16]. Experiments were conducted using a sample that contained 0.15% ethanol to validate the methodology suggested in this study. Ten times the SD can be used to derive the limit of quantification, or LOQ for short, which is the lowest concentration that can be quantitatively measured at a certain confidence level [16]. A sample containing 0.1% ethanol was prepared and examined to determine the LOQ value. The SD value of the results was multiplied 10 times and the LOQ was calculated. Additionally, the SD value was multiplied by the *t*-value to calculate the method detection limit (MDL) at a certain confidence level.

Precision measures the variability of data acquired under various situations (e.g., different analysts, instruments, or days) to assess the repeatability and intermediate precision of the procedure. The term SDR, or Standard Deviation of Reproducibility, describes the standard deviation that is linked to a measurement method's reproducibility. It also measures the variation in results that arises when various operators, tools, or labs carry out the same measurement in identical circumstances.

Relative standard deviation of reproducibility (RSDr%), a concept related to reproducibility, is calculated by dividing the SDR (standard deviation of repeatability) measurements by the mean value and

multiplying the result by 100. %RSDr is useful for SDR, a standard deviation related to the repeatability of a measurement method. SDR quantifies the variability in results that occurs when the same operator, using the same instrument, performs repeated measurements under the same conditions. Relative standard deviation of repeatability (RSDr%), like RSDr%, is the relative standard deviation associated with repeatability. It's calculated by dividing the SDR by the mean value of the measurements and multiplying by 100 to express it as a percentage [16].

The method was applied to ethanol solutions at different concentrations by different analysts on different days, both intraday and interday, and %RSDr intraday and %RSDr interday values were calculated from the results obtained. By calculating the proportion of ethanol that can be recovered from spiked samples in comparison to the expected concentration, recovery assesses the method's accuracy [17,18]. The Horwitz equation estimates the relative standard deviation (RSD) expected when replicating measurements within a laboratory or among different laboratories. This is particularly useful for assessing the precision of analytical methods [18]. Predicted relative standard deviation (PRSDr and PRSDr) is a statistical measure used to estimate the precision or variability of a future set of measurements based on existing data. It is calculated using regression analysis or other statistical methods to predict the variability of future measurements under similar conditions [18].

RSDr% and RSDr% values can be calculated from the equations given in [Formula 1](#) and [Formula 2](#) below.

$$PRSDr\% = 2^{1-0.5 \times \log C} \times 0.66 \quad (1)$$

$$PRSDr\% = 2^{1-0.5 \times \log C} \quad (2)$$

Where *C* is the concentration of the measured analyte.

Both formulas should provide an estimate of the repeatability, and reproducibility relative standard deviation as a percentage relative to the concentration of the analyte being measured. For this, three distinct concentrations of recovery, repeatability, and reproducibility tests were carried out by two analysts. Measurement uncertainty accounts for all possible influences on the measurement process, including instrument limits and interference from other substances in samples.

The expanded measurement uncertainty (*U*) was determined by multiplying the combined uncertainty, which encompasses RSDr%, RSDr%, and mean recovery%, by a coverage factor (*k*) of 2 [19].

**Table 1.** Analytical parameters applied in the linearity studies

	Calibration concentration, %				
	1	2	3	4	5
	0.10	0.25	0.50	1.00	2.00
Calibration range, %	0.10 – 2.00				
a	0.0629				
b	0.0012				
R <sup>2</sup>	0.9997				
y = ax + b	y = 0.0629x – 0.0012				
Measurement Range, %	0.10 – 10.00				

### 2.5. Statistical analysis

XLSTAT software (Addinsoft (2024), XLSTAT statistical and data analysis solution, New York, USA, <https://www.xlstat.com>), in conjunction with the Microsoft Excel application. Using the results of the Cochran and Grubbs tests, outliers were examined and eliminated. The least-squares method was used to complete the linear regression model.

## 3. Results and discussion

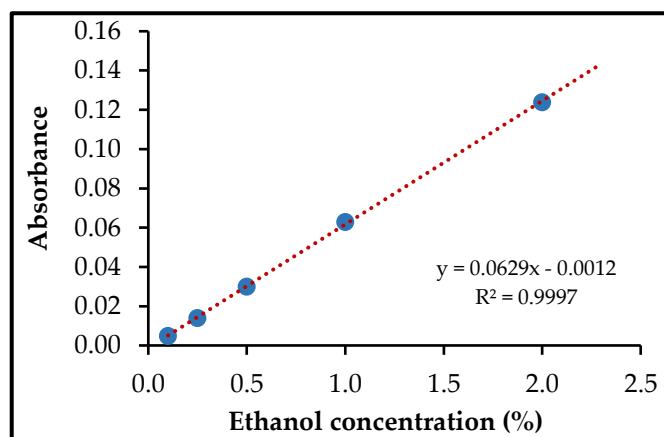
A single laboratory validation was completed by the Harmonized Guidelines for Single-Laboratory Validation of Methods of Analysis. Selectivity, linearity, LOD, LOQ, recovery, precision, and measurement uncertainty metrics were employed as the method's performance characteristics [20].

### 3.1. Selectivity

Selectivity is a crucial aspect of any analytical method, including spectrophotometry. Selectivity refers to the method's ability to distinguish between the analyte of interest and other substances present in the sample matrix. In other words, it determines how specifically the method can detect the target analyte amidst potentially interfering compounds. Ethanol undergoes oxidation by sodium dichromate (Na<sub>2</sub>Cr<sub>2</sub>O<sub>7</sub>) in an acidic medium to form acetic acid and chromium ions. The excess dichromate ions present after the reaction were determined by their absorption at 578 wavelengths using the UV-Vis spectrophotometer. Before initiating the validation phase, the selectivity of the method was evaluated against compounds that occur naturally. The analysis involved comparing the absorbance of representative blank samples (*n* = 10) with that of spiked samples (*n* = 10). The results indicated that at 578 nm, the blank samples exhibited no interference [20].

### 3.2. Linearity and measurement range

Plotting the peak areas of the standard solutions, which were the three series of five distinct concentrations, produced a calibration curve. The formula for the calibration curve is  $y = ax + b$ , where  $x$  is the standard

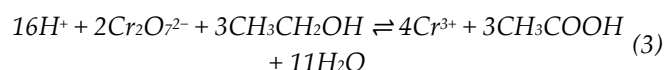
**Figure 2.** Calibration curve for ethanol analysis

solution's concentration in percentage and  $y$  is the standard solution's peak area measured in absorbance. In the studied range, good linearity was found, with an  $R^2$  value greater than 0.999 (Table 1 and Fig. 2) [21,22].

Utilizing mass or volume concentration and other analytical parameters is fundamental in establishing a reliable spectrophotometric analysis method. The mass or volume concentration provides crucial information about the amount of the substance present in the solution, allowing for accurate quantification.

Table 1 displays the standard calibration plot for the suggested procedure. The method yielded a standard calibration plot demonstrating robust linearity within the 0.10–2.00% ethanol range. The standard calibration plot for the recommended method is depicted in Fig. 2.

According to Eq. (1), the colorimetric approach is based on the reaction of ethanol and potassium dichromate in acidic solutions, which produces Cr<sup>3+</sup> and acetic acid [23].



The compound's absorbance was measured to make this approximation. Higher ethanol percentages result in a greater blue color (Cr<sup>3+</sup>); for example, if a molecule appears blue in solution, it presumably absorbs red light, according to Eq. (1) (Fig. 3).

It was discovered that the measurement range operating chart's regression coefficient was higher than 0.995. The F test was used to examine regression at a 95% confidence level. In beer samples, it was discovered to be linear at ethanol concentrations of 0.10–10.00%.

### 3.3. Limit of detection and limit of quantification

The exact LOD and LOQ values are determined by several variables, such as the analyte's unique properties, sample matrix, instrument sensitivity, and analytical technique employed.

**Table 2.** Analytical parameters LOD, LOQ and MDL

Spike Concentration = 0.15%				
	Analyst 1	Analyst 2	Ethanol (%)	Recovery (%)
Sample 1	0.15	0.17	0.16	107.67
Sample 2	0.13	0.20	0.17	111.03
Sample 3	0.10	0.18	0.14	93.33
Sample 4	0.18	0.10	0.14	92.33
Sample 5	0.19	0.14	0.16	109.83
Sample 6	0.12	0.15	0.13	88.50
Sample 7	0.14	0.16	0.15	100.47
Sample 8	0.14	0.17	0.15	102.50
Sample 9	0.10	0.15	0.13	84.70
Sample 10	0.15	0.19	0.17	113.33
<b>Mean</b>	<b>0.15</b>			
<b>Std Dev.</b>	<b>0.02</b>			
<b>MDL %</b>	<b>0.04</b>			
<b>LOD %</b>	<b>0.05</b>			
<b>LOQ %</b>	<b>0.15</b>			
Spike Level (10xMDL>Spike):		0.43 >0.15		OK, Meets Criteria
Spike Level (MDL<Spike)		0.04 <0.15		OK, Meets Criteria
S/N Estimate (ave./sd):		9.88 <10		OK, Meets Criteria
Ave. % Recovery (98–102%)		100.37		Acceptable

Higher sensitivity is indicated by lower LOD and LOQ values, which is advantageous in many analytical applications, especially in environmental sectors. The lowest concentration of an analyte that can be accurately identified but not always measured is known as the limit of detection, or LOD. The smallest concentration of analytes yields a signal that stands out from the noise. The concentration corresponding to a signal-to-noise ratio (S/N) 3:1 is typically used to calculate LOD.

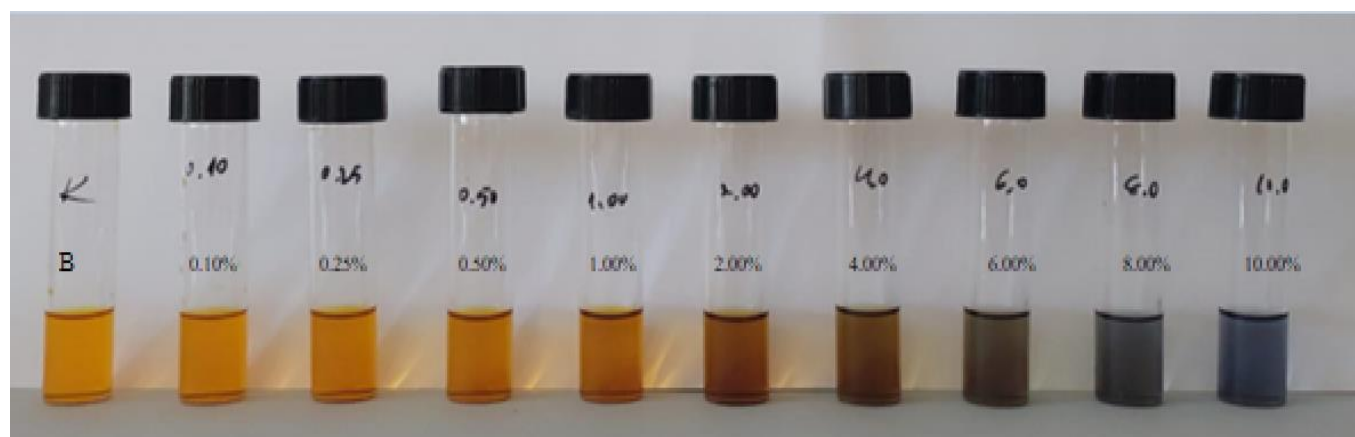
As stated above, the lowest concentration of an analyte at which a measurement can be made with sufficient accuracy and precision is known as the limit of quantification, or LOQ. Typically, the concentration that corresponds to a 10:1 or 3:1 signal-to-noise ratio is used to calculate it. The LOD and LOQ values of the technique were determined by analyzing ten blank samples that had been fortified with 0.15% ethanol. In compliance with the Analytical Detection Limit Guidance [24], the LOD and LOQ values were established.

The SD of the response (s) values was computed by three points three times the response SD to estimate the LOD. Additionally, the projected LOD values were

confirmed in compliance with the guidelines [24]. Ten times the response SD was used to calculate the LOQ values. The LOD values for ethanol were identified at 0.05%. The MDL values were established at 0.04%, and the LOQ values were determined to be 0.15% (Table 2). The LOD and LOQ values in a study on the analysis of ethanol in beers were determined to be 0.09% and 0.27%, respectively [23].

### 3.4. Precision

In the precision study, the concentrations were determined according to the maximum and minimum alcohol contents of beers listed in TGK 2006/33 (Low-alcohol beer, non-alcoholic beer, lager, and high-alcohol beer) [20]. Six blank samples treated with ethanol at 0.5%, 3.0%, and 6.0% levels were examined to measure precision. For the repeatability test, samples were prepared in six repetitions, and the same operators finished the analyses in a single day. To determine the within-laboratory repeatability, ten replicate samples were assessed over three days by two different operators over a month.

**Figure 3.** Color pictures with an alcohol percentage of 0.10–10.00%

**Table 3.** Analytical parameters RSD<sub>r</sub>% and RSD<sub>R</sub>%

Analyte	Intra-day (n=6)				Inter-day (n=6)				
	Fortification level (%)	Determination level (%)	SD <sub>r</sub> (%)	Precision RSD <sub>r</sub> (%)	0.66×Horwitz value	Determination level (%)	SD <sub>R</sub> (%)	Precision RSD <sub>R</sub> (%)	Horwitz value
					PRSD <sub>r</sub> (%)				PRSD <sub>R</sub> (%)
Ethanol	0.5 <sup>a</sup>	0.49	0.01	2.36	2.94	0.50	0.020	4.12	4.45
	3.0 <sup>b</sup>	2.94	0.05	1.85	2.24	2.95	0.032	3.19	3.40
	6.0 <sup>c</sup>	5.96	0.10	1.65	2.02	6.03	0.026	2.65	3.05

a: % Alcohol by volume (20 °C): Low alcohol beer > 0.50, <3.0 and Non-alcoholic beer < 0.50 %, b: % Alcohol by volume (20 °C): Beer > 3.00, <6.0% c: % Alcohol by volume (20 °C): High alcohol beer > 6.00, <10.0% (TGK 2006/33, 2006)

Table 3 displays the results for the within-laboratory reproducibility represented with SD<sub>R</sub> (reproducibility SD), RSD<sub>R</sub>% (relative SD), the repeatability stated with the SD<sub>r</sub> (Repeatability SD), and the relative SD (RSD<sub>r</sub>%). PRSD<sub>r</sub>% and PRSD<sub>R</sub>% values predicted by the Horwitz equation cannot be exceeded by reproducibility (RSD<sub>r</sub>%) and repeatability (RSD<sub>R</sub>%) values acquired from experimental tests.

RSD<sub>r</sub>% and RSD<sub>R</sub>% values of experimental studies were found to be lower than the reference values (Table 3) obtained by applying the Horwitz equation at each of the three concentration levels. These results demonstrated that the proposed method meets the defined minimal performance threshold for Horwitz values PRSD<sub>r</sub>% and PRSD<sub>R</sub>%. Therefore, the precision of the approach is sufficient.

$$\text{Reproducibility limit} = 2.8 \times \text{SD}_R \quad (4)$$

The repeatability limit of the analysts was determined using the calculation in Formula 3, and it was discovered to be appropriate for the investigated 0.5%, 3.0%, and 6.0% concentrations. Furthermore, it was discovered that the general repeatability control was appropriate for the identical concentrations under investigation.

The RSD<sub>R</sub>% value was determined to be less than 5% in the interday repeatability investigation on ethanol analysis in beers [23]. Repeatability results in another study ranged from 0.47 to 0.62% [26].

### 3.5. Recovery

Table 4 provides analytical parameters for recovery percentages. To conduct the recovery investigation, samples that had been spiked with ethanol at three distinct concentrations (0.5%, 3.0%, and 6.0% low alcohol beer, non-alcoholic beer, beer, and high alcohol beer)

were generated. The suggested procedure for determining the amount of ethanol in beer was applied to the six replicates of the spiked samples. The recovery values obtained (Table 4) fell between 97% and 103% of the values advised by the Association of Analytical Societies (AOAC) in 2016. Thus, it can be concluded that the suggested method for determining the amount of ethanol in beer and nonalcoholic beer samples produced satisfactory findings [18].

In the recovery investigation, samples were treated with varying quantities of ethanol. The amount of ethanol in the beers was then measured through analysis, and a percentage of recovery was computed. Between 97% and 103% of the values advised by the AOAC (2016) were found to be recovery values from this procedure [18]. This demonstrates that the approach yields acceptable outcomes. A recovery number of 97% to 103% shows that the procedure is accurate because the spiked samples recover almost the expected amount of ethanol. This is a good result since it demonstrates that the method can accurately detect the quantity of ethanol in beers that fall within the designated concentration levels. Achieving recovery percentage values near 100% is typically preferred in analytical chemistry since it shows that the technique analyzes the target analyte precisely and without experiencing appreciable loss or interference.

Consequently, outcomes falling within this range show that the method is reliable and appropriate for figuring out how much ethanol is in beer.

### 3.6. Measurement uncertainty

According to ISO 17025/2017 [27], laboratories that are accredited must evaluate the uncertainty of their analytical results. Various methods have been offered for calculating this uncertainty, including the Eurachem/Citac Guide CG 4 [28], and NMKL 4 [29].

**Table 4.** Analytical parameters of recovery %

Analyte	Fortification level, %	Recovery, % (n= 6)			
		Low-alcohol beer Recovery, %	Non-alcoholic beer Recovery, %	Beer Recovery, %	High Alcohol Beer Recovery, %
Ethanol	0.5	102.00 ± 1.91	98.40 ± 1.48	99.40 ± 1.43	97.65 ± 1.67
	3.0	98.85 ± 1.21	98.84 ± 1.33	98.76 ± 1.54	98.41 ± 1.54
	6.0	99.53 ± 1.11	98.53 ± 1.13	98.12 ± 1.66	98.54 ± 1.53

**Table 5.** Analytical parameters of measurement uncertainty

Measurement Uncertainty			
Parameter	Value (X)	u(X)	u(X)/X
Trueness (bias)	100.00	0.34	0.003
Repeatability	100.00	2.36	0.024
Reproducibility	100.00	4.12	0.041
Relative combined uncertainty =			0.048
* Expanded measurement uncertainty) =			0.095

\*95% confidence level,  $k = 2$

We employed the analytical validation parameters that were derived at each stage of the procedure in this investigation. Table 5 provides analytical parameters for measurement uncertainty. Measurement uncertainty estimation was performed using data from method performance and validation.

As a result, the likelihood of incorporating every uncertainty component has peaked. Six sources of uncertainty have been considered in order to determine the relative uncertainty (u): (a) volume; (b) mass; (c) calibration curve; (d) technique reproducibility and repeatability; (e) preparation of standards, and (f) precision. Using a coverage factor of 2, which roughly corresponds to a 95% confidence level (Eurachem/Citac Guide CG 4 2000), a relative expanded measurement uncertainty was computed, yielding values of 9.5% (0.095) in beers [28].

### 3.7. Analysis results of beers purchased from the market

Table 6 provides information on the ABV of samples of non-alcoholic beer and beer that is purchased commercially. The ABV values of the non-alcoholic beer samples are significantly lower, ranging from roughly 0.47% to 0.50%, compared to the beer samples, which have ABV values between 4.96% and 5.05%.

The alcohol content is the main distinction between market-bought beer and non-alcoholic beer. The ABV of regular beers usually ranges from 0.5% to 6.0% [25,30]. By contrast, non-alcoholic beers have an ABV of less than 0.5%, about the same as orange juice's alcohol concentration. According to research on the alcohol content of Turkish beers, the ethanol percentage was found to be between 4.2% and 5.2% [31].

## 4. Conclusions

A spectrophotometric technique based on the distillation of ethanol by micro water vapor distillation followed by sodium dichromate oxidation was developed to quantify the quantity of ethanol present in beer matrices. It was discovered that the method's performance characteristics met the minimal requirements set forth by the Harmonized Guidelines for Single-Laboratory Validation of Methods of Analysis. The verified approach offers quick and affordable procedures along with precise and accurate results.

**Table 6.** Alcohol analysis results of commercially purchased non-alcoholic beer and beer samples ( $n = 3$ )

Sample	Alcohol ABV (%)
Sample 1 beer	5.04 ± 0.03
Sample 2 beer	5.02 ± 0.06
Sample 3 beer	4.99 ± 0.03
Sample 4 beer	5.05 ± 0.02
Sample 5 beer	4.96 ± 0.01
Sample 6 beer	4.98 ± 0.03
Sample 7 non-alcoholic beer	0.48 ± 0.03
Sample 8 non-alcoholic beer	0.50 ± 0.02
Sample 9 non-alcoholic beer	0.47 ± 0.02
Sample 10 non-alcoholic beer	0.50 ± 0.02

With sample preparation and detection processes, the suggested method is ideally suited to meet the needs for sensitive and accurate ethanol beer detection. The method demonstrates high sensitivity, allowing for the detection of ethanol in beer matrices even at low concentrations. This sensitivity is important for meeting regulatory requirements and ensuring product compliance. Overall, the described spectrophotometric technique offers a robust and efficient approach for quantifying ethanol in beer matrices, meeting the requirements for method validation and providing reliable results for quality control purposes.

## Funding

The TÜBİTAK (Turkish Scientific and Technological Research Council)-funded were supported the project titled "Using Ohmic Assisted Vacuum Evaporation System in Non-Alcoholic Beer Production", Project No. 222O168.

## Declarations

Approval from an Ethical Perspective: There are no research involving humans or animals in this article.

This study was produced from the doctoral thesis of the Arda Akdoğan.

Permission to Publish: To publish this work, the writers consented.

Conflicting Interests: There are no pertinent financial or non-financial interests that the authors need to disclose.

## References

- [1] V. Popescu, A. Soceanu, S. Dobrinan and G. Stanciu, A study of beer bitterness loss during the various stages of the Romanian beer production process, *J Inst of Brew*, 119, 2013, 111–115.
- [2] P. S. Horacio, B. A. Veiga, L. F. Luz, C. A. Levek, A. R. de Souza and A. P. Scheer, Simulation of vacuum distillation to produce alcohol-free beer, *J Inst of Brew*, 126, 2020, 77–82.
- [3] S. Sohrabvandi, S. M. Mousavi, S. H. Razavi, A. M. Mortazavian and K. Rezaei, Alcohol-free beer: methods of production,

- sensorial defects, and healthful effects, *Food Rev Int*, 26 2010, 35–352.
- [4] R. Halama, P. Broz, P. Izak, M. Kacirkova, M. Dienstbier and J. Olsovská, Beer dealcoholization using pervaporation, *Kvasny Prumysl*, 65, 2019, 65–71.
- [5] C. A. Blanco, C. Andres-Iglesias and O. Montero, 2016, Low-alcohol beers: flavor compounds, defects, and improvement strategies, *Crit Rev in Food Sci and Nut*, 56, 2016, 1379–1388.
- [6] L. Cloninger, Alcohol determination of malt-based beverages by rapid distillation, *J Am Soc Brew Chem*, 76, 2018, 21–23.
- [7] M. Catarino, A. Mendes, Non-alcoholic beer-a new industrial process. *Sep Puri Technol*, 79, 2011, 342–351.
- [8] C. Andres-Iglesias, J. Garcia-Serna, O. Montero, C.A. Blanco, Simulation and flavor compound analysis of dealcoholized beer via one-step vacuum distillation, *Food Res Int*, 76, 2015, 751–760.
- [9] Z. M. Jiang, B. Y. Yang, X. Liu, S. Zhang, J. Shan, J. Liu, X. R. A.Wang, A novel approach for the production of a non-alcohol beer ( $\leq 0.5\%$  abv) by a combination of limited fermentation and vacuum distillation, *J Inst Brew*, 123, 2017, 533–536.
- [10] M. Catarino, A. Mendes, L. M. Madeira, A. Ferreira, Alcohol removal from beer by reverse osmosis, *Sep Sci Technol*, 42, 2007, 3011–3027.
- [11] E. Akyilmaz, and E. Dinçkaya, Development of a catalase based biosensor for alcohol determination in beer samples, *Talanta*, 61, 2003, 113–118.
- [12] S. Castritius, A. Kron, T. Schäfer, M. Rädle, D. Harms, Determination of alcohol and extract concentration in beer samples using a combined method of near-infrared (NIR) spectroscopy and refractometry, *J Agr Food Chem*, 58, 2010, 12634–12641.
- [13] G. K. Buckee, A. P. Mundy, Determination of ethanol in beer by gas-chromatography (direct-injection) - collaborative trial, *J Inst Brew*, 99,1993, 381–384.
- [14] S. Engelhard, H. G. Löhmannsröben F. Schael, Quantifying ethanol content of beer using interpretive near-infrared spectroscopy, *Appl Spectrosc*, 58, 2004, 1205–1209.
- [15] S. Sumbhate, S. Nayak, D., A. GouplaeTlwarl, R.S. Jadon, Colorimetric method for the estimation of ethanol in alcoholic-drinks, *J Anal Tech*, 1, 2012, 1–6.
- [16] C. Baltacı, Z. Aksit, Validation of HPLC Method for the determination of 5-hydroxymethylfurfural in pestil, köme, jam, marmalade and pekmez, *Hittite Journal of Science & Engineering* 3, 2016, 91–97
- [17] ISO 5725, 1994, Accuracy (Trueness and Precision) of Measurement Methods and Results”, Parts 1-6, International Standard ISO 5725-1:1994, 5725-2:1994, 5725-3:1994, 5725-4:1994, 5725-5:1994, and 5725-6:1994. (1994).
- [18] AOAC, 2016, Appendix F: Guidelines for standard method performance requirements. *AOAC Official Methods of Analysis*, 9.
- [19] O. Golge, A. Koluman, B. Kabak, Validation of a modified QuEChERS method for the determination of 167 pesticides in milk and milk Products by LC-MS/MS, *Food Ana Met*, 11, 2018,1122–1148.
- [20] M. Thompson, S.L.R. Ellison, R. Wood, Harmonized guidelines for single laboratory validation of methods of analysis (IUPAC Technical Report), *Pure Appl Chem*, 74, 2002, 835–855.
- [21] N. Phaduncharoen, P. Patrojanasophon, P. Opanasopit, T. Ngawhirunpat, A. Chinsriwongkul, T. Rojanarata, Smartphone-based Ellman’s colourimetric methods for the analysis of d-penicillamine formulation and thiolated polymer, *Int J Pharm*, 558, 2019, 120–127.
- [22] J.N. Miller, Basic statistical methods for analytical chemistry. Part 2. Calibration and regression methods. A review, *Analyst*, 116, 1991, 3–14
- [23] L. Curbani, J. Genlinsky, E. M. Borges, Determination of ethanol in beers using a flatbed scanner and automated digital image analysis, *Food Anal Meth*, 13, 2020, 249–259.
- [24] Analytical Detection Limit Guidance & Laboratory Guide for Determining Method Detection Limits, Wisconsin Department of Natural Resources Laboratory Certification Program, April 1996.
- [25] Turkish Food Codex (2006) Turkish food codex beer communiqué (Communiqué no: 2006/33), Ankara.
- [26] D.W. Lachenmeier, T. Pflaum, A. Nieborowsky, S. Mayer, J. Rehm, Alcohol-free spirits as novel alcohol placebo—A viable approach to reduce alcohol-related harms, *Int. J. Drug Policy*, 32, 2016, 1–2.
- [27] TS EN ISO/IEC 17025., 2017, General requirements for the competence of testing and calibration laboratories, Türk Standartları Enstitüsü Ankara.
- [28] Eurachem/Citac, 2000, Guide CG 4, Quantifying Uncertainty in Analytical Measurement, Third Edition.
- [29] NMKL Procedure No. 4., Validation of chemical analytical methods Page: 1 of 45 Version: 3 Date: June 2009 Approved: Ole Bjørn Jensen.
- [30] K. Bellut, E.K. Arendt, Chance and challenge: non-saccharomyces yeasts in nonalcoholic and low alcohol beer brewing—a review, *J Am Soc Brew Chem*, 77, 2019, 77–91
- [31] O. Destanoğlu, İ. Ateş, Determination and evaluation of methanol, ethanol, and higher alcohols in legally and illegally produced alcoholic beverages, *J Turkish Chem Soci, Section A: Chem*, 6, 2019, 21–28.



## Voltammetric methods for determination of Allura Red AC in foods and beverages

Elif Şişman , Fatma Ağın\* 

Karadeniz Technical University, Faculty of Pharmacy, Department of Analytical Chemistry, 61080, Trabzon, Türkiye

### Abstract

Allura Red AC, is one of the azo group dyes, finds extensive application in foods and beverages such as fruit juices, baked goods, meat products, and confections. The substantial consumption of Allura Red AC has been associated with potential adverse effects on human health, like food intolerance, allergies, cancer, attention deficit hyperactivity disorder, multiple sclerosis, brain damage, cardiac diseases, nausea, and asthma, largely attributed to the reaction involving aromatic azo compounds. Therefore, controlling amount of the Allura Red AC in food and beverage is very crucial. The voltammetric analysis of Allura Red AC offers numerous benefits, including high sensitivity, selectivity, and rapidity. Furthermore, these methods are characterized by their robustness, reproducibility, and user-friendliness. This review is gathered to the comparison of voltammetric methods being in the literature for determination of Allura Red AC in foods and beverages.

**Keywords:** Allura Red AC, cyclic voltammetry, differential pulse voltammetry, square wave voltammetry, stripping voltammetry

### 1. Introduction

The rapid development of the food industry leads a rising number of specific products with certain shape, taste, smell, color, etc. For this reason, to improve the organoleptic properties of foods, various food additives are used such as coloring agents, sweeteners, thickeners and preservatives. Dyes have a special role in this regard, as the taste and quality of food are often associated with its color [1].

The persistent application of such colorants raises significant safety concerns, impacting both human well-being and environmental health. Recognizing the potential for enduring harm stemming from these food colorants, both the European Food Safety Authority and the US Food and Drug Administration have established stringent regulations governing their usage [2]. These regulatory bodies aim to ensure that consumers can enjoy food products being free from harm, defining precise threshold values that indicate safe levels of exposure to these additives [3].

Dyes utilized in food can be classified into two broad categories: natural dyes and synthetic dyes. Natural dyes are derived from plant, animal, or mineral sources. They have been used for centuries to impart color to various foods and beverages [1].

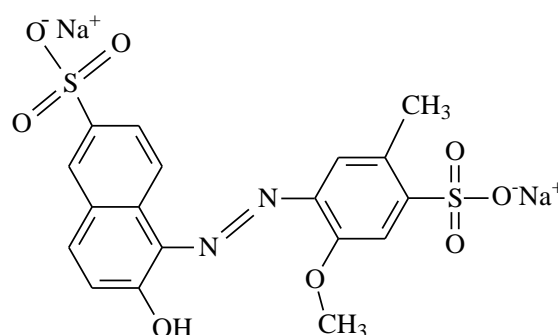


**Figure 1.** Molecular structure of Allura Red AC

Plant-based dyes are obtained from different parts of plants such as roots, berries, leaves, or flowers and they include turmeric (yellow), beetroot (red), spirulina (blue-green), and annatto (yellow-orange). Animal-based dyes; certain dyes are obtained from animal sources, particularly insects. One well-known example is carmine or cochineal, achieved from the bodies of female cochineal insects and provides a red color. Mineral-based dyes: these dyes are obtained from minerals and are often used in the form of pigments. For instance, titanium dioxide is used as a white pigment, and iron oxide provides shades of red, brown, and yellow. Natural dyes are generally considered safe, but they may

have limitations in terms of stability, availability, and color range. Additionally, some individuals may have allergies or sensitivities to specific natural dyes [4].

Synthetic food dyes are chemically synthesized compounds that are specifically designed for use as food colorants. They offer a wide range of colors and are typically more stable compared to natural dyes. These dyes are classified into azo dyes, indigotine dyes, triphenylmethane dyes, xanthene dyes and quinoline dyes. Azo dyes have azo group in the molecular structure as the chromophore, which is largest group of color accounting more than half of global dyes production. They are commonly used in various industries, including the food industry, to enhance the appearance of products. Allura Red AC is one of the mostly used synthetic dyes in food industry that could be found in a variety of food and beverage products, including candies, beverages, and bakery products [5].

Allura Red AC designated as E-129 is a water-soluble monoazo dye, disodium 6-hydroxy-5-(6-methoxy-4-sulfo-m-tolylazo)naphthalene-2-sulfonate (Fig. 1). This synthetic dye has exhibited signs of both behavioral and physiological toxicity in laboratory rats when administered at extremely high doses, exceeding 10% of their diet [6,7]. In the past, numerous studies have investigated the toxicity and carcinogenic effects of Allura Red AC [8,9]. Allura Red AC has the potential to induce behavioral effects in both humans and animals, notably causing increased hyperactivity in children. Furthermore, certain studies have demonstrated the existence of aromatic amide or amine functional groups in the chemical compositions of Allura Red AC's degradation products. Allura Red AC is absorbed through the gastrointestinal tract and then entered the bloodstream, where it binds to proteins during its transportation and metabolism. It is essential to regulate the excessive use of Allura Red AC in food and beverage products. In numerous nations, the utilization of various food dyes, including Allura Red AC, has controlled, or prohibited due to its toxic properties. In the process of safety assessment, Joint FAO/WHO Expert Committee on Food Additives and the European Scientific Committee for Food, are the international scientific expert committees, established an acceptable daily intake for Allura Red AC ranging from 0 to 7 mg/kg of body weight per day. To address human health concerns, numerous analytical methods have been developed for the determination of Allura Red AC [5]. Allura Red AC has been determined by high-performance liquid chromatography [10], spectrophotometry [8], electrophoresis [11] and voltammetry [12].

## 2. Electroanalytical Methods

Electroanalytical methods typically involve in voltammetry, polarography, potentiometry, amperometry, and coulometry. Electroanalytical methods offer several advantages over other instrumental methods in analytical chemistry such as sensitivity, selectivity, speed, cost-effectiveness, and versatility, making them valuable tools for chemical analysis in numerous fields. Among these, voltammetry and polarography stand out as the most frequently employed electroanalytical methods. These techniques enable the identification and evaluating of organic compounds, with a detection limit as low as  $10^{-7}$  M [13].

The voltammetric method effectiveness is influenced via the material of the working electrode, as the reply obtained relies on the electrochemical reactions taking place at the interface between the electrode and the solution. Moreover, it's crucial to take into account both the composition and the structure of the working electrode material, because they can impact on the voltammetric method performance. The physical form of the working electrode may also influence the diffusion and electron transfer processes associated with analyte detection [14–18]. The voltammetric techniques contain cyclic voltammetry (CV), linear sweep voltammetry (LSV), differential pulse voltammetry (DPV), square wave voltammetry (SWV), and stripping voltammetry [19].

CV serves as an initial and frequently employed voltammetric method due to its ability to offer valuable insights into both the thermodynamic and kinetic aspects of various chemical systems. This method excels at swiftly revealing the redox behavior across a broad spectrum of potentials. It stands out as the primary electroanalytical technique for gaining qualitative insights into the electrochemical reactions of electroactive samples [20–21].

LSV represents the most straight forward approach involving the systematic application of a varying potential to the working electrode to monitor changes in current over both potential and time. Also, the applied potential boundaries depend on factors such as the working electrode material, and the supporting electrolyte composition. This method entails a linear progression of the working electrode's potential over time, starting from an initial potential and concluding at a final potential. The direction of the scan rate can be denoted to demonstrate the potential scan direction, with positive for an anodic sweep and negative for a cathodic sweep. LSV is an exceptionally valuable electroanalytical technique, particularly when employing solid electrodes, as it offers swift analysis with a detection limit of approximately  $10^{-6}$  M [22–25].

Pulse methods involve the application of varying potential pulses, with the corresponding current response measured at specific time intervals defined by the pulse duration. The DPV method proves highly effective in the detection of minute quantities of electroactive compounds. The waveform utilized in differential pulse voltammetry typically resembles a staircase. This method involves measuring of current at two key points: initially before the pulse is applied, and then at the end of the pulse. Thus, the differential pulse voltammogram is generated based on as a function of the potential, derived from the disparity between these two current measurements and then the dual current measurement approach enables the detection of analytes in solutions even at low concentrations. Because differential pulse voltammograms exhibit peak shapes, they are particularly well-suited for analytical purposes [26,27].

SWV employs a substantial amplitude differential approach characterized by symmetrical square waveforms. Within this technique, current measurements are taken twice during each cycle of the square wave, specifically at the end of both the forward and reverse pulses. The difference between these current values is graphed against the staircase potential. Peak currents yielded through SWV are nearly quadruple those observed in comparison to differential pulse voltammetry. The priority advantage of square wave voltammetry lies in its rapidity, as it can be completed within a matter of seconds, in contrast to the 2-3 minutes required for a full voltammogram using DPV. This rapidity and sensitivity make SWV particularly valuable for quantitative analyzes [20,28].

Stripping voltammetric techniques have gained significant popularity owing to their low quantification limit (typically around  $10^{-8}$  or  $10^{-9}$  M), as well as their precision, accuracy, and cost-effectiveness when compared to alternative analytical methods. These stripping methods are typically divided into two separate stages. First, there is the electrochemical deposition or accumulation step, during which the electroactive compound accumulates on the working electrode. Following the accumulation step, the subsequent phase is the stripping measurement, which entails the dissolution of the deposited analyte. Stripping voltammetry methods encompass various versions depending on how the preconcentration and stripping steps are applied. When the potential is initially maintained at a negative level before initiating a positive-direction scan, the technique is referred to as anodic stripping voltammetry. Following a predetermined deposition period, the potential is then systematically scanned in an anodic direction using a voltammetric approach. Cathodic stripping

voltammetry involves the anodic deposition of the analyte followed by its stripping during a negative potential scan. In terms of application, cathodic stripping voltammetry can be seen as the inverse of anodic stripping voltammetry [29].

Adsorptive stripping voltammetry offers notable advantages, including heightened sensitivity and superior selectivity when compared to alternative voltammetric techniques. When the concentration step involves adsorption, the method is categorized as adsorptive stripping voltammetry. In the realm of electrochemistry, the process of ions or molecules adhering to the electrode surface is referred to as adsorption. The quantity of adsorbate present on the electrode surface holds significant importance, as it directly influences the voltammetric response. Adsorptive stripping voltammetry stands out for its excellent selectivity and sensitivity, making it particularly well-suited for the precise determination of trace and ultra-trace concentrations of analyte in samples [30,31].

This paper includes studies of the voltammetric analysis of Allura Red AC in foods and beverages, and we have reviewed general voltammetric methods for selective detection of Allura Red AC to ensure the safety of food and beverage products. Voltammetric sensors were developed to detect the presence of Allura Red AC in a wide range of food and beverage products to provide a new perspective. For this purpose, the voltammetric determination studies of Allura Red AC in the literature are assembled, also these studies are chronologically listed in Table 1.

### 3. Voltammetric determination studies for Allura Red AC

A carbon paste electrode (CPE) modified by silica gel impregnated with cetylpyridinium chloride (SG/CPCl) was developed by Pliuta *et al.* This innovative electrode has proven highly effective for the precise determination of Allura Red AC in Britton-Robinson buffer (BRB) solution at pH 2.0. CV was used to examine the redox characteristics of Allura Red AC on the developed sensor, and it showed an oxidation peak at +0.95V. The electro-oxidation of Allura Red AC was defined irreversible and adsorption-controlled process. After the optimal conditions for SWV were determined, the calibration curve exhibited excellent linearity within two concentration ranges: 0.04 – 0.2  $\mu\text{M}$  and 0.2 – 1.0  $\mu\text{M}$  with a low limit of detection of 0.005  $\mu\text{M}$  and a limit of quantification of 0.015  $\mu\text{M}$ . The newly developed sensor has showed satisfactory results in analyzing both model solutions and jelly candies [12].

**Table 1.** The voltammetric studies for determination of Allura Red AC

Electrode Type	Method	Medium	Linear Range ( $\mu\text{M}$ )	LOD ( $\mu\text{M}$ )	Recovery (%)	Ref.
PAMI/GCE	SWV	0.5 M HCl	10.0 – 300.0	1.4	—	[49]
MWCNT/GCE	DPV	PBS, pH 7.0	0.1 – 1.2 ( $r = 0.991$ )	0.05	98.1 – 100.6 (soft drink)	[48]
Gr/TiO <sub>2</sub> /CPE	SWV	0.1 M H <sub>2</sub> SO <sub>4</sub>	0.00067 – 0.21 ( $r = 0.997$ )	0.00034	100.8 – 101.6 (soft drink) 97.12 – 102.1 (sausage)	[40]
IL/EGPE	SWSV	BRB, pH 6.0	0.1 – 10.0 ( $r = 0.999$ )	0.00179	96.0 – 99.2 (soft drink)	[39]
SbF/SPCE	DPV	AcB, pH 4.0	1.0 – 5.0	0.3	—	[50]
MWCNT/IL/GO/GCE	SWSV	BRB, pH 7.0	0.0008 – 0.5	0.0005	100.0 – 106.8 (alcoholic beverages)	[51]
PC/GCE	DPV	PBS, pH 7.0	0.005 – 0.8	0.0034	—	[52]
PDDA/Gr/Ni/GCE	DPV	PBS, pH 3.0	0.05 – 10.0 ( $r = 0.9993$ )	0.008	95.0 – 97.6 (strawberry juice)	[38]
IRGO/Au/GCE	SWV	BRB, pH 5.0	0.0006 – 0.2 ( $r = 0.998$ )	0.00043	—	[53]
CPB/GCE	SWAdSV	PBS, pH 3.3	0.06 – 11.5 ( $r = 0.999$ )	0.032	95.5 (cherry gelatin) 104.2 (chili sauce) 97.85 (strawberry juice)	[37]
MWCNT/GCE	DPV	PBS, pH 6.0	0.1 – 9.0 ( $r = 0.996$ )	0.014	95.0 – 118.0 (red isotonic drink) 94.0 – 130.0 (lilac isotonic drink) 91.5 (chili sauce)	[35]
Co <sub>2</sub> O <sub>4</sub> /CPE	SWV	PBS, pH 3.1	0.1 – 1.0 ( $r = 0.995$ )	0.05	89.7 (isotonic drink) 96.3 (soft drink)	[36]
m-AgSAE	DPAAdSV	—	0.01 – 0.4 ( $r = 0.996$ )	0.0012	—	
p-AgSAE	DCAdSV	AcB, pH 3.6	0.008 – 0.6 ( $r = 0.9926$ )	0.0034	—	[54]
IL/CB/CTS/ECH/GCE	SWAdSV	PBS, pH 4.0	0.0398 – 0.909 ( $r = 0.9998$ )	0.00091	87.5 – 108.3 (soft drink powder)	[33]
TiO <sub>2</sub> /ErGO/GCE	DPV	PBS, pH 7.0	0.3 – 5.0 ( $r = 0.991$ ) 0.01 5.0 – 800 ( $r = 0.992$ )	0.05	98.42 – 106.0 (milk drink)	[34]
Er-BTC/CPE	DPV	PBS, pH 6.0	0.001 – 0.1 ( $r = 0.99$ )	0.0003	—	[47]
SG/CPCI/CPE	SWV	BRB, pH 2.0	0.04 – 0.2 ( $r = 0.992$ ) 0.2 – 1.0 ( $r = 0.998$ )	0.005	—	[12]
Ptre/PGE	DPV	PBS, pH 7.0	0.25 – 100.0 ( $r = 0.992$ )	0.075	98.4 – 99.6 (energy drink) 99.4 – 100.8 (cherry juice)	[32]
MoO <sub>3</sub> /CPE	SWV	PBS, pH 6.5	0.36 – 6.0	0.38	96.0 (gelatin) 95.0 (syrup)	[41]
In <sup>3+</sup> /NiO RLHNSs/GCE	DPV	PBS, pH 4.0	– 700.0 ( $r = 0.9999$ )	0.0041	99.0 – 101.2 (soft drinks) 96.3 – 101.0 (soft drink)	[45]
F-nanodiamond@SiO <sub>2</sub> @TiO <sub>2</sub> /SPE	DPV	BRB, pH 3.0	0.001 – 0.12 ( $r = 0.985$ ) 0.12 – 8.65 ( $r = 0.991$ )	0.00122	95.0 – 106.0 (powder) 95.0 – 102.8 (orange juice) 99.4 – 102.7 (candy)	[43]
Mn <sub>3</sub> O <sub>4</sub> @C/SPM	DPV	—	0.1 – 168.4 ( $r = 0.92441$ ) 168.4 – 1748.4 ( $r = 0.97599$ )	0.033	98.6 – 100.68 (sports drink)	[44]
SHU/PCFE	DPV	PBS, pH 4.0	0.001 – 0.1 ( $r = 0.9988$ ) 0.1 – 2.0 ( $r = 0.9490$ )	0.00036	98.0 – 101.0 (beverages) 100.0 – 105.0 (pharmaceuticals) 100.0 (lollipop)	[42]
ErGO/GCE	DPAAdSV	BRB, pH 2.5	0.1 – 0.8 ( $r = 0.997$ )	0.028	96.2 – 102.3 (soft drink)	[46]

In their study focused on the electrochemical analysis of Allura Red AC, Uruc *et al.* prepared an anodically pretreated pencil graphite electrode (Ptre/PGE) which has oxygen-containing groups. The anodic pretreatment procedure involved the application of a constant potential of +1.8 V for a duration of 250 seconds in pH 9.0 phosphate buffer solution (PBS) accomplished by chronoamperometry method. When the studies were carried out with CV and DPV methods on Allura Red AC in pH 7.0 PBS, a significant and notable increase in the anodic peak current was observed for Ptre/PGE compared to the unmodified PGE. Under optimized conditions for DPV, the calibration curve, reflecting the response of Ptre/PGE to varying concentrations of Allura Red AC, showed a linear relationship within the concentration range from 0.25 to 100  $\mu\text{M}$ , with a limit of detection and limit of quantification values of 0.075  $\mu\text{M}$  and 0.251  $\mu\text{M}$ , respectively. The developed sensor was effectively applied for assessing the presence of Allura Red AC in cherry juice and energy drink samples. It exhibited impressive performance, delivering relative standard deviation values within the range of 1.14%

and recovery rates ranging from 98.4 to 100.8% [32].

In another study, a novel sensor for sensitive voltammetric determination of Allura Red AC and Brilliant Blue FCF was developed by incorporating carbon black (CB) nanoparticles and the ionic liquid (IL) (1-butyl-3-methylimidazolium tetrafluoroborate) within a crosslinked film made from chitosan (CTS) and epichlorohydrin (ECH). This film was applied over the surface of a glassy carbon electrode (GCE), allowing for efficient detection of Allura Red AC in soft drink powders. The electrochemical behavior of the Allura Red AC colorant was examined using CV in PBS at pH 4.0. The analysis revealed an irreversible oxidation peak occurring at approximately +0.9 V. Moreover, the redox process of Allura Red AC on the IL/CB/CTS/ECH/GCE was found to be controlled by a combination of diffusion and adsorption processes. The optimization of experimental parameters effecting the sensor response was carried out systematically using square-wave adsorptive anodic stripping voltammetry (SWAdASV). Under the ideal experimental conditions, the SWAdASV method demonstrated a linear analytical curve within

the concentration range of 0.0398 to 0.909  $\mu\text{M}$ , accompanied by a notably low limit of detection of 0.00091  $\mu\text{M}$ . The precision of the suggested sensor was assessed through intra and inter-day repeatability experiments and relative standard deviations was calculated as 3.5–6.7% and 7.6–11.1%, respectively. Furthermore, interference and recovery experiments were conducted, demonstrating the proposed sensor has good accuracy and selectivity, with recovery values ranging from 87.5 to 108.3% [33].

Li and co-workers prepared an electrochemical sensor by modifying a GCE with titania/electro-reduced graphene oxide nanohybrids ( $\text{TiO}_2/\text{ErGO}$ ) for the detection of Allura Red AC. Notably, when compared to pure ErGO and  $\text{TiO}_2$  nanoparticles, the  $\text{TiO}_2/\text{ErGO}$  nanohybrids exhibited a significant enhancement in electrocatalytic activity and voltammetric response for Allura Red AC. In 0.1 M PBS at pH 7.0, which serves as the optimal supporting electrolyte, Allura Red AC showed an oxidation peak at +0.62 V in DPV. Additionally, cyclic voltammetric studies revealed that the electrochemical oxidation process of Allura Red AC was diffusion-limited quasi-reversible. Using the DPV method, it was observed that within the concentration range of 0.3–5.0  $\mu\text{M}$ , the anodic peak currents of Allura Red AC exhibited a linear correlation with its concentrations. However, this linear relationship shifted to a semi-logarithmic relationship in a higher concentration region (5.0–800  $\mu\text{M}$ ). The detection limit was calculated as 0.05  $\mu\text{M}$ . The suggested  $\text{TiO}_2/\text{ErGO}/\text{GCE}$  exhibited good reproducibility and stability in both determination and storage. It reliably and accurately detected the concentration of Allura Red AC in milk drinks, with recovery results between 98.42–106.0% and relative standard deviation values within the range of 0.85 to 4.86 % [34].

Sierra-Rosales and colleagues have introduced a rapid and simple electrochemical sensor for the determination of Allura Red AC in isotonic sports drinks. This sensor was prepared from GCE modified with multi-walled carbon nanotubes (MWCNT). The electrochemical behavior of the colorant was investigated by CV on the MWCNT/GCE, revealing an anodic peak at +0.72 V, along with a small cathodic peak at +0.72 V on the reverse scan. This process was found to be mixed adsorptive-diffusion controlled. In differential pulse voltammograms, the sensor demonstrated a linear response to Allura Red AC within the concentration range of 0.1–9.0  $\mu\text{M}$ , with a detection limit of 0.014  $\mu\text{M}$  in isotonic sports drinks. The method also showed good recovery results in both red and lilac isotonic sport drinks, with relative standard values below 3 % and 5 %, respectively [35].

A novel CPE composed of cobalt (II, III) oxide was prepared by Penagos-Llanos et al. for the detection of Allura Red AC. The presence of  $\text{Co}_3\text{O}_4$  resulted in a remarkable enhancement of the cathodic peak current for Allura Red AC, with an increase of over 50% in CV and a 65% boost in SWV, as compared to an unmodified CPE. In PBS at pH of 3.1 serving as the supporting electrolyte, Allura Red AC exhibited a linear response in the concentration range of 0.1 to 1.0  $\mu\text{M}$ , with a remarkable detection limit of 0.05  $\mu\text{M}$ . This technique was successfully applied to chili sauce, soft drink and isotonic drink beverages containing Allura Red AC, displaying the good accuracy of the developed method. Furthermore, studies have proven that the sensor is sensitive, stable, and selective [36].

Nagles and García-Beltrán have offered a new and simple approach for the detection of Allura Red AC in cherry gelatin, chili sauce, and strawberry juice. This method is based on utilizing square-wave adsorptive stripping voltammetry (SWAdSV) on GCE, with the presence of cetylpyridinium bromide (CPB). In PBS at pH 3.3, the oxidation peak of Allura Red AC occurred at 0.81 V. However, with the addition of small quantities of CPB, an aggregate of Allura Red AC and CPB formed, causing a notable shift in oxidation to nearly 0.14 V and a concurrent increase in current by approximately 50%. This method was effectively applied for the analysis of Allura Red AC, demonstrating linearity within the concentration range of 0.06 to 11.5  $\mu\text{M}$ , and achieving a low limit of detection as low as 0.032  $\mu\text{M}$ . Furthermore, this method has proven effective when applied to real samples, yielding satisfactory recovery results within the range of 95.5 to 104.2%. The authors also have highlighted that when utilizing CPB/GCE, it is possible to perform at least 60 measurements with little loss of reliability, and each measurement can be completed in just 60 seconds [37].

In another study, Yu et al. have introduced a novel and highly sensitive electrochemical sensor that based on a composite material consisting of poly(diallyldimethylammonium chloride) (PDDA) functionalized graphene (Gr) and nickel nanoparticles, which is utilized to modify a GCE for the detection of Allura Red AC. The sensor demonstrated a significantly enhanced electrochemical activity towards Allura Red AC. The observed improvement could be attributed to the synergistic effect arising from the enlarged active surface area and enhanced electron transfer efficiency achieved through the combined utilization of Gr and Ni nanoparticles. The electro-oxidation process of Allura Red AC on PDDA/Gr/Ni/GCE was detected irreversible and adsorption-controlled. The differential pulse stripping voltammetry (DPSV) responses to various concentrations of Allura Red AC in PBS at pH 3.0

exhibited a linear correlation within the range of 0.05–10.0  $\mu\text{M}$ , with a detection limit as low as 0.008  $\mu\text{M}$ . The method was successfully applied to strawberry juice samples and proved its accuracy with 96–97.6% recovery values and relative standard deviation lower than 5% [38].

Zhang et al. devised a practical and highly responsive technique for quantifying Allura Red AC and Ponceau-4R simultaneously. This approach involved the utilization of an expanded graphite paste electrode (EGPE) that was modified with an IL (1-butyl-3-methylimidazolium hexafluorophosphate), in combination with square-wave stripping voltammetry (SWSV). The high conductivity of IL resulted in a significant improvement in the electrocatalytic oxidation signal of Allura Red AC at +0.72 V when comparing it to EGPE. In BRB solution at pH of 6.0, the linear range for the concentration of Allura Red AC spanned from 1.0 to 10.0  $\mu\text{M}$ , with an impressive detection limit of 0.0179  $\mu\text{M}$ . To assess its practical applicability, the developed method was applied for the quantification of Allura Red AC in both orange and grapefruit juices under optimized experimental parameters. The recoveries achieved using this method for Allura Red ranged from 96.0 to 99.2%, which strongly indicate the good accuracy of the proposed method. The electrode design also demonstrated excellent characteristics in terms of reproducibility, stability, and reusability [39].

A CPE was effectively modified using mesoporous  $\text{TiO}_2$  combined with graphene (Gr/ $\text{TiO}_2$ ). This modification resulted in a notable enhancement effect, significantly increasing the oxidation signal of Allura Red AC at +0.89 V when analyzed using SWV. The electro-oxidation of Allura Red AC was found irreversible and adsorption-controlled electrode process. 0.1 M  $\text{H}_2\text{SO}_4$  solution was used as the supporting electrolyte for detecting Allura Red AC. Under the optimal conditions, it was observed that the oxidation current of Allura Red AC exhibited proportionality to its concentration within the range of 0.00067 to 0.21  $\mu\text{M}$ , and the limit of detection was obtained as 0.00034  $\mu\text{M}$ . To assess its practical utility, this developed method was put to the test in detecting Allura Red AC within soft drink and sausage samples. The authors also emphasized the excellent reproducibility in fabricating the method and its precision in detection [40].

In a study presented by Nagles et al., a novel application involving  $\text{MoO}_3$  combined with CPE was introduced to create a micro-composite electrode. This electrode was designed for the purpose of quantifying Allura Red AC and Paracetamol simultaneously, using SWV. The anodic peak current for Allura Red AC was 80% higher when compared to an unmodified CPE. The relationship between concentration of Allura Red AC

and oxidation peak current was linear in the range of 0.36–6.0  $\mu\text{M}$  with the detection limit of 0.38  $\mu\text{M}$  in PBS at pH 6.5. The accuracy of the proposed method was evaluated by testing its ability to detect Allura Red AC in real samples of syrup and strawberry-flavored gelatin, indicating recovery values of 95% and 96%, respectively. Stability and potential interferences were thoroughly assessed, and the results obtained were very acceptable [41].

In another study, shungite (SHU), a natural mineral as a modifier on a planar carbon fiber electrode (PCFE), has proven to be advantageous for creating a favorable electrode interface for the electrochemical oxidation of Allura Red AC. This modification has led to several positive effects, including an expansion of the electroactive surface area, a reduction in electron transfer resistance, and the enhancement of electrocatalytic effects. In analytical applications employing DPV, PBS with a pH of 4.0 was used as supporting electrolyte. The developed sensor exhibited the capability to quantify Allura Red AC within the concentration ranges of 0.001 to 0.1  $\mu\text{M}$  and 0.1 to 2.0  $\mu\text{M}$ , with impressively low detection limit of 0.00036  $\mu\text{M}$ . The practical utility of the SHU/PCFE was demonstrated by testing it with drink samples, lollipops, and pharmaceuticals. The results demonstrated its accuracy, as evidenced by excellent recovery values with relative standard deviations consistently lower than 5%. Additionally, this convenient and cost-effective sensor exhibited good repeatability, stability, and anti-interference capacity [42].

Mehmandoust et al. developed a sensitive and innovative electrochemical sensor designed for the detection of Allura Red AC in the presence of Tartrazine. This sensor was prepared by modifying a screen-printed electrode with functionalized nanodiamonds coated with silicon dioxide and titanium dioxide nanoparticles (F-nanodiamond@ $\text{SiO}_2$ @ $\text{TiO}_2$ /SPE). The electrochemical response of F-nanodiamond@ $\text{SiO}_2$ @ $\text{TiO}_2$ /SPE in the electro-oxidation of Allura Red AC was investigated by using CV and the results revealed that the oxidation reaction occurring on the electrode surface was a diffusion-controlled process. In BRB at pH 3.0 using DPV, the fabricated electrode exhibited two extensive dynamic ranges for Allura Red AC quantification: 0.01–0.12  $\mu\text{M}$  and 0.12–8.65  $\mu\text{M}$  and it achieved a detection limit as low as 0.00122  $\mu\text{M}$ . The successful detection of Allura Red AC in various food samples such as soft drinks, powders, orange juice, and candy demonstrated the sensor's practical applicability for determining Allura Red AC with satisfactory recovery rates. Furthermore, the modified electrode indicates outstanding attributes in terms of repeatability, reproducibility, selectivity, and stability [43].

A core-shell architecture was ingeniously crafted, featuring  $\text{Mn}_3\text{O}_4@\text{C}$  nanocubes, to construct an exceptionally sensitive screen-printed microchip (SPM) for the precise detection of Allura Red AC. This nanocomposite capitalizes on the strengths of  $\text{Mn}_3\text{O}_4@\text{C}$ , characterized by its high electrocatalytic activity and chemical stability. The electrochemical behavior of the prepared  $\text{Mn}_3\text{O}_4@\text{C}$  nanocubes was compared with that of both the unmodified electrode and  $\text{MnCO}_3$  nanocubes by CV. Notably, the  $\text{Mn}_3\text{O}_4@\text{C}$  nanocubes exhibited the highest redox currents, proving the robust redox capabilities of coexisting  $\text{Mn}^{2+}$  and  $\text{Mn}^{3+}$ . The newly Allura Red AC sensor exhibited excellent selectivity, featured with impressively large linear detection ranges from 0.1 to 168.4  $\mu\text{M}$  and from 168.4 to 1748.4  $\mu\text{M}$ , with a low detection limit of 0.033  $\mu\text{M}$ . The accuracy of the prepared Allura Red AC sensor was assessed in real samples of various sports drinks using a standard addition method. The obtained recovery results ranged from 98.60% to 100.67%, indicating the sensor's excellent performance in accurately quantifying Allura Red AC in these samples [44].

In their recent research, Moarefdoust and colleagues aimed to identify Allura Red AC through the creation of a novel electrochemical sensor by developing a raspberry-like  $\text{In}^{3+}/\text{NiO}$  hierarchical nanostructure ( $\text{In}^{3+}/\text{NiO}$  RLHNSs) modified GCE. The electrochemical behavior of Allura Red AC was investigated with three different electrodes ( $\text{In}^{3+}/\text{NiO}$  RLHNSs/GCE,  $\text{NiO}$  RLHNSs/GCE, and bare GCE) in 0.1 M PBS at pH 4.0 by CV. Notably, the anodic peak current obtained using the  $\text{In}^{3+}/\text{NiO}$  RLHNSs/GCE exhibited a significant increase, approximately 3.4 and 1.5 times higher than that of the bare GCE and  $\text{NiO}$  RLHNSs/GCE, respectively. These results indicated the successful grafting of  $\text{In}^{3+}/\text{NiO}$  RLHNSs onto the electrode surface, leading to a substantial enhancement in electrode sensitivity for Allura Red AC. Also, it was determined that Allura Red AC responses on the developed electrode surface continued with a diffusion-controlled process. Using DPV, a linear relationship was evident between the concentration of Allura Red AC and the corresponding peak current (0.01 – 700.0  $\mu\text{M}$ ). The calculated values for the limit of detection and the limit of quantification were 0.0041 and 0.0136  $\mu\text{M}$ , respectively. The proposed sensor's applicability was evaluated using strawberry and fruit juice samples, and the mean recovery rate for Allura Red AC was found in the range of 99.0% to 101.2%, which confirms the good accuracy of the developed method [45].

The electrochemical characteristics of Allura Red AC on a GCE that had been modified with ErGO were studied using CV and differential pulse adsorptive anodic stripping voltammetry (DPAdASV). The

electrochemical behavior of Allura Red AC on the ErGO/GCE indicated semi-reversible oxidation, and it was observed that Allura Red AC adsorbed onto the surface of the ErGO/GCE. In the supporting electrolyte consisting of a BRB solution with a pH of 2.5, the anodic peak current exhibited a linear increase with the concentration of Allura Red AC, ranging from 0.1 to 0.8  $\mu\text{M}$ . The method's calculated limit of detection and limit of quantification were 0.028 and 0.093  $\mu\text{M}$ , respectively. The ErGO/GCE was successfully employed for determining Allura Red AC in soft drinks, offering both high sensitivity and accuracy. This method is characterized by its simplicity and cost-effectiveness [46].

Cai et al. developed a modified CPE using erbium nitrate and 1,3,5-benzenetricarboxylic acid (Er-BTC) for the sensitive electroanalytical analysis of azo dyes and flavonoids in drink and tea samples. PBS with a pH of 6.0 served as the supporting electrolyte for the simultaneous detection of Allura Red AC and Rhodamine B using DPV. It was observed that as the concentration of Allura Red AC ranged from 0.001 to 0.1  $\mu\text{M}$ , there was a linear increase in the oxidation peak currents. The detection limit was obtained as low as 0.0003  $\mu\text{M}$ . When the practical applicability of the method was tested on various drink and tea samples, it was found that the relative standard deviation remained below 5%. This indicates the method's reliability and consistency in different sample types [47].

An electrochemical sensor was developed for the rapid and simple detection of Allura Red AC and Ponceau 4R. This sensor was created by modifying a GCE with a film of MWCNT. The MWCNT film sensor, owing to its substantial surface area and efficient accumulation capability, significantly enhances the oxidation signal of Allura Red AC. The electro-oxidation process of Allura Red AC on the MWCNT/GCE was determined to be irreversible and diffusion-controlled. The detection parameters, including pH value, the amount of MWCNT, accumulation potential and time were optimized for the best results. By DPV, it was observed that the obtained peak currents showed a linear relationship with concentrations of Allura Red AC in the range of 0.1 to 1.2  $\mu\text{M}$  and the limit of detection for this analysis was determined to be 0.05  $\mu\text{M}$ . To evaluate its performance in real sample analysis, the new method was applied to detect Allura Red AC in several soft drinks. The recovery values that obtained ranged between 98.1% and 100.6% suggest that the detection of Allura Red AC using MWCNT/GCE is accurate and feasible [48].

In their research, Silva et al. described the fabrication process of a polyallylamine (PAMI) modified GCE. They subsequently employed this modified electrode for the

electro-reduction of Allura Red AC within complex food samples using SWV. Given the complex nature of the sample matrices to be analyzed, a multi-commutated flow system was devised. This system facilitated the seamless execution of the standard additions method, all while operating automatically and maintaining a continuous flow of samples. After optimizing the parameters of SWV, it was observed that the linear range for the quantification of Allura Red AC in a 0.5 M HCl solution extended from 10.0 to 300.0  $\mu\text{M}$ , achieving a detection limit of 1.4  $\mu\text{M}$ . The method was successfully applied to determine the concentration of Allura Red AC in gelatin powder and alcoholic beverages [49].

Rodríguez et al. demonstrated the effectiveness of combining sequential injection analysis with DPV detection, using Antimony film modified screen-printed carbon electrodes (SbF/SPCE), for the analysis of Allura Red AC in food samples. Acetate buffer (AcB) solution of pH 4.0 was selected as the supporting electrolyte for this analysis. The study revealed a linear relationship between the peak height and the concentration of the dye within the range of 1.0 to 5.0  $\mu\text{M}$ , with a detection limit calculated as 0.3  $\mu\text{M}$ . The method was put into practical use for the determination of Allura Red AC in real samples, including flavored cornflour, tomato bouillon cubes, candy, gelatin powder, and isotonic drinks [50].

A modified GCE was fabricated by dispersing MWCNTs into an IL and graphene oxide (GO) mixture. The MWCNTs were effectively dispersed within the IL-GO mixture, leading to excellent dispersion properties and a significantly increased surface area for the composite. This enhanced the electrode's capability to absorb Allura Red AC, making it a promising platform for analytical applications. In BRB with a pH of 7.0, the oxidation peak current of Allura Red AC exhibited a linear increase as its concentration was raised (0.0008–0.5  $\mu\text{M}$ ), and the limit of detection was found 0.0005  $\mu\text{M}$ . To assess its potential application, MWCNT/IL/GO/GCE was employed for the concurrent detection of Allura Red AC, Ponceau 4R, and Tartrazine in alcoholic beverages using SWSV technique, and the obtained recovery values were between 100.0–106.8% for Allura Red AC [51].

A series of porous carbon (PC) was synthesized by utilizing calcium carbonate nanoparticles as a hard template and starch as the carbon source. Through the surface modification of PC on a GCE, Cheng et al. successfully established a highly sensitive electrochemical sensing platform for the detection of Allura Red AC. As a result of the calibration study performed with DPV, the linearity range and limit of detection values for Allura Red AC in PBS at pH 7.0 were found to be 0.005–0.8  $\mu\text{M}$  and 0.0034  $\mu\text{M}$ , respectively. Reproducibility and interference studies were carried

out with PC/GCE, demonstrating satisfactory results. To evaluate its practical applicability, the developed method was utilized in various drink samples [52].

In another study, to synthesize high dispersible nanocomposites, 1-allyl-3-methylimidazolium chloride functionalized reduced graphene oxide (IRGO) was used to load Au nanoparticles (Au). The prepared IRGO/Au nanocomposites were employed to modify a GCE. SWV was performed to investigate the electrochemical behavior of Allura Red AC on the surface of the IRGO/Au/GCE in BRB at pH 5.0, and the results indicated that the developed sensor could greatly facilitate the electro-oxidation of Allura Red AC. The SWV peak current for Allura Red AC exhibited an increase with rising concentrations within the range of 0.0006 to 0.2  $\mu\text{M}$ , demonstrating a low detection limit of 0.00043  $\mu\text{M}$ . To validate the practical applicability of the proposed sensor, the IRGO/Au/GCE was utilized for the quantification of Allura Red AC in chocolate, jelly, tea, and juice samples [53].

Lastly, a novel method was successfully developed to determine Allura Red AC in commercial beverages by Tvorynska et al. This method utilized two types of silver solid amalgam electrodes: the mercury meniscus modified amalgam electrode (m-AgSAE) and the liquid mercury-free polished amalgam electrode (p-AgSAE). The analysis was conducted using both differential pulse adsorptive stripping voltammetry (DPAdSV) and direct current adsorptive stripping voltammetry (DCAdSV) techniques. Due to the substantial increase in the reduction peak current of Allura Red AC observed on both m-AgSAE and p-AgSAE, which is a result of its adsorption at the electrode surface, the amalgam electrodes demonstrate wide linear ranges and high sensitivity for the quantification of Allura Red AC. In AcB with a pH of 3.6, the peak current of Allura Red AC exhibited a linear relationship with its concentration in the range of 0.01 to 0.4  $\mu\text{M}$  when using DPAdSV and 0.008 to 0.6  $\mu\text{M}$  when employing DCAdSV on the m-AgSAE electrode. The calculated detection limits for this analysis were determined to be 0.0012 and 0.0034, respectively. When utilizing the p-AgSAE, the linearity for the analysis of Allura Red AC was from 0.08 to 0.6  $\mu\text{M}$  and detection limit was obtained 0.03  $\mu\text{M}$ , by the DCAdSV technique [54].

## 4. Conclusion

Allura Red AC, which is a group of azo dyes in the food and beverage coloring, plays a key role in the food processing sector. Because the excessive consumption of this synthetic toxic dye can cause adverse effects on the human health, voltammetric methods were developed for detecting the presence of Allura Red AC in food and



beverage samples. No study compiling the voltammetric determination of Allura Red AC in foods and beverages has been found in the literature. The voltammetric studies carried out for determination of Allura Red AC from food and beverage samples in the literature have been reviewed and evaluated on account of used method, obtained linear range and limit of detection values. Considering the methods used in these studies, DPV method was used the most, followed by stripping methods and SWV. When compared in terms of the linear range values have been obtained in these studies, it has been seen that the widest range was acquired with DPV method and the  $\text{In}^{3+}/\text{NiO}$  RLHNSs/GCE. Then limit of detection values have been evaluated for these studies, the lowest limit of detection value was obtained SWV and  $\text{Gr}/\text{TiO}_2/\text{CPE}$ . The concentration of Allura Red AC in foods and beverages can be determined at very low limits via voltammetric methods. Also, these methods provided good recovery, accurate and precise results. In conclusion, the determination of Allura Red AC can be carried out accurately and reliably by voltammetric methods in food and beverage samples.

### Conflicts of Interest:

The authors declare no conflict of interest.

### Author Contributions

**EŞ:** Writing-original draft.

**FA:** Supervision, writing-review & editing.

### References

- [1] O.I. Lipskikh, E.I. Korotkova, P. Khristunova Ye, J. Barek, B. Kratochvil, Sensors for voltammetric determination of food azo dyes - A critical review, *Electrochim Acta*, 260, 2018, 974-985.
- [2] N. Martins, C.L. Roriz, P. Morales, L. Barros, I.C.F.R. Ferreira, Food colorants: challenges, opportunities and current desires of agro-industries to ensure consumer expectations and regulatory practices, *Trends Food Sci*, 52, 2016, 1-15.
- [3] P. Amchova, H. Kotolova, J. Ruda-Kucerova, Health safety issues of synthetic food colorants, *Regul Toxicol Pharmacol*, 73, 2015, 914-922.
- [4] S. Adeel, S. Rafi, M.A. Mustaan, M. Salman, A. Ghaffar, *Handbook of Renewable Materials for Coloration and Finishing* (1. edition), 2018, USA, Wiley.
- [5] K. Rovina, S. Siddiquee, S.M. Shaarani, Extraction, analytical and advanced methods for detection of Allura Red AC (E129) in food and beverages products, *Front Microbiol*, 7, 2016, 798.
- [6] A.H. Alghamdi, Determination of Allura Red in some food samples by adsorptive stripping voltammetry, *J AOAC Int*, 88, 2005, 1387-1393.
- [7] C.V. Vorhees, R.E. Butcher, R.L. Brunner, V. Wootten, T.J. Sobotka, Developmental toxicity and psychotoxicity of FD and C red dye no. 40 (Allura Red AC) in rats, *Toxicology*, 28, 1983, 207-217.
- [8] E. Dinç, E. Baydan, M. Kanbur, F. Onur, Spectrophotometric multicomponent determination of sunset yellow, tartrazine and allura red in soft drink powder by double divisor-ratio spectra derivative, inverse least-squares and principal component regression methods, *Talanta*, 58, 2005, 579-594.
- [9] M.G. Kiseleva, V.V. Pimenova, K.I. Eller, Optimization of conditions for the HPLC determination of synthetic dyes in food, *J Anal Chem*, 58, 2003, 685-690.
- [10] N. Yoshioka, K. Ichihashi, Determination of 40 synthetic food colors in drinks and candies by high-performance liquid chromatography using a short column with photodiode array detection, *Talanta*, 74, 2008, 1408-1413.
- [11] K.L. Kuo, H.Y. Huang, Y.Z. Hsieh, High-performance capillary electrophoretic analysis of synthetic food colorants, *Chromatographia*, 47, 1998, 249-256.
- [12] K. Pliuta, A. Chebotarev, A. Pliuta, D. Snigur, Voltammetric determination of Allura Red AC onto carbone-paste electrode modified by silica with embedded cetylpyridinium chloride, *Electroanalysis*, 33, 2021, 987-992.
- [13] D. Harvey, *Modern Analytical Chemistry* (1. edition), 2000, USA, McGraw-Hill Companies.
- [14] J. Wang, *Analytical Electrochemistry* (2. edition), 2000, USA, New York: Wiley-VCH.
- [15] J.P. Hart, *Electroanalysis of Biologically Important Compounds* (1. edition), 1990, UK, Chichester.
- [16] R. Kellner, J.M. Mermet, M. Otto, M. Valcárcel, H.M. Widmer, *Analytical Chemistry: A Modern Approach to Analytical Science* (2. edition), 2004, USA, Weinheim: Wiley-VCH.
- [17] D.K. Gosser, *Cyclic Voltammetry: Simulation and Analysis of Reaction Mechanisms* (1. edition), 1993, USA, New York: Wiley-VCH.
- [18] G. Christian, *Analytical Chemistry* (7. edition), 2013, USA, NJ: Wiley.
- [19] F. Ađın, A Review of voltametric methods for determination of dopamine agonists, *Curr Anal Chem*, 17, 2021, 1104-1113.
- [20] V.K. Gupta, R. Jain, K. Radhapyari, N. Jadon, S. Agarwal, Voltammetric techniques for the assay of pharmaceuticals - A review, *Anal Biochem*, 408, 2011, 179-196.
- [21] B. Uslu, S.A. Ozkan, Electroanalytical application of carbon based electrodes to the pharmaceuticals, *Anal. Lett.* 40, 2007, 817-853.
- [22] A.J. Bard, L.R. Faulkner, *Electrochemical Methods, Fundamentals and Applications* (2. edition), 2000, USA, New York: Wiley.
- [23] C.G. Zoski, *Handbook of Electrochemistry* (1. edition), 2007, Holland, Amsterdam.
- [24] D. Harvey, *Modern Analytical Chemistry* (1. edition), 2000, USA, McGraw-Hill Companies.
- [25] S.A. Ozkan, Principles and techniques of electroanalytical stripping methods for pharmaceutically active compounds in forms and biological samples, *Curr Pharm Anal*, 5, 2009, 127-143.
- [26] F. Scholz, *Electroanalytical Methods* (2. edition), 2010, Germany, Berlin, Heidelberg: Springer-Verlag.
- [27] F. Ađın, S. Atal, Electroanalytical determination of anti-inflammatory drug tenoxicam in pharmaceutical dosage forms, *Turk J Pharm Sci*, 16, 2019, 184-191.
- [28] V. Mirceski, S. Komorsky-Lovric, M. Lovric, *Square Wave Voltammetry* (1. edition), 2007, Germany, Berlin.
- [29] B. Uslu, S.A. Ozkan, Electroanalytical methods for the determination of pharmaceuticals: A review of recent trends and developments, *Anal Lett*, 44, 2011, 2644-2702.
- [30] P.T. Kissinger, W.R. Heineman, *Laboratory Techniques in Electroanalytical Chemistry* (2. edition), 1996, USA, New York.
- [31] J. Wang, *Analytical Electrochemistry* (2. edition), 2006, USA, Wiley.
- [32] S. Uruc, O. Gorduk, Y. Sahin, Electroanalytical determination of Allura Red in beverage samples using an anodically pretreated graphite electrode, *Int. J. Environ. Anal. Chem*, 2021, 1-19.

- [33] T.A. Silva, A. Wong, O. Fatibello-Filho, Electrochemical sensor based on ionic liquid and carbon black for voltammetric determination of Allura red colorant at nanomolar levels in soft drink powders, *Talanta*, 209, 2020, 120588.
- [34] G. Li, J. Wu, H. Jin, Y. Xia, J. Liu, Q. He, et al., Titania/electro-reduced graphene oxide nanohybrid as an efficient electrochemical sensor for the determination of Allura Red, *Nanomaterials*, 10, 2020, 307.
- [35] P. Sierra-Rosales, C. Toledo-Neira, P. Ortúzar-Salazar, J.A. Squella, MWCNT modified electrode for voltammetric determination of Allura Red and brilliant blue FCF in isotonic sport drinks, *Electroanalysis*, 31, 2019, 883-890.
- [36] J. Penagos-Llanos, O. García-Beltrán, J.A. Calderón, E. Nagles, J.J. Hurtado, Carbon paste composite with  $\text{Co}_3\text{O}_4$  as a new electrochemical sensor for the detection of Allura Red by reduction, *Electroanalysis*, 31, 2019, 695-703.
- [37] E. Nagles, O. García-Beltrán, Determination of Allura Red in the presence of cetylpyridinium bromide by square-wave adsorptive stripping voltammetry on a glassy carbon electrode, *Anal Sci*, 34, 2018, 1171-1175.
- [38] L. Yu, M. Shi, X. Yue, L. Qu, Detection of Allura Red based on the composite of poly (diallyldimethylammonium chloride) functionalized graphene and nickel nanoparticles modified electrode, *Sens. Actuators B Chem*, 225, 2016, 398-404.
- [39] J. Zhang, S. Zhang, X. Wang, W. Wang, Z. Chen, Simultaneous determination of Ponceau-4R and Allura Red in soft drinks based on the ionic liquid modified expanded graphite paste electrode, *Int. J. Environ. Anal. Chem*, 95, 2015, 581-591.
- [40] T. Gan, J. Sun, H. Zhu, J. Zhu, D. Liu, Synthesis and characterization of graphene and ordered mesoporous  $\text{TiO}_2$  as electrocatalyst for the determination of azo colorants, *J Solid State Electrochem*, 17, 2013, 2193-2201.
- [41] E. Nagles, M. Ceroni, C. Villanueva Huerta, J.J. Hurtado, Simultaneous electrochemical determination of paracetamol and Allura Red in pharmaceutical doses and food using a Mo (VI) oxide-carbon paste microcomposite, *Electroanalysis*, 33, 2021, 2335-2344.
- [42] M.A. Bukharinova, E.I. Khamzina, N.Y. Stozhko, A.V. Tarasov, Highly sensitive voltammetric determination of Allura Red (E129) food colourant on a planar carbon fiber sensor modified with shungite, *Anal. Chim. Acta*, 2023, 341481.
- [43] M. Mehmamdoust, P. Pourhakkak, F. Hasannia, Ö. Özalp, M. Soyak, N. Erk, A reusable and sensitive electrochemical sensor for determination of Allura red in the presence of Tartrazine based on functionalized nanodiamond@ $\text{SiO}_2$ @ $\text{TiO}_2$ ; an electrochemical and molecular docking investigation, *Food Chem. Toxicol*, 164, 2022, 113080.
- [44] K. Zhang, H. Zeng, J. Feng, Z. Liu, Z. Chu, W. Jin, Screen-printing of core-shell  $\text{Mn}_3\text{O}_4$ @C nanocubes based sensing microchip performing ultrasensitive recognition of allura red, *Food Chem. Toxicol.*, 162, 2022, 112908.
- [45] M.M. Moarefdoust, S. Jahani, M. Moradalizadeh, M.M. Motaghi, M.M. Foroughi, Effect of positive In(III) doped in nickel oxide nanostructure at modified glassy carbon electrode for determination of Allura Red in soft drink powders, *Monatsh. Chem*, 152, 2021, 1515-1525.
- [46] T.G.H. Le, T.M. Nguyen, T.T.N. Pham, T.B. Do, M.G.H. Dang, T.T.K. Nguyen, Electrochemical study of allura red at glassy carbon electrode modified with the reduced graphene oxide and its determination in food by adsorptive stripping voltammetry, *Anal. Bioanal. Electrochem*, 15, 2023, 371-381.
- [47] Y. Cai, W. Huang, K. Wu, Morphology-controlled electrochemical sensing of erbium-benzenetricarboxylic acid frameworks for azo dyes and flavonoids, *Sens. Actuators B Chem*, 304, 2020, 127-370.
- [48] Y. Zhang, X. Zhang, X. Lu, J. Yang, K. Wu, Multi-wall carbon nanotube film-based electrochemical sensor for rapid detection of Ponceau 4R and Allura Red, *Food Chem*, 122, 2010, 909-913.
- [49] M.L.S. Silva, M.B.Q. Garcia, J.L. Lima, E. Barrado, Voltammetric determination of food colorants using a polyallylamine modified tubular electrode in a multicommutated flow system, *Talanta*, 72, 2007, 282-288.
- [50] J.A. Rodríguez, M.G. Juárez, C.A. Galán-Vidal, J.M. Miranda, E. Barrado, Determination of allura red and tartrazine in food samples by sequential injection analysis combined with voltammetric detection at antimony film electrode, *Electroanalysis*, 27, 2015, 2329-2334.
- [51] M. Wang, J. Zhao, A facile method used for simultaneous determination of ponceau 4R, allura red and tartrazine in alcoholic beverages, *J. Electrochem. Soc*, 162, 2015, H321.
- [52] Q. Cheng, S. Xia, J. Tong, K. Wu, Highly-sensitive electrochemical sensing platforms for food colourants based on the property-tuning of porous carbon, *Anal. Chim. Acta*, 887, 2015, 75-81.
- [53] M. Cui, M. Wang, B. Xu, X. Shi, D. Han, J. Guo, Determination of allura red using composites of water-dispersible reduced graphene oxide-loaded Au nanoparticles based on ionic liquid, *Int. J. Environ. Anal. Chem*, 96, 2016, 1117-1127.
- [54] S. Tvorynska, B. Josypčuk, J. Barek, L. Dubenska, Electrochemical behavior and sensitive methods of the voltammetric determination of food azo dyes amaranth and allura red AC on amalgam electrodes, *Food Anal. Methods*, 12, 2019, 409-421.



## A comprehensive review on carbon quantum dots

Mussarat JABEEN<sup>1\*</sup> , Iqra Mutaza<sup>2</sup> 

<sup>1</sup> Govt. Sadiq College Women University, Department of Chemistry, Bahawalpur 63100, Pakistan

<sup>2</sup> University of Central Punjab, Faculty of Science & Technology, Department of Chemistry, Lahore 54000, Pakistan

### Abstract

Over the past few decades, carbon quantum dots (CQDs) gained remarkable attention due to their distinctive properties and wide-ranging applications. Usually, CQDs are nano-sized materials, showcase of outstanding optical, electronic, and chemical characteristics. Their synthesis involves the controlled carbonization of diverse carbon-rich precursors, such as organic molecules or waste materials. Their optical properties, including adjustable fluorescence, make them ideal for implementation in bioimaging, sensors, and optoelectronic devices. Their diminutive size, biocompatibility, and minimal toxicity enhance their suitability for applications in biology and medicine. Furthermore, researchers have delved into exploring the potential of CQDs in energy-related domains, such as photo-catalysis, solar cells, and super-capacitors, leveraging their unique electronic structure and catalytic capabilities. Ongoing research continues to uncover their synthesis and fascinating applications due to low toxicity. This review provides comprehensive information on CQDs, including their synthesis, characteristics, and attractive applications.

**Keywords:** Carbon quantum dots, bio-imaging, photo-catalyst, nano-medicine, chemical sensor

### 1. Introduction

From the past few decades, researches on carbon quantum dots have significantly increased due to their dramatic and fascinating applications [1]. Carbon quantum dots are a novel class of fluorescent materials from the nano-carbon family with a dimension of less than 10nm that include carbon as one of their constituent parts [2]. Due to their unique properties, such as biocompatibility, ease of surface modification, good photoluminescence, exceptional water+ solubility, and low toxicity, carbon quantum dots have recently emerged as a possible rival for inorganic quantum dots. For example, applications like photo-catalysis in vitro and in vivo bio-imaging, light emitting diodes (LEDs), organic solar cells (OSCs), DSSCs (dye-sensitized solar cells), drug carriers in biomedicine, chemical and biological sensors, as well as photodynamic and photothermal therapies, all utilize CQDs [3]. However, the search for low-cost synthesis/fabrication materials that are also non-toxic, eco-friendly, and biocompatible has been ongoing for some time. C-dots can be made using two different approaches: top-down and bottom-up. For example, laser ablation, electrochemical syntheses, and electric discharges are all top-down techniques [4]. Meanwhile, bottom-up methods include

carbonization of sugars like glucose and sucrose, ascorbic acid, and citric acid [5]. To improve water solubility and luminescent properties, additional synthetic procedures, techniques, stages/levels, hazardous agents, and equipment are required [6]. An urgently needed one-step, facile approach with economic chemistry is required to produce self-passivated photo luminescent C-dots. In particular, it is possible to control the size, shape, and physical properties of the carbon nanoparticles by careful selection of the carbon source and surface modifier [7]. However substantial production of C-dots with tailored composition, structure, morphology and size by a simple and cheap method remains still challenging.

### 2. Semiconductor Quantum Dots

Semiconductor nanocrystals are the latest developed nanomaterial, also known as QDs, that has piqued many people's curiosity [8]. A broad range of studies have been conducted on semi-conductor quantum dots, which have found them durable, tunable-fluorescence-emission, high productivity, and with new visual characteristics [9]. The most often utilized fluorescent

**Citation:** M. Jabeen, I. Mutaza, Comprehensive review on carbon quantum dots, Turk J Anal Chem, 6(1), 2024, 50–60.

**Author of correspondence:** [dr.mussaratjabeen@gmail.com](mailto:dr.mussaratjabeen@gmail.com)

**Received:** March 11, 2024

**Tel:** +92 (333) 520 78 22

**Accepted:** April 24, 2024

**Fax:** N/A

compounds are organic dyes, CdSe, and ZnS quantum dots (QDs). These are some of the most frequently utilized fluorescent compounds [8], which use heavy toxic metals (either with low concentrations). Therefore, these QDs are not considered useful in biomedical applications [10]. The disadvantages arise due to photobleaching, quenching of dye molecules, and the toxicity of QDs [11].

Photo-luminescent materials have gained popularity due to their auspicious, diversified, and broad range of uses [12]. Because excitons are restricted in spatial dimensions, QDs exhibit the characteristics that fall between bulk semiconductors and discrete molecules [13]. When stimulated by photons and/or an electric field with greater energy than the band gap, quantum dots produce photons to release the absorbed energy [14]. Furthermore, because of the quantum confinement phenomenon, the emission energy can be adjusted by varying the composition and particle size of quantum dots.

### 3. Carbon Quantum Dots

Researchers have conducted a broad range of studies for investigating nanotechnology and creating nanomaterials. These nanomaterials are the particles that have been reduced to the nanoscale size and display significantly different characteristics than what they do on a large scale. For example, when the system size decreases, the "quantum size effect" becomes more apparent, causing the electrical characteristics of solids to change [15]. Meanwhile, increasing the exterior part to capacity proportion dramatically alters the mechanical, thermal, and catalytic characteristics of constituents [16]. Nanomaterials' specific characteristics allow for novel uses [7]. Carbon nanotubes, along with fullerenes, as well as nanoparticles composed of different materials such as silver, gold, silica, zinc, and titanium, are usually employed in a variety of goods in the market [17].

The systematic studies and the combination of both nanotechnology and biotechnology are quite appealing for the provision of analytical tools and techniques, and provide an efficient platform for the studies and/or research in biological sciences [18]. Quantum dots have been utilized as strong fluorescent probes for imaging biological targets [19], illness diagnosis and prognosis, tracking cell/protein interactions, and cell viability [20]. Traditional organic dyes have a restricted excitation range, poor fluorescence intensity, and a short lifespan [16]. QDs, on the other hand, have broad emission spectra but a limited, powerful, and modified emission range [21]. With their brilliant emission and exceptional

photostability, they allow a real-time monitoring of particles [17].

Because of their simplicity of functionalization and low cost of synthesis, carbon nanomaterials have shown significant promise in applications such as optoelectronics, bioimaging, and catalysis [22]. However, chemical changes frequently result in unwanted consequences such as low water solubility, limiting their potential in a variety of applications [23].

Carbon QDS, or CQDs, are not very old, and a type of carbon-nanomaterial which has intrinsically high-water solubility, photoluminescent quantum yield, and size-dependent fluorescence, has demonstrated even more potential in these applications [24]. Chemical treatment retains or even improves these characteristics, elevating CQDs above many carbon nanomaterials [24].

#### 3.1. Discovery of CQDs

Xu et al. (2004) [25] unintentionally discovered CQDs during the process of the disintegration and filtration of the SWCNTs (carbon nanotube) [26]. This prompted further research to harness CQD fluorescence characteristics and produce a new class of very small sized practical fluorescent nanomaterials [27].

C-dots particles are found to be very interesting among researchers due to their uniqueness in integration of bright-light photoluminescence, high water solubility, easy functional activity, lower toxicity values, and photostability with higher values [12]. The simple synthesis processes achievable by several methods from a range of initiating materials [28, 29]. Unlike nanodiamonds, which emit light owing to point defects found in the  $sp^3$  hybridized carbon structures due to differences in carbon atom arrangement, energy emission from C-dots exhibits several characteristics along with fully recharged electrons and carbon materials [30].

#### 3.2. Optical Properties of CQDs

The most fascinating element of CQDs is their variable photoluminescence (PL) properties, which are produced by the quantum confinement phenomena. The excited electron transfers from the conduction band towards the valence band of the absorbed photon's wavelength [31]. Light emitted by QDs can have wavelengths ranging from ultraviolet to infrared [32].

The major distinguishing feature of fluorescent CQDs or FCQDs is that the hue of fluorescence varies with size [31]. Quantum dots of various sizes produce high-energy light (Blue). Furthermore, large quantum dots produce light with a low energy (Red) [33].

#### 3.3. Quantum Confinement Effect

Bulk semiconductor materials contain a fully occupied valence band and also a conduction band, which is

separated by relatively small band gap distance (less than 4 eV), acting like insulators at ambient temperature and displaying electrical conductivity when triggered externally [34]. The valence band receives energy through the conduction band when the energy is higher than the band gap, and it also allows electric current to flow. The valence and conduction bands in nanoparticles are divided into different energy levels, with the energy difference between the closest feasible valence and conduction levels increasing with particle size [35,36].

A dot is formed when a bulk substance is reduced to 1nm-10nm in all three dimensions [14]. The band gap between the conduction band and the valence band grows as the number of atoms decreases from bulk material to quantum dots. The number of electrons that jump from the conduction band to the valence band is determined by the energy gap between the conduction and valence bands, which is directly proportional to the number of atoms present in the material [37].

Because QDs have broad absorption spectra, they may be excited by a wide variety of wavelengths. This feature may be used to concurrently stimulate several colored QDs with a single wavelength. The emission spectra of QDs are narrow. This can be easily adjusted by making changes to the size, composition, and surface coating [36]. When quantum dots are produced, the number of atoms in each cluster of material may vary, resulting in fluorescent carbon quantum dots of varying sizes displaying distinct colors [17]. Color of QDs depends on size, decreasing size from 6nm to 2nm, energy bandgap increases and color changed red>yellow>green>blue (decreasing size order) [38]. This is caused by the quantum confinement effect.

- i) As the nanoparticle's size shrinks, the exciton (electron-hole pair) becomes more restricted.
- ii) As the exciton is restricted further, the recombination energy increases. This is caused by the quantum confinement effect.

During the synthesis process, the size of quantum dots may be adjusted [33].

### 3.4. Review on Various Synthetic Methods

Carbon dots can be synthesized from different materials including lemon juice [5], wheat straws [39], milk [40], apple juice [41], aspirin [42], coffee grounds [43], egg yolk [44], and chocolate [45]. There are two basic approaches to the synthesis of carbon dots [15]; top-down methods, and bottom-up methods.

In the top-down method, the carbon particles (bulk material) are usually broken down, which results in different products, such as carbon soot, graphite, graphite oxide, nanodiamonds, and/or nanotubes. These materials are produced by using different processes such

as the laser ablation, electrochemical oxidation, and/or electrochemical oxidation [46]. Unlike the top-down method, the bottom-up method involves the carbonization of tiny organic molecules to produce CDs, which are frequently manufactured utilizing combustion/thermal/hydrothermal, supported synthesis, microwave/ultrasonic-aided processes in which CQDs usually generated from molecular precursors [47].

#### 3.4.1. The Top-down Approaches

##### 3.4.1.1. The Arc-discharge Methods

C-dots were discovered by Xu et al. while purifying arc-discharge dust-derived single-walled nanotubes (SWCNTs). Carbonaceous materials were divided into a number of components with varying degrees of fluorescence based on their size. The researchers used 3.3 M HNO<sub>3</sub> to add carboxyl-functional groups to the arc soot, which improves the substance's hydrophilicity. They then extracted the dust/soot using a NaOH solution (pH 8.4) to create a stable black suspension. Gel electrophoresis was used to separate the suspension into SWCNTs, short tubular carbons, and fluorescent Carbon dots. Lack of poly aromatic hydrocarbon (PAH) characteristic C-H bond out of plane bending modes in the FTIR spectrum showed that the PL was not derived from PAH sources [25].

##### 3.4.1.2. The Electrochemical Oxidation

For the first time, electrochemical synthesis of C-dots in a solution was shown by Zhou et al. (2007). They grew multiwall carbon nanotubes (MWCNTs) on carbon paper made from scrolled grapheme layers using chemical vapor deposition. A degassed acetonitrile solution with 0.1 M tetrabutylammonium perchlorate (TBA+ClO<sub>4</sub>) served as the electrolyte, and the nanotubes were used as the working electrode in an electrochemical cell along with a Pt wire counter electrode and an Ag/AgClO<sub>4</sub> reference electrode, as well as a Pt wire counter electrode and a reference electrode. When developed, they were spherical and emitted photoluminescence. When no MWCNTs were used in the carbon paper, no C-dots were generated. Chi and colleagues also created C-dots in phosphate buffer solution (pH 7.0) using a Pt mesh counter electrode and an Ag/AgCl reference electrode assembly by electrochemically oxidizing graphite rods [48].

##### 3.4.1.3. Laser-Ablation Methods

Argon was used to heat-press a mixture of graphite powder and cement, which was then baked, cured, and annealed at 900°C and 75 kg/cm<sup>2</sup>. To enhance C-Dot fluorescence, different non-toxic polymeric agents [47] such as poly(ethylene glycol) diamine (PEDG), poly(propionyl ethylene-imine-ethyleneimine) (PEIE) [49],

terminated polyethylene glycol diamine [50], and poly(propionyl-ethylenimine-coethylenimine) (PEIE-EI) [49]. After dialysis against water, followed by centrifugation, a highly fluorescent product was obtained from the fluorescently pure C-dots [51]. It was necessary to design and execute a slightly modified technique utilizing  $^{13}\text{C}$  powder and more rigorous control in order to produce C-dots with a high quantum yield of 20% [52]. For 2 hours, the authors of the study used a pulsed Nd:YAG laser to irradiate graphite or carbon black mixed in diamine hydrate, diethanolamine, or PEG200N, which acted as a surface passivating agent.

### 3.4.2. Bottom-up Approaches

#### 3.4.2.1. Combustion/Thermal/Hydrothermal Methods

Unscented candle soot and natural gas burner soot are also excellent sources of C-dots. To make multicolor luminous C-dots from candle combustion soot, Mao et al. used an oxidative acid treatment to the C-dot surfaces, adding -OH and -COOH groups [53]. Polyacrylamide gel electrophoresis (PAGE) fractionation was employed to clean up the particles after they had been separated.

Thermally degrading low-temperature melting molecular precursors were used to produce surface passivated C-dots in a single procedure [54]. Careful selection of the carbon source and surface modification increased control over the C-dots' form and physical properties. The EDTA salts were converted using a one-step pyrolytic process into extremely blue luminous C-dots with a PL QY of 31.6–40.6%. Chemical oxidation of carbohydrates was a significant technique for generating C-dots [55]. To increase water solubility and other PL properties, most synthesis methods call for a number of steps, a strong acid, and further treatment with other compounds. Wu et al. created hydrophilic C-dots with a high yield via controlled carbonization of sucrose, as reported in *Science* [55]. Green luminescent C-dots were differentiated from non-luminous C-dots that emitted blue fluorescence after being functionalized with PEG, and this was accomplished effectively. The hydrothermal technique was also utilized by other researchers for the production of C-dots with a high quantum yield from chemical precursors including glucose, fructose, saccharide, and ascorbic acid as compared to others [56]. We recently synthesized huge quantities of highly photoluminescent C-dots on a massive scale using hydrothermal treatment of cheap orange juice that is readily available. Because of their high photo-stability and low toxicity, these C-dots have shown to be excellent probes for cellular imaging. Using hydrothermal treatment of soya milk, Zhu et al. created bi-functional fluorescent C-dots with strong electro-catalytic activity for oxygen reduction [57].

#### 3.4.2.2. Microwave/Ultrasonic Synthesis

To make C-dots with electro-chemiluminescence properties, Yang says he used a microwave pyrolysis approach by mixing PEG200 with a saccharide (such as glucose or fructose) in water to make a transparent solution, which was then heated for 2–10 min in a 500 W microwave oven to produce electro-chemiluminescence [58]. The length of the microwave heating influences the size and PL properties of these C-dots (5 minutes in this case). Kang et al. created C-dots that showed vividly colored PL from glucose or active carbon in the visible to near-infrared spectral region using an ultrasonic treatment method [59]. Also, using hydrogen peroxide as a catalyst, the same group devised a one-step ultrasonic treatment to generate water-soluble bright C-dots from active carbon [56]. It was found that these C-dots generated bright and colorful photoluminescence throughout the whole visible to near-infrared spectral range, despite their up-conversion fluorescent properties. One-pot ultrasonic synthesis was utilized in a recent research to produce photocatalytically active fluorescent N-doped C-dots (NCDs), which were then used in the visible light photo degradation of methyl orange [60]. Figure 2.5 depicts the photodegradation of methyl orange utilizing fluorescent N-doped C-dots (NCDs) with photocatalytic activity [60].

#### 3.4.2.3. Supported Synthetic Methods

With this method, the C dots may be made to have a monodisperse structure while still being synthesized using a supported synthetic approach. The support helps to keep the C-dots separate during high-temperature treatment, which prevents nanoparticle aggregation. For C-dot formation, Li and colleagues used surfactant-modified silica spheres as supports; the silica spheres were then removed using a 2 M NaOH solution etched with a diamond pen [61]. Using 3M  $\text{HNO}_3$ , the surface was passivated and oxidized to produce hydrophilic photoluminescent C-dots. When developing C-dots, Giannelis and colleagues used an ion-exchanged version of NaY zeolite [54]. To make hydrophilic C-dots, Zhu et al. utilized mesoporous silica (MS) spheres as nanoreactors. After calcination and support removal, MS spheres were impregnated with a complex salts and citric acid solution, resulting in monodisperse, hydrophilic C-dots [62].

## 3.5. Applications of CQDs

### 3.5.1. The Chemical sensing

CQDs have proven useful in chemical sensing, e.g., mercury ( $\text{Hg}^{2+}$ ) must be identified as soon as possible since it poses a major hazard to both the environment and human health. CQDs have been used in chemical sensing applications because of their low toxicity, water

solubility, high photostability, and remarkable chemical stability. The selective detection of  $\text{Hg}^{2+}$  in aqueous solutions and live cells was one of the first successful attempts to utilize CQDs in chemical sensing [6]. Fluorescence emissions from both CQD solution and CQDs immobilized in sol-gel were found to be  $\text{Hg}^{2+}$ -dependent, as shown by Goncalves and colleagues in their study. Fluorescent probes included laser-ablated CQDs,  $\text{NH}_2$ -PEG200, and N-acetyl-L cysteine-passivated CQDs. The team of Goncalves and associates used micromolar quantities of  $\text{Hg}^{2+}$  with a Stern–Volmer constant of  $1.3105 \text{ M}^{-1}$ . Barman and Sadhukhan (2012) found that fluorescence intensity in CQDs could be successfully reduced. This means that the quenching induced by  $\text{Hg}^{2+}$  is most likely due to static quenching as a consequence of the formation of a stable non-fluorescent complex between CQD and  $\text{Hg}^{2+}$ , given the high value of the Stern–Volmer constant. Substituting N-CQDs for the laser-ablated CQDs led to a substantial improvement in sensitivity down to nanomolar levels, as later found. Again, it is speculated that static quenching is responsible for the loss of fluorescence; but this time, the value of the Stern–Volmer constant is two orders of magnitude higher:  $1.4107 \text{ M}^{-1}$ . The significantly improved  $\text{Hg}^{2+}$  sensing ability of N-CQDs has been attributed to the presence of nitrogen element, most likely in the form of  $-\text{CN}$  groups on the N-CQD surface [63]. The  $\text{Hg}^{2+}$ -CQD system, developed more recently by Yan and colleagues, enables the selective detection of  $\text{Hg}^{2+}$  in aqueous solution and in live cells. When compared to conventional synthesis methods, the authors were able to achieve quantum yields of 65.5 and 55.4 percent using citric acid and 1,2-ethyldiamine (CQD-1 and CQ-2, respectively). These quantum yields were much higher than those of the usual technique. They looked into the influence of  $\text{Hg}^{2+}$  on CQD-1 and CQD-2's fluorescence emission quenching effectiveness and selectivity. Both CQDs served as selective and sensitive fluorescence probes, respectively, for the detection of mercury levels in aqueous solutions and live cells. After injecting 20 mM of  $\text{Hg}^{2+}$ , the fluorescence became more intense.

The intensity of CQD-1 was reduced by 80% in the first hour, whereas the intensity of CQD-2 was reduced by 55% in the first hour and stayed constant afterwards. This shows that CQD-1 and CQD-2 may be used as  $\text{Hg}^{2+}$  chemical sensing probes in a wide range of applications [64]. The  $\text{Hg}^{2+}$  selectivity of CQD-1 and CQD-2 was then determined by measuring the quantity of fluorescence quenching produced by different metal ions added to the cells at 20 mM concentrations. Using  $\text{Hg}^{2+}$ , the most potent metal ion tested, scientists were able to significantly reduce the fluorescence of the CQD-1 and CQD-2 fluorescent materials. Reversible quenching of

fluorescence was shown in these CQDs, making them useful as reversible fluorescent probes. This was demonstrated in the studies. The detection of  $\text{Hg}^{2+}$  in growing cells was also made with efficient and successful efforts [64].

Some of the additional elements identified by CQDs in chemical sensing include  $\text{Cu}^{2+}$  [65],  $\text{Fe}^{3+}$  [66],  $\text{Pb}^{2+}$  [20],  $\text{Cr}^{4+}$  [67], and  $\text{Ag}^+$  [68]. The bulk of the methods proposed are based, as previously mentioned, on the fluorescence quenching produced by metal ions, similar to the  $\text{Hg}^{2+}$  sensing approach.  $\text{Cu}^{2+}$  was discovered to be selectively detected utilizing CQDs modified with lysine and bovine serum albumin in aqueous samples such as tap water described by Liu et al (CQDs-BSA-Lys). Sensitive detection of  $\text{Cu}^{2+}$  in solution was achieved using the coordination reaction of  $\text{Cu}^{2+}$  with the  $-\text{COOH}$  and  $-\text{NH}_2$  groups of the CQDs-BSA-Lys [69]. CQD-based fluorescent probes with higher sensitivity were developed by covering them with more sensitive metal-organic frameworks (ZIF-8 – zinc imidazolate frameworks) and silica nanoparticles rather than polymeric materials [70]. A new class of ultrasensitive nanocomposite fluorescence probes has been developed by Lin and colleagues by using CQDs coated with b-PEI and encapsulated in ZIF-8. It was discovered that by using the synergistic effects of the strong fluorescence of the CQDs and the selective accumulation action of ZIF-8 hosts, CQD-ZIF-8 nano composite probes could detect  $\text{Cu}^{2+}$  concentrations down to 80 parts per million (ppm) [52]. To make more CQD-metal-organic framework probes, the same method may be employed, which would enable very sensitive and selective detection for many analytes like concentration of metal ions, detect pH, citrate ion concentration in a single experiment.

A few examples of reactive oxygen species are  $\text{CN}^-$  [71],  $\text{S}^{2-}$  [72],  $\text{ClO}^-$  [73], and  $\text{I}^-$  [74]. Instead of using the fluorescence quenching method to measure metal ions, many anion assays use the fluorescence rise (also known as fluorescence recovery) of previously quenched CQD-metal complexes. CQD fluorescence was recovered by creating more stable complexes between  $\text{I}^-$  and metal ions in the  $\text{I}^-$ -assay, which displaced the CQDs from the CQD-metal complexes. The authors, Z. Yang et al. (2013), state that Ascorbic acid, 4-nitrophenol, quercetin, 2,4-dinitrophenol, and APTS-GO were also tested for chromium [67], as were other minor inorganic substances [75]. Variations in the synthesis of CQDs have serious consequences because studies suggest that the fluorescence characteristics of CQDs are strongly dependent on the composition of CQDs and residue chemical groups on their surface; different starting materials and procedures invariably result in CQDs with significantly different physicochemical properties overall, and optical properties specifically. CQDs must

be standardized, and their performance must be evaluated, as soon as possible [13].

### 3.5.2. Biosensing

CQDs were used in immunoassays and biomarker studies in addition to biosensing using antibodies and their gene-recombinant fragments [76]. In immunoassays, CQDs are mainly employed as fluorescent labels. Posthuma-Trumpie and colleagues studied the utilization of CQDs in lateral flow and microarray immunoassays [77]. Because they are less costly, more stable, and more sensitive, CQDs were chosen for this study over other commonly used fluorescent markers. CQDs have been found to be more sensitive as labels in lateral flow tests than gold or latex nanoparticles (LFA). As recently as 2019, researchers discovered that the pico-molar range was capable of accurately detecting CQDs.

NALFA serves as a good generic example of nucleic acid LFA. The amplicons' distinguishing tags are recognized by the appropriate antibodies, and the CQDs attached to the amplicons generate fluorescence signals [78]. For the rapid and specific detection of 4,4'-dibrominated biphenyl (PBB15), a persistent organic pollutant that has been shown to disrupt the endocrine system, Bu and colleagues developed an immune-sensor based on the principles of Forrester resonance energy transfer (FRET) and homogenous immunoassay. Gold nanoparticles (AuNPs) functionalized with anti-PBB15 antibody have been used as fluorescence acceptors, whereas PBB15 antigens have been CQD-labeled have been used as donors. Because of the FRET phenomena, the AuNPs were able to reduce the CQDs' fluorescence. Fluorescence recovery happened when the CQD-labeled antigens were competitively immune-reacted off of AuNP's surface with PBB15 added to the solution. Using antibodies and antigens specific to the analyte, this immunosensor may be used as a model for the future creation of immunoassays for the detection of other analytes [79]. The fluorescence dye was successfully quenched by the addition of single-stranded DNA to the CQDs, and this technique was used to identify nucleic acids with such great selectivity that even a single base mismatch could be detected first. The newly generated cs-DNA desorbed from the CQD surface when single-stranded DNA (ss-DNA) hybridized with its matching target to make a double-stranded DNA (ds-DNA). This allowed the fluorescence to return [80]. Single-nucleotide polymorphisms may be detected using this technology's ability to detect changes in fluorescence intensity. The use of nucleic acid binders called aptamers, selected from a large nucleic acid library, has also been shown in another CQD application [13]. Most of the time, aptamers are linked to a conformational

change in the target that can be detected in the radiometric response. When used in conjunction with thrombin-functionalized CQDs, this technique creates a sandwich-structure with aptamer-functionalized silica nanoparticles by creating a specific interaction between thrombin and a particular aptamer [80]. With a detection limit of 1.0 nM, this thrombin assay was shown to be one of the most sensitive fluorescence assays available for thrombin. Stable fluorescent CQDs made using a one-step microwave pyrolysis method previously reported were used to identify the proteins after they were separated using gel electrophoresis. Protein staining was a breeze with these CQDs since they worked so well.

Conventional staining agents like Coomassie Brilliant Blue and Ag<sup>+</sup> work extremely well or even better in terms of sensitivity than [80]. According to the researchers, water-soluble CQDs made from rice straws thermally burned in a furnace with insufficient air flow were used to rapidly identify and count bacteria cells in sewage water. These CQDs engaged with the receptors only when they came into touch with the bacterial cell membrane [81]. In addition to macro-biomolecules, CQDs have shown promise as fluorescent probes for the detection of small bio-analytes such as anti-bacterial drugs. This was clearly shown by Niu and Gao's experiments. Luminescent N-CQDs were initially synthesized from glutamic acid using a one-step pyrolysis method. These N-CQDs were utilized in a number of applications for the detection of amoxicillin, a popular antibiotic used to treat bacterial infections. The researchers found that amoxicillin molecules effectively separate N-CQDs from one another, decreasing the frequency of non-radiative transitions, which ultimately led to an increase in fluorescence intensity [82]. CQDs were also utilized to detect previously undetectable small bio-analyte including dopamine, ascorbic acid, and glucose. Some of these CQD-based methods utilize dopamine as a carbon source and generate highly fluorescent CQDs, which may be used to detect dopamine without the need of labelling chemicals. Using dopamine, researchers were able to restore the fluorescence of a previously quenched Fe<sup>3+</sup> CQD complex in a manner similar to the anion sensing described earlier. In the range of 0.1–10 mM, the increase in fluorescence was shown to be proportional to an increase in dopamine concentration, with a detection limit of just over 68 nM. [71]. Dopamine, on the other hand, was shown to be an efficient quencher in another study. The differences in the techniques and carbon sources used to make CQDs likely account for this discrepancy. Consistency in CQD synthesis is crucial to prevent data misunderstanding of data [70].



### 3.5.3. Bio-imaging

CQDs provide numerous advantages over semiconductor quantum dots due to their comparable optical properties and outstanding chemical and photochemical durability [12]. First and foremost, carbon does not pollute the environment in any way. These features make CQDs an appealing technology as an alternative to semiconductor quantum dots for studying biological systems both in vitro and in vivo [72]. Cytotoxicity is caused by surface passivating chemicals on the CQD surface, not by the carbon core of the CQDs [83]. Surface passivating compounds with low cytotoxicity have been proven to be safe at high dosages for in vivo imaging. Mice were given 8–40 mg/kg (CQD/weight) of PEGylated CQDs intravenously, and no adverse effects could be detected up to 28 days later for the evaluation of toxicity [84]. To test whether CQDs are detrimental at exposure levels and durations beyond what is typically used in in-vivo imaging studies, researchers gave mice various dosages of CQDs or NaCl as a control. Physiological indicators were all similar. Despite liver and spleen CQD levels being higher than those reported in the other organs, no abnormalities were seen in the tissues. Additionally, the health of cells exposed to various doses of CQDs was evaluated. Cell viability was reported to be more than 95% at CQD dosages up to 1.8 mg/ml. As a result of these results, CQDs have been shown to be much more biocompatible than semiconductor quantum dots as a result of these results [85]. Even at low concentrations and/or short incubation times, it is feasible to use CQDs modified with high cytotoxicity agents for in vivo applications. It has been shown that organic dye-conjugated CQDs are effective fluorescent H<sub>2</sub>S probes. When organic dye-conjugated CQDs were exposed to residues of H<sub>2</sub>S, a FRET reaction took place, changing the blue emission into a green emission [12]. H<sub>2</sub>S has already been shown to cross cell membranes through simple diffusion [84]. A fluorescence microscope was used to investigate the ability of organic dye-conjugated CQDs to detect changes in physiologically relevant H<sub>2</sub>S levels in live cells. Additionally, CQDs synthesized using N-( $\beta$ -aminoethyl)- $\gamma$ -aminopropyl methyl-dimethoxysilane as a carbon source interacted preferentially with Cu<sup>2+</sup> owing to the presence of ethylenediamine residues on their surface [85]. RhB-doped silica nanoparticles were coated with these CQDs to produce dual-emission Cu<sup>2+</sup> probes. Cu<sup>2+</sup> significantly reduced the fluorescence of CQDs but had no effect on RhB. These probes worked well for imaging Cu<sup>2+</sup> in live cells [85]. The images taken by Hsu et al. showed that the cytoplasm and membrane were the primary locations of CQDs. Passivated PPEI-EI water-soluble CQDs have been shown to label MCF-7 cells' cell membrane and cytoplasm, but not their nucleus [86]. COS-7 cells' membranes and cytoplasm

were labelled with CQDs produced from activated carbon alone [84]. Only cells treated with silica-encapsulated CQDs exhibited the highest light in the cytoplasm [81]. Fowley and colleagues created CQDs that passed the membrane of Chinese hamster ovary cells and landed in the cytoplasm using a biocompatible amphiphilic polymer [86]. Researchers led by Hu have created CQDs with a 54.3% quantum yield b-PEI coating that are uniformly dispersed throughout the cytoplasm [63].

Surface passivating chemicals and surface passivation mode influence CQDs localization, as shown by these examples. It is common practice to apply CQDs to cells before imaging to enable uptake by the cells and utilization within them. When CQD internalization was tested at 481°C, no CQDs were found within the cells. As reported, CQDs enter cells through endocytosis [87, 88]. One possible way to enhance CQD absorption is by coupling them with membrane translocation peptides to facilitate this process [89]. CQDs are unique labelling agents due to their variety of emission colors. Consequently, researchers can now select and control the excitation and emission wavelengths more easily [65]. The multicolor emissions they produce when stimulated at different wavelengths were also observed when folic acid passivated CQDs were used in HepG2 cells [84]. Bacteria and yeast cells utilized several excitation modes to stimulate green CQDs produced from sugar cane juice [90]. The strong fluorescence intensity required for cell imaging [89]. Even without any surface passivating compounds, thermally combusted soot CQDs treated with acid efficiently translocated into Ehrlich ascites carcinoma cells. If the excitation wavelength is sufficiently red-shifted, CQDs may emit in the near infrared (NIR). Despite their low NIR emission, CQDs have great potential for in vivo fluorescence tracking studies [91]. This is due to the fact that the animal's body is almost transparent in the near-infrared spectrum. Yang's team was the first to use CQDs in live mice as a contrast agent [91]. PEG1500N-passivated CQDs were administered subcutaneously into mice, and the animals continued to emit bright fluorescence for 24 hours after the injection. This study found that intravenously administered CQDs mostly exit the body through urine extraction. The same group observed lymph vessel movement using ZnS-doped CQDs [92].

### 3.5.4. Nano-medicine

CQDs are an ideal alternative to other fluorescent nanomaterials since they are tiny fluorescent nanoparticles that can be synthesized rapidly and inexpensively using various synthetic methods [93]. As CQDs show no apparent signs of toxicity in animals,

they hold great promise for application in nano-medicine [94]. CQDs were administered intravenously to mice in vivo and used in photodynamic treatment to treat transdermal tumors with no effect on thrombin activity or blood coagulation [95]. The production of singlet oxygen species, which leads to cell death, and the localization and concentration of photosensitizers in cancer tissue are induced using a specific wavelength of irradiation. The strong tumor-to-background fluorescence contrast and the low fluorescence levels in other tissues and organs indicate that CQDs might be used as photosensitizers due to their ability to selectively concentrate within tumors [96].

PPEI-EI functionalized small CQDs (PPEI-CQDs) showed a significant photodynamic impact on Du145 and PC3 cells when exposed to UV light. The observed photodynamic impact was caused by the photo-induced production of singlet oxygen (Type II process) and other reactive oxygen species and radicals (Type I mechanism) [97]. Due to the size of its bandgap, TiO<sub>2</sub> is a typical semiconductor photo-catalyst that can only be activated by UV light [98]. CQDs also used to treat deep-seated tumors like colon and bladder cancer [99]. CQDs combined with conventional photosensitizer (protoporphyrin IX). The up-conversions activated the photosensitizer without causing any negative side effects thanks to FRET. Fluorescence emission is produced by excitation of the CQDs at 800 nm. In comparison to clinical photodynamic treatment, the excitation light at 800 nm from the phototherapeutic window may penetrate four times deeper into human tissue than clinical photodynamic therapy [100].

CQDs significantly used for radiotherapy as well as phototherapy. Silver-coated PEG-CQDs (C-Ag-PEG CQDs) were employed as radiosensitizers in Du145 cells. To enhance their therapeutic selectivity, low-energy X-ray exposure generated electrons that damaged cancer cells around the CQDs but did not affect healthy cells [101]. bPEI-coated CQDs efficiently used as nanocarriers for gene delivery to the retinal cells due to high number of amino groups on their surfaces. The bPEI was successfully delivered into cells without any issues. Because of its high positive charge density and proton-sponge activity, biotin gathers and condenses genetic material to form toroidal complexes that cells can easily uptake through endocytosis [102].

Zheng & coworkers used chemical coupling to attach an anticancer Pt<sup>4+</sup>-based pro-drug – oxidized oxaliplatin (Oxa(VI)-COOH) to CQD surfaces [103]. When exposed to light, the quinoline molecules on the CQDs' surfaces serve as release triggers, allowing researchers to monitor the dispersion of drug-CQDs conjugates. In addition to pH-triggered drug release, several mechanisms for the

release of medicines have been investigated [104]. Folic acid was used as a navigation molecule on the CQDs surface because of its association with almost all types of cancer cells. CQDs were used to evaluate the loading capacity of DOX, and the release kinetics were found to follow first order kinetics at a physiological pH, providing for a good release profile.

Interestingly, the DOX-loaded CQDs killed cancer cells more quickly and were less harmful to normal cells than free DOX because of the better targeting ability of the folic acid molecule [105].

## 4. Conclusion

In conclusion, CQDs represent a fascinating class of nano-sized carbon-based materials that have garnered significant scientific interest in recent decades. Their distinct qualities, including optical, electrical, and chemical characteristics, make them ideal candidates for a variety of applications. The controllable fluorescence and biocompatibility of CQDs have led to their utilization in domains such as bioimaging and sensors, highlighting their promise for medical and technological advancements. Furthermore, the study of CQDs in energy-related applications, such as photocatalysis and solar cells, demonstrates their potential importance in sustainable technology. As new synthesis methods are discovered, the multifarious nature of CQDs presents them as exciting and valuable materials with far-reaching ramifications in a various scientific technological field. This comprehensive review highlights the synthesis, properties, and applications of CQDs, which will serve as an informative foundation for future research.

## References

- [1] P. Kumar, S. Dua, R. Kaur, M. Kumar, G. Bhatt, A review on advancements in carbon quantum dots and their application in photovoltaics, *RSC Advances* 12 (8), 4714-4759, 2022.
- [2] M. Farshbaf, S. Davaran, F. Rahimi, N. Annabi, R. Salehi, A. Akbarzadeh, Carbon quantum dots: recent progresses on synthesis, surface modification and applications, *Artificial Cells, Nanomedicine, and Biotechnology* 46 (7), 1331-1348, 2018.
- [3] M. Pourmadadi, E. Rahmani, M. Rajabzadeh-Khosroshahi, A. Samadi, R. Behzadmehr, A. Rahdar, L. F. R. Ferreira, Properties and application of carbon quantum dots (CQDs) in biosensors for disease detection: A comprehensive review, *J Drug Deliv Sci Tec* 80 104156, 2023.
- [4] T. J. Pillar-Little, N. Wanninayake, L. Nease, D. K. Heidary, E. C. Glazer, D. Y. Kim, Superior photodynamic effect of carbon quantum dots through both type I and type II pathways: Detailed comparison study of top-down-synthesized and bottom-up-synthesized carbon quantum dots, *Carbon* 140 616-623, 2018.
- [5] A. Tadesse, D. Rama Devi, M. Hagos, G. Battu, K. Basavaiah, Facile green synthesis of fluorescent carbon quantum dots from

- citrus lemon juice for live cell imaging, *Asian Journal of Nanoscience and Materials* 1 (1), 36-46, 2018.
- [6] Y. Guo, Z. Wang, H. Shao, X. Jiang, Hydrothermal synthesis of highly fluorescent carbon nanoparticles from sodium citrate and their use for the detection of mercury ions, *Carbon* 52 583-589, 2013.
- [7] K. Dimos, Carbon Quantum Dots: Surface Passivation and Functionalization, *Curr Org Chem* 20 (6), 682-695, 2016.
- [8] M. Bangal, S. Ashtaputer, S. Marathe, A. Ethiraj, N. Hebalkar, S. W. Gosavi, J. Urban, S. K. Kulkarni, Semiconductor Nanoparticles, in: D. R. S. Somayajulu, K. P. Lieb (Eds.) *IWNMS 2004*, Springer Berlin Heidelberg, Berlin, Heidelberg, 2005, pp. 81-94.
- [9] W. Zhou, J. J. Coleman, Semiconductor quantum dots, *Curr Opin Solid St M* 20 (6), 352-360, 2016.
- [10] A. M. Wagner, J. M. Knipe, G. Orive, N. A. Peppas, Quantum dots in biomedical applications, *Acta Biomater* 94 44-63, 2019.
- [11] A. Gour, S. Ramteke, N. K. Jain, Pharmaceutical Applications of Quantum Dots, *AAPS Pharm Sci Tech* 22 (7), 233, 2021.
- [12] H. Li, Z. Kang, Y. Liu, S.-T. Lee, Carbon nanodots: synthesis, properties and applications, *J Mater Chem* 22 (46), 24230-24253, 2012.
- [13] S. Y. Lim, W. Shen, Z. Gao, Carbon quantum dots and their applications, *Chem Soc Rev* 44 (1), 362-381, 2015.
- [14] K. J. Mintz, Y. Zhou, R. M. Leblanc, Recent development of carbon quantum dots regarding their optical properties, photoluminescence mechanism, and core structure, *Nanoscale* 11 (11), 4634-4652, 2019.
- [15] P. Anilkumar, X. Wang, L. Cao, S. Sahu, J.-H. Liu, P. Wang, K. Korch, K. N. Tackett II, A. Parenzan, Y.-P. Sun, Toward quantitatively fluorescent carbon-based "quantum" dots, *Nanoscale* 3 (5), 2023-2027, 2011.
- [16] P. Namdari, B. Negahdari, A. Eatemadi, Synthesis, properties and biomedical applications of carbon-based quantum dots: An updated review, *Biomed Pharmacother* 87 209-222, 2017.
- [17] A. S. Barnard, S. P. Russo, I. K. Snook, Size dependent phase stability of carbon nanoparticles: Nanodiamond versus fullerenes, *J Chem Phys* 118 (11), 5094-5097, 2003.
- [18] J. M. Klostranec, W. C. W. Chan, Quantum Dots in Biological and Biomedical Research: Recent Progress and Present Challenges, *Adv Mater* 18 (15), 1953-1964, 2006.
- [19] S. C. Ray, A. Saha, N. R. Jana, R. Sarkar, Fluorescent Carbon Nanoparticles: Synthesis, Characterization, and Bioimaging Application, *J Phys Chem C* 113 (43), 18546-18551, 2009.
- [20] X. Wang, K. Qu, B. Xu, J. Ren, X. Qu, Multicolor luminescent carbon nanoparticles: Synthesis, supramolecular assembly with porphyrin, intrinsic peroxidase-like catalytic activity and applications, *Nano Research* 4 (9), 908-920, 2011.
- [21] P. Koutsogiannis, E. Thomou, H. Stamatis, D. Gournis, P. Rudolf, Advances in fluorescent carbon dots for biomedical applications, *Advances in Physics: X* 5 (1), 1758592, 2020.
- [22] D. L. Zhao, T.-S. Chung, Applications of carbon quantum dots (CQDs) in membrane technologies: A review, *Water Research* 147 43-49, 2018.
- [23] Y. Zhang, D. Petibone, Y. Xu, M. Mahmood, A. Karmakar, D. Casciano, S. Ali, A. S. Biris, Toxicity and efficacy of carbon nanotubes and graphene: the utility of carbon-based nanoparticles in nanomedicine, *Drug metabolism reviews* 46 (2), 232-46, 2014.
- [24] A. Truskewycz, S. Beker, A. S. Ball, I. Cole, Photoluminescence measurements of carbon quantum dots within three-dimensional hydrogel matrices using a high throughput 96 well plate method, *MethodsX* 6 437-441, 2019.
- [25] X. Xu, R. Ray, Y. Gu, H. J. Ploehn, L. Gearheart, K. Raker, W. A. Scrivens, Electrophoretic analysis and purification of fluorescent single-walled carbon nanotube fragments, *J Am Chem Soc* 126 (40), 12736-7, 2004.
- [26] P. K. Yadav, S. Chandra, V. Kumar, D. Kumar, S. H. Hasan, Carbon Quantum Dots: Synthesis, Structure, Properties, and Catalytic Applications for Organic Synthesis, *Catalysts* 13 (2), 422, 2023.
- [27] X. Liu, J. Hao, J. Liu, H. Tao, Green synthesis of carbon quantum dots from lignite coal and the application in Fe<sup>3+</sup> detection, *IOP Conference Series: Earth and Environmental Science* 113 (1), 012063, 2018.
- [28] R. Wang, K.-Q. Lu, Z.-R. Tang, Y.-J. Xu, Recent progress in carbon quantum dots: synthesis, properties and applications in photocatalysis, *J Mater Chem A* 5 (8), 3717-3734, 2017.
- [29] R. Das, R. Bandyopadhyay, P. Pramanik, Carbon quantum dots from natural resource: A review, *Mater Today Chem* 8 96-109, 2018.
- [30] M. J. Molaei, Principles, mechanisms, and application of carbon quantum dots in sensors: a review, *Anal Method* 12 (10), 1266-1287, 2020.
- [31] T. Takagahara, K. Takeda, Theory of the quantum confinement effect on excitons in quantum dots of indirect-gap materials, *Physical Review B* 46 (23), 15578-15581, 1992.
- [32] H.-L. Yang, L.-F. Bai, Z.-R. Geng, H. Chen, L.-T. Xu, Y.-C. Xie, D.-J. Wang, H.-W. Gu, X.-M. Wang, Carbon quantum dots: Preparation, optical properties, and biomedical applications, *Mater Today Adv* 18 100376, 2023.
- [33] T. Yuan, T. Meng, P. He, Y. Shi, Y. Li, X. Li, L. Fan, S. Yang, Carbon quantum dots: an emerging material for optoelectronic applications, *J Mater Chem C* 7 (23), 6820-6835, 2019.
- [34] A. M. Smith, H. Duan, M. N. Rhyner, G. Ruan, S. Nie, A systematic examination of surface coatings on the optical and chemical properties of semiconductor quantum dots, *Physical chemistry chemical physics : PCCP* 8 (33), 3895-903, 2006.
- [35] D. Ozyurt, M. A. Kobaisi, R. K. Hocking, B. Fox, Properties, synthesis, and applications of carbon dots: A review, *Carbon Trends* 12 100276, 2023.
- [36] Z. Liu, H. Zou, N. Wang, T. Yang, Z. Peng, J. Wang, N. Li, C. Huang, Photoluminescence of carbon quantum dots: coarsely adjusted by quantum confinement effects and finely by surface trap states, *Sci China Chem* 61 (4), 490-496, 2018.
- [37] Y. K. Chang, H. H. Hsieh, W. F. Pong, M. H. Tsai, F. Z. Chien, P. K. Tseng, L. C. Chen, T. Y. Wang, K. H. Chen, D. M. Bhusari, J. R. Yang, S. T. Lin, Quantum Confinement Effect in Diamond Nanocrystals Studied by X-Ray-Absorption Spectroscopy, *Phys Rev Lett* 82 (26), 5377-5380, 1999.
- [38] O. D. Neikov, N. A. Yefimov, Chapter 9 - Nanopowders, in: O. D. Neikov, S. S. Naboychenko, N. A. Yefimov (Eds.), *Handbook of Non-Ferrous Metal Powders (Second Edition)*, Elsevier, Oxford, pp. 271-311, 2019.
- [39] M. Yuan, R. Zhong, H. Gao, W. Li, X. Yun, J. Liu, X. Zhao, G. Zhao, F. Zhang, One-step, green, and economic synthesis of water-soluble photoluminescent carbon dots by hydrothermal treatment of wheat straw, and their bio-applications in labeling, imaging, and sensing, *Appl Surf Sci* 355 1136-1144, 2015.
- [40] D. Wang, L. Zhu, C. McCleese, C. Burda, J.-F. Chen, L. Dai, Fluorescent carbon dots from milk by microwave cooking, *RSC Advances* 6 (47), 41516-41521, 2016.
- [41] S. Borna, R. E. Sabzi, S. Pirsia, Synthesis of carbon quantum dots from apple juice and graphite: investigation of fluorescence and structural properties and use as an electrochemical sensor for measuring Letrozole, *J Mater Sci: Materials in Electronics* 32 (8), 10866-10879, 2021.
- [42] X. Xu, K. Zhang, L. Zhao, C. Li, W. Bu, Y. Shen, Z. Gu, B. Chang, C. Zheng, C. Lin, H. Sun, B. Yang, Aspirin-Based Carbon Dots, a Good Biocompatibility of Material Applied for Bioimaging and Anti-Inflammation, *ACS Appl Mater Inter* 8 (48), 32706-32716, 2016.
- [43] L. Wang, W. Li, B. Wu, Z. Li, S. Wang, Y. Liu, D. Pan, M. Wu, Facile synthesis of fluorescent graphene quantum dots from

- coffee grounds for bioimaging and sensing, *Chem Eng J* 300 75-82, 2016.
- [44] Y. Zhao, Y. Zhang, X. Liu, H. Kong, Y. Wang, G. Qin, P. Cao, X. Song, X. Yan, Q. Wang, H. Qu, Novel carbon quantum dots from egg yolk oil and their haemostatic effects, *Scientific Reports* 7 (1), 4452, 2017.
- [45] Y. Liu, Q. Zhou, J. Li, M. Lei, X. Yan, Selective and sensitive chemosensor for lead ions using fluorescent carbon dots prepared from chocolate by one-step hydrothermal method, *Sensor Actuator B: Chem* 237 597-604, 2016.
- [46] F. Limosani, E. M. Bauer, Top-Down N-Doped Carbon Quantum Dots for Multiple Purposes: Heavy Metal Detection and Intracellular Fluorescence, 11 (9), 2021.
- [47] L. Cao, X. Wang, M. J. Mezziani, F. Lu, H. Wang, P. G. Luo, Y. Lin, B. A. Harruff, L. M. Veca, D. Murray, S.-Y. Xie, Y.-P. Sun, Carbon Dots for Multiphoton Bioimaging, *J Am Chem Soc* 129 (37), 11318-11319, 2007.
- [48] L. Zheng, Y. Chi, Y. Dong, J. Lin, B. Wang, Electrochemiluminescence of Water-Soluble Carbon Nanocrystals Released Electrochemically from Graphite, *J Am Chem Soc* 131 (13), 4564-4565, 2009.
- [49] A. Khayal, V. Dawane, M. A. Amin, V. Tirth, V. K. Yadav, A. Algahtani, S. H. Khan, S. Islam, K. K. Yadav, B.-H. Jeon, Advances in the Methods for the Synthesis of Carbon Dots and Their Emerging Applications, *Polymers* 13 (18), 3190, 2021.
- [50] [50] Z.-A. Qiao, Y. Wang, Y. Gao, H. Li, T. Dai, Y. Liu, Q. Huo, Commercially activated carbon as the source for producing multicolor photoluminescent carbon dots by chemical oxidation, *Chem Commun* 46 (46), 8812-8814, 2010.
- [51] H. B. Ahmed, H. E. Emam, Environmentally exploitable biocide/fluorescent metal marker carbon quantum dots, *RSC Adv* 10 (70), 42916-42929, 2020.
- [52] Y.-P. Sun, X. Wang, F. Lu, L. Cao, M. J. Mezziani, P. G. Luo, L. Gu, L. M. Veca, Doped Carbon Nanoparticles as a New Platform for Highly Photoluminescent Dots, *J Phys Chem C* 112 (47), 18295-18298, 2008.
- [53] C. H. Lei, X. E. Zhao, S. L. Jiao, L. He, Y. Li, S. Y. Zhu, J. M. You, A turn-on fluorescent sensor for the detection of melamine based on the anti-quenching ability of Hg<sup>2+</sup> to carbon nanodots, *Anal Method* 8 (22), 4438-4444, 2016.
- [54] A. B. Bourlinos, A. Stassinopoulos, D. Anglos, R. Zboril, V. Georgakilas, E. P. Giannelis, Photoluminescent Carbogenic Dots, *Chem Mater* 20 (14), 4539-4541, 2008.
- [55] M. J. Krysmann, A. Kellarakis, P. Dallas, E. P. Giannelis, Formation Mechanism of Carbogenic Nanoparticles with Dual Photoluminescence Emission, *J Am Chem Soc* 134 (2), 747-750, 2012.
- [56] X. He, H. Li, Y. Liu, H. Huang, Z. Kang, S.-T. Lee, Water soluble carbon nanoparticles: Hydrothermal synthesis and excellent photoluminescence properties, *Colloid Surface B* 87 (2), 326-332, 2011.
- [57] C. Zhu, J. Zhai, S. Dong, Bifunctional fluorescent carbon nanodots: green synthesis via soy milk and application as metal-free electrocatalysts for oxygen reduction, *Chem Commun* 48 (75), 9367-9369, 2012.
- [58] H. Li, R. Liu, W. Kong, J. Liu, Y. Liu, L. Zhou, X. Zhang, S.-T. Lee, Z. Kang, Carbon quantum dots with photo-generated proton property as efficient visible light controlled acid catalyst, *Nanoscale* 6 (2), 867-873, 2014.
- [59] H. Li, X. He, Y. Liu, H. Huang, S. Lian, S.-T. Lee, Z. Kang, One-step ultrasonic synthesis of water-soluble carbon nanoparticles with excellent photoluminescent properties, *Carbon* 49 (2), 605-609, 2011.
- [60] Z. Ma, H. Ming, H. Huang, Y. Liu, Z. Kang, One-step ultrasonic synthesis of fluorescent N-doped carbon dots from glucose and their visible-light sensitive photocatalytic ability, *New J Chem* 36 (4), 861-864, 2012.
- [61] R. Liu, D. Wu, S. Liu, K. Koynov, W. Knoll, Q. Li, An Aqueous Route to Multicolor Photoluminescent Carbon Dots Using Silica Spheres as Carriers, *Angew Chem Int Edit* 48 (25), 4598-4601, 2009.
- [62] J. Zong, Y. Zhu, X. Yang, J. Shen, C. Li, Synthesis of photoluminescent carbogenic dots using mesoporous silica spheres as nanoreactors, *Chem Commun* 47 (2), 764-766, 2011.
- [63] L. Lu, R. Helgeson, R. M. Jones, D. McBranch, D. Whitten, Superquenching in Cyanine Pendant Poly(L-lysine) Dyes: Dependence on Molecular Weight, Solvent, and Aggregation, *J Am Chem Soc* 124 (3), 483-488, 2002.
- [64] F. Yan, Y. Zou, M. Wang, X. Mu, N. Yang, L. Chen, Highly photoluminescent carbon dots-based fluorescent chemosensors for sensitive and selective detection of mercury ions and application of imaging in living cells, *Sensor Actuator B-Chem* 192 488-495, 2014.
- [65] S. Zhang, Q. Wang, G. Tian, H. Ge, A fluorescent turn-off/on method for detection of Cu<sup>2+</sup> and oxalate using carbon dots as fluorescent probes in aqueous solution, *Mater Lett* 115 233-236, 2014.
- [66] Y.-L. Zhang, L. Wang, H.-C. Zhang, Y. Liu, H.-Y. Wang, Z.-H. Kang, S.-T. Lee, Graphitic carbon quantum dots as a fluorescent sensing platform for highly efficient detection of Fe<sup>3+</sup> ions, *RSC Advances* 3 (11), 3733-3738, 2013.
- [67] M. Zheng, Z. Xie, D. Qu, D. Li, P. Du, X. Jing, Z. Sun, On-Off-On Fluorescent Carbon Dot Nanosensor for Recognition of Chromium(VI) and Ascorbic Acid Based on the Inner Filter Effect, *ACS Appl Mater Inter* 5 (24), 13242-13247, 2013.
- [68] Z. Qian, J. Ma, X. Shan, H. Feng, L. Shao, J. Chen, Highly Luminescent N-Doped Carbon Quantum Dots as an Effective Multifunctional Fluorescence Sensing Platform, *Chem – A Eur J* 20 (8), 2254-2263, 2014.
- [69] J.-M. Liu, L.-p. Lin, X.-X. Wang, L. Jiao, M.-L. Cui, S.-L. Jiang, W.-L. Cai, L.-H. Zhang, Z.-Y. Zheng, Zr(H<sub>2</sub>O)<sub>2</sub>EDTA modulated luminescent carbon dots as fluorescent probes for fluoride detection, *Analyst* 138 (1), 278-283, 2013.
- [70] X. Lin, G. Gao, L. Zheng, Y. Chi, G. Chen, Encapsulation of Strongly Fluorescent Carbon Quantum Dots in Metal-Organic Frameworks for Enhancing Chemical Sensing, *Anal Chem* 86 (2), 1223-1228, 2014.
- [71] X. Hou, F. Zeng, F. Du, S. Wu, Carbon-dot-based fluorescent turn-on sensor for selectively detecting sulfide anions in totally aqueous media and imaging inside live cells, *Nanotechnology* 24 (33), 335502, 2013.
- [72] S.-L. Hu, K.-Y. Niu, J. Sun, J. Yang, N.-Q. Zhao, X.-W. Du, One-step synthesis of fluorescent carbon nanoparticles by laser irradiation, *J Mater Chem* 19 (4), 484-488, 2009.
- [73] B. Yin, J. Deng, X. Peng, Q. Long, J. Zhao, Q. Lu, Q. Chen, H. Li, H. Tang, Y. Zhang, S. Yao, Green synthesis of carbon dots with down- and up-conversion fluorescent properties for sensitive detection of hypochlorite with a dual-readout assay, *Analyst* 138 (21), 6551-6557, 2013.
- [74] Z. Yang, Z. Li, M. Xu, Y. Ma, J. Zhang, Y. Su, F. Gao, H. Wei, L. Zhang, Controllable Synthesis of Fluorescent Carbon Dots and Their Detection Application as Nanoprobes, *Nano-Micro Letters* 5 (4), 247-259, 2013.
- [75] Y. Zhou, Z.-b. Qu, Y. Zeng, T. Zhou, G. Shi, A novel composite of graphene quantum dots and molecularly imprinted polymer for fluorescent detection of parantrophenol, *Biosens Bioelectron* 52 317-323, 2014.
- [76] C. Ji, Y. Zhou, R. M. Leblanc, Z. Peng, Recent Developments of Carbon Dots in Biosensing: A Review, *ACS Sensors* 5 (9), 2724-2741, 2020.
- [77] X. Terzapulo, A. Kassenova, R. Bukasov, Immunoassays: Analytical and Clinical Performance, Challenges, and Perspectives of SERS Detection in Comparison with Fluorescent Spectroscopic Detection, *Int J mol sci* 25 (4), 1-33, 2024.

- [78] Y. Yu, C. Li, C. Chen, H. Huang, C. Liang, Y. Lou, X.-B. Chen, Z. Shi, S. Feng, Saccharomyces-derived carbon dots for biosensing pH and vitamin B 12, *Talanta* 195 117-126, 2019.
- [79] Y. Dai, Z. Liu, Y. Bai, Z. Chen, J. Qin, F. Feng, A novel highly fluorescent S, N, O co-doped carbon dots for biosensing and bioimaging of copper ions in live cells, *RSC Advances* 8 (73), 42246-42252, 2018.
- [80] H. Shi, J. Wei, L. Qiang, X. Chen, X. Meng, Fluorescent carbon dots for biolmaging and biosensing applications, *J biomed nanotechnol* 10 (10), 2677-99, 2014.
- [81] T. Sarkar, H. B. Bohidar, P. R. Solanki, Carbon dots-modified chitosan based electrochemical biosensing platform for detection of vitamin D, *Int j biol macromol* 109 687-697, 2018.
- [82] M. Pan, Z. Xu, Q. Jiang, J. Feng, J. Sun, F. Wang, Interfacial engineering of carbon dots with benzenediboric acid for fluorescent biosensing, *1 (2)*, 765-771, 2019.
- [83] Q. Zhang, R. Shi, Q. Li, T. Maimaiti, S. Lan, P. Ouyang, B. Ouyang, Y. Bai, B. Yu, S.-T. Yang, Low toxicity of fluorescent carbon quantum dots to white rot fungus *Phanerochaete chrysosporium*, *J Environ Chem Eng* 9 (1), 104633, 2021.
- [84] V. Sharma, P. Tiwari, S. M. Mobin, Sustainable carbon-dots: recent advances in green carbon dots for sensing and bioimaging, *J Mater Chem B* 5 (45), 8904-8924, 2017.
- [85] F. Du, Y. Ming, F. Zeng, C. Yu, S. Wu, A low cytotoxic and ratiometric fluorescent nanosensor based on carbon-dots for intracellular pH sensing and mapping, *Nanotechnology* 24 (36), 365101, 2013.
- [86] S. Barman, M. Sadhukhan, Facile bulk production of highly blue fluorescent graphitic carbon nitride quantum dots and their application as highly selective and sensitive sensors for the detection of mercuric and iodide ions in aqueous media, *J Mater Chem* 22 (41), 21832-21837, 2012.
- [87] G. Sahay, D. Y. Alakhova, A. V. Kabanov, Endocytosis of nanomedicines, *Journal of controlled release: official journal of the Controlled Release Society* 145 (3), 182-95, 2010.
- [88] L. W. Zhang, N. A. Monteiro-Riviere, Mechanisms of Quantum Dot Nanoparticle Cellular Uptake, *Toxicol Sci* 110 (1), 138-155, 2009.
- [89] X. T. Zheng, A. Ananthanarayanan, K. Q. Luo, P. Chen, Glowing Graphene Quantum Dots and Carbon Dots: Properties, Syntheses, and Biological Applications, *Small* 11 (14), 1620-1636, 2015.
- [90] T. S, R. S. D, Green synthesis of highly fluorescent carbon quantum dots from sugarcane bagasse pulp, *Appl Surf Sci* 390 435-443, 2016.
- [91] K. Qu, J. Wang, J. Ren, X. Qu, Carbon Dots Prepared by Hydrothermal Treatment of Dopamine as an Effective Fluorescent Sensing Platform for the Label-Free Detection of Iron(III) Ions and Dopamine, *Chem – A Eur J* 19 (22), 7243-7249, 2013.
- [92] A. Hamidu, W. G. Pitt, Recent Breakthroughs in Using Quantum Dots for Cancer Imaging and Drug Delivery Purposes, *Nanomater (Basel, Switzerland)* 13 (18), 1-35, 2023.
- [93] P. Devi, S. Saini, K.-H. Kim, The advanced role of carbon quantum dots in nanomedical applications, *Biosens Bioelectron* 141 111158, 2019.
- [94] S. Chaudhary, A. Umar, K. Bhasin, S. Singh, Applications of Carbon Dots in Nanomedicine, *J Biomed Nanotechnol* 13, 591-637 13 (6), 591-637, 2017.
- [95] K. Soumya, N. More, M. Choppadandi, D. A. Aishwarya, G. Singh, G. Kapusetti, A comprehensive review on carbon quantum dots as an effective photosensitizer and drug delivery system for cancer treatment, *Biomed Technol* 4 11-20, 2023.
- [96] H. Wang, S. Yang, L. Chen, Y. Li, P. He, G. Wang, H. Dong, P. Ma, G. Ding, Tumor diagnosis using carbon-based quantum dots: Detection based on the hallmarks of cancer, *Bioact mater* 33 174-222, 2024.
- [97] K. Naik, S. Chaudhary, L. Ye, A. S. Parmar, A Strategic Review on Carbon Quantum Dots for Cancer-Diagnostics and Treatment, *Front Bioeng Biotech* 10 2022.
- [98] V. Etacheri, C. Di Valentin, J. Schneider, D. Bahnemann, S. C. Pillai, Visible-light activation of TiO<sub>2</sub> photocatalysts: Advances in theory and experiments, *J Photoch Photobio C* 25 1-29, 2015.
- [99] S. Masha, O. S. Oluwafemi, Synthesis of blue and green emitting carbon-based quantum dots (CBQDs) and their cell viability against colon and bladder cancer cell lines, *Mater Lett* 283 128790, 2021.
- [100] C. Fowley, N. Nomikou, A. P. McHale, B. McCaughan, J. F. Callan, Extending the tissue penetration capability of conventional photosensitisers: a carbon quantum dot-protoporphyrin IX conjugate for use in two-photon excited photodynamic therapy, *Chem commun (Cambridge, England)* 49 (79), 8934-6, 2013.
- [101] S. Bayda, E. Amadio, Carbon dots for cancer nanomedicine: a bright future, *Nanoscale Adv.* 3 (18), 5183-5221, 2021.
- [102] M. R. Biswal, S. Bhatia, Carbon Dot Nanoparticles: Exploring the Potential Use for Gene Delivery in Ophthalmic Diseases, *Nanomaterials (Basel, Switzerland)* 11 (4), 2021.
- [103] D. Tolan, V. Gandin, L. Morrison, A. El-Nahas, C. Marzano, D. Montagner, A. Erxleben, Oxidative Stress Induced by Pt(IV) Prodrugs Based on the Cisplatin Scaffold and Indole Carboxylic Acids in Axial Position, *Sci Rep.* 6 29367, 2016.
- [104] A. Ray Chowdhuri, S. Tripathy, C. Haldar, S. Roy, S. K. Sahu, Single step synthesis of carbon dot embedded chitosan nanoparticles for cell imaging and hydrophobic drug delivery, *J Mater Chem B* 3 (47), 9122-9131, 2015.
- [105] X. Li, K. Vinothini, T. Ramesh, M. Rajan, Combined photodynamic-chemotherapy investigation of cancer cells using carbon quantum dot-based drug carrier system, *Drug delivery* 27 (1), 791-804, 2020.



